# Search for Dark Sectors and Dark Photons decaying into lepton jets with the ATLAS experiment

**Bernardo Ricci**

Erice 2024

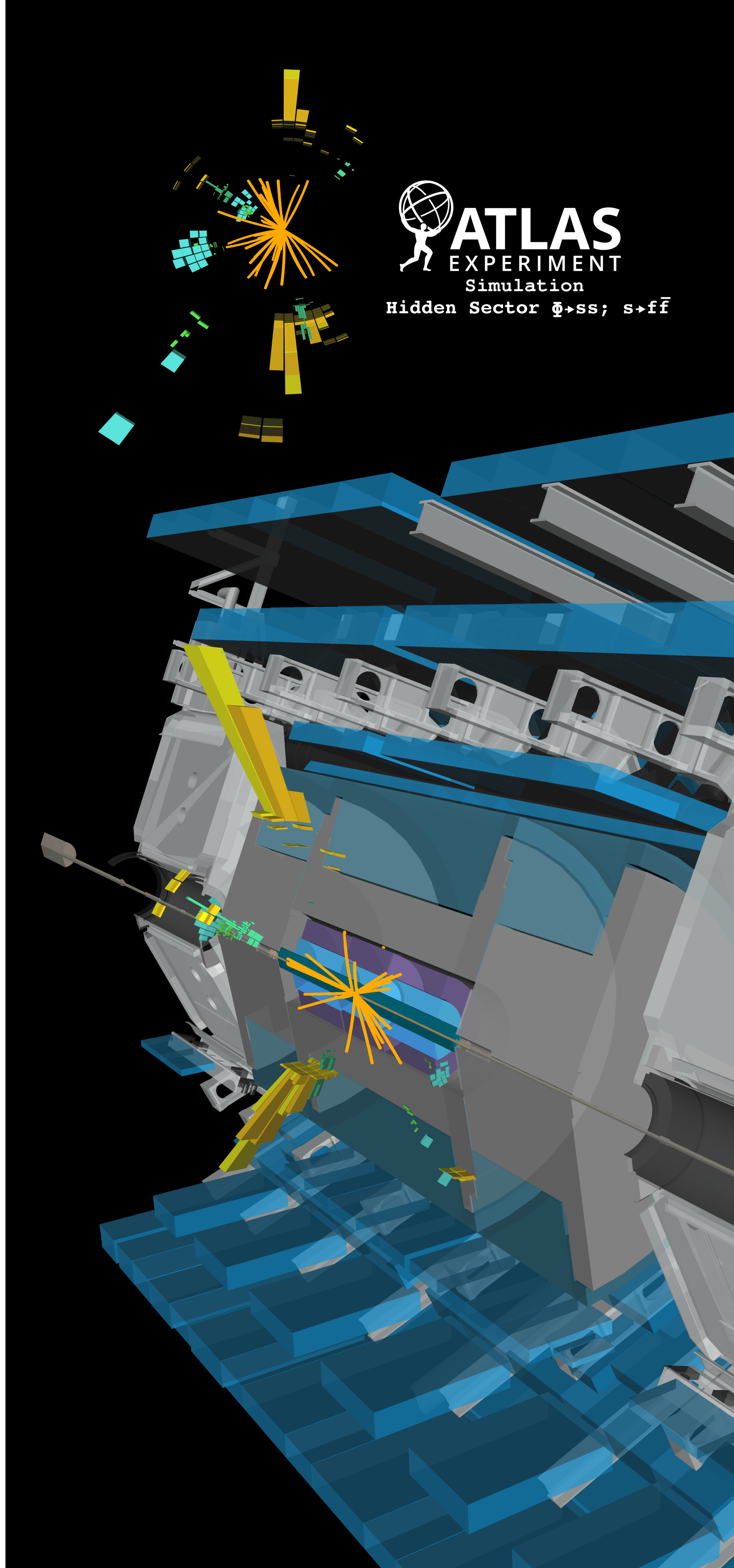

# Dark Sector through portals

- Investigated possibility: Dark Matter is a stable state of a new **Dark Sector**
- Minimal Dark Sector Model: $U(1)_d$ spontaneously broken by a Dark Higgs Mechanism → short-range interaction, the **Dark Photon** $\gamma_d$ can be massive and decay
- Minimum assumption: the existence of a vector portal ($\epsilon$) between the Dark Sector and the Standard Model is required

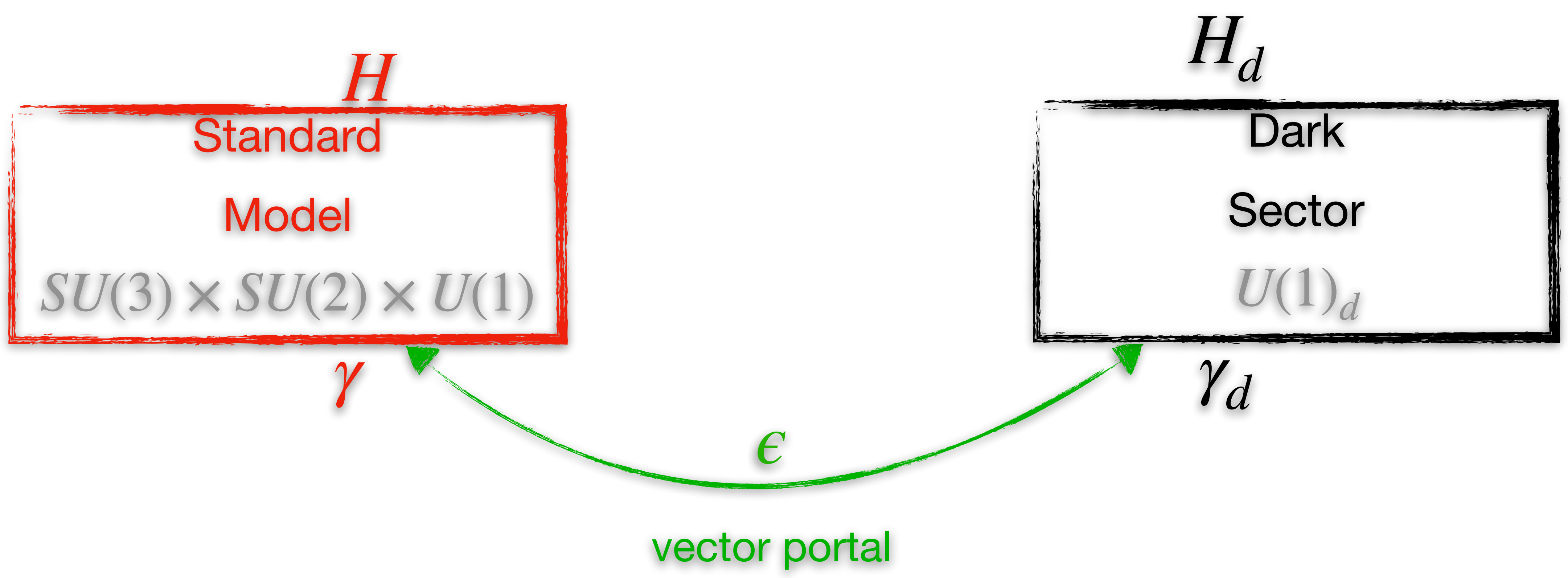


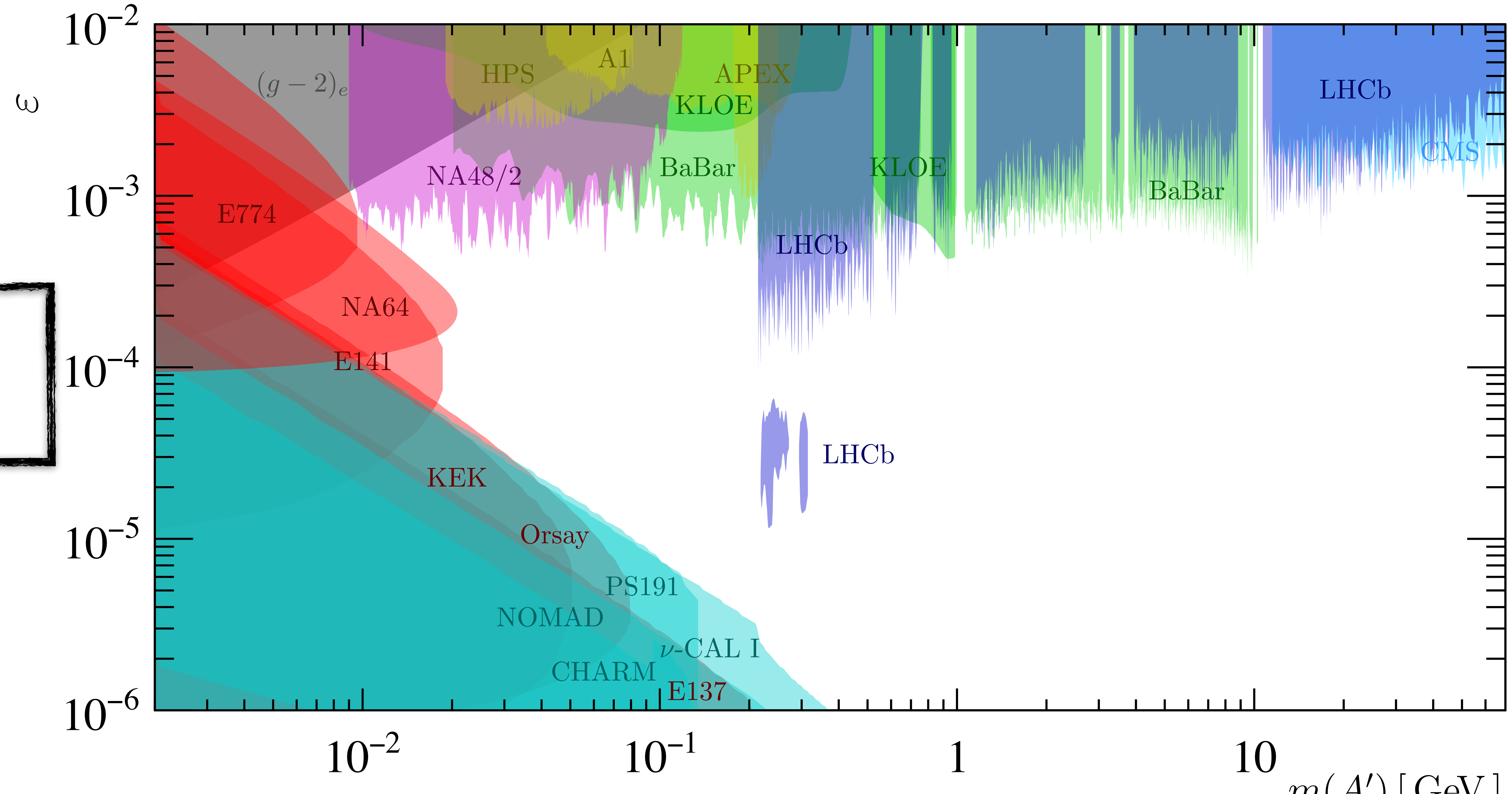


https://arxiv.org/abs/1801.04847

# Dark Sector through portals

- Investigated possibility: Dark Matter is a stable state of a new **Dark Sector**
- Minimal Dark Sector Model: $U(1)_d$ spontaneously broken by a Dark Higgs Mechanism → short-range interaction, the **Dark Photon** $\gamma_d$ can be massive and decay
- Minimum assumption: the existence of a vector portal ($\epsilon$) between the Dark Sector and the Standard Model is required
- $BR(H \rightarrow und) < 11\%$ —> Higgs Boson can decay in Dark Sector particles through the Higgs portal

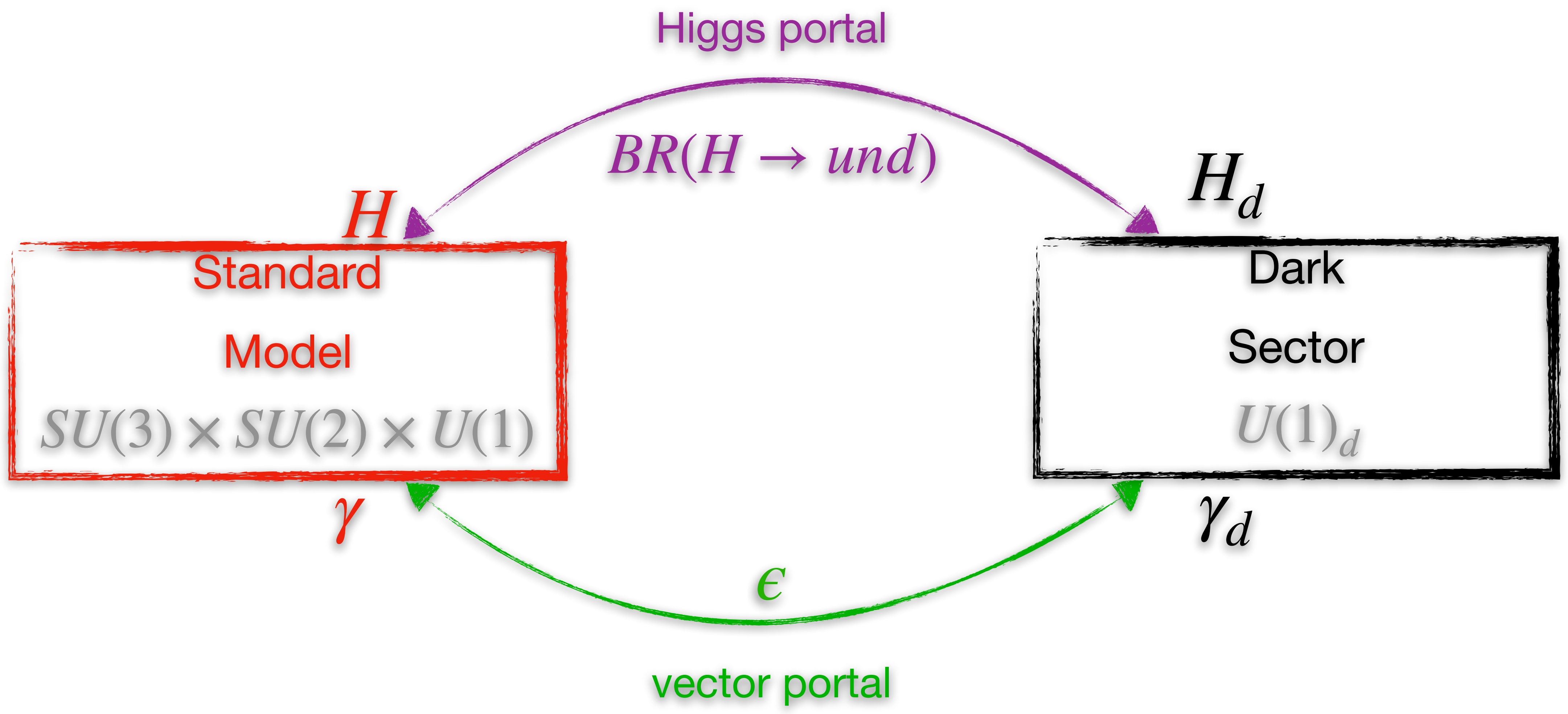


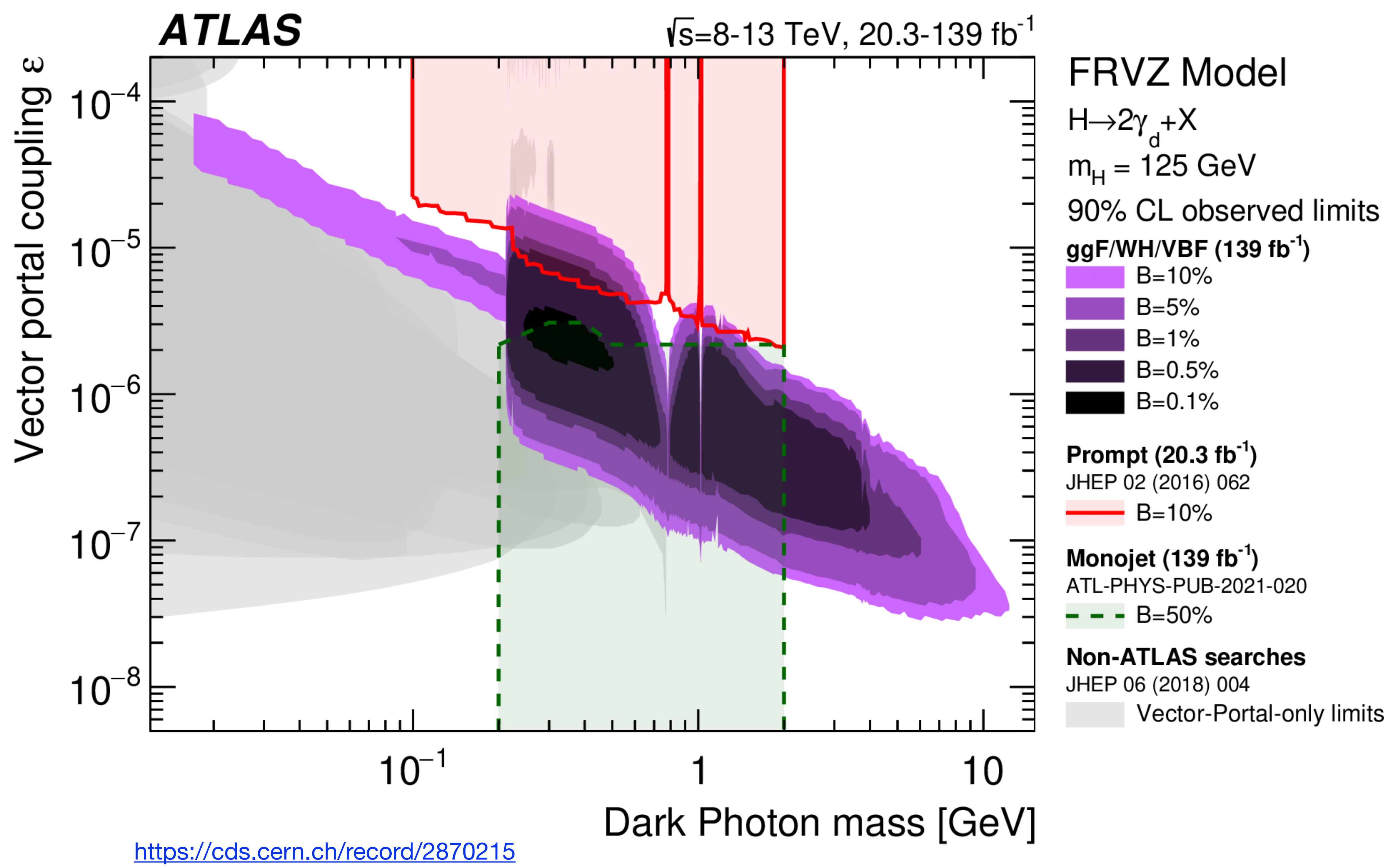


https://cds.cern.ch/record/2870215

# Prompt decay of Dark Photon

Prompt decay —> The Dark Photon decays in the ID

Free Parameters of the Dark Sector:

- $BR(H \rightarrow und)$ affects the number of events
- $\epsilon$ affects where the Dark Photon decays ($\tau_{\gamma_d} \propto \epsilon^{-2}$)
- $m_{\gamma_d}$ determine the $BR$ of $\gamma_d$ in Standard Model particles

$$\tau_{\gamma_d} \propto \left(\frac{10^{-4}}{\epsilon}\right)^2 \left(\frac{100MeV}{m_{\gamma_d}}\right)$$

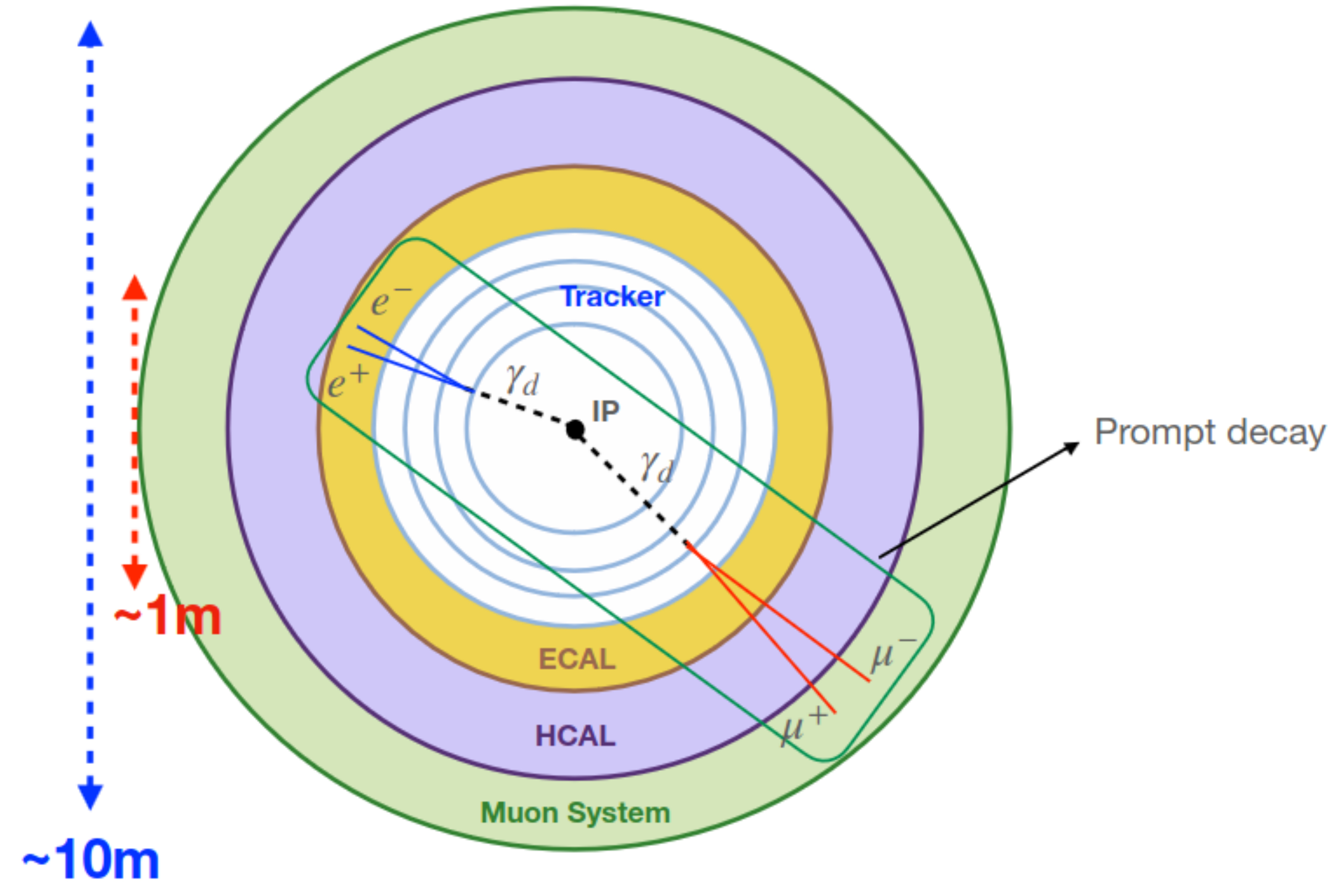


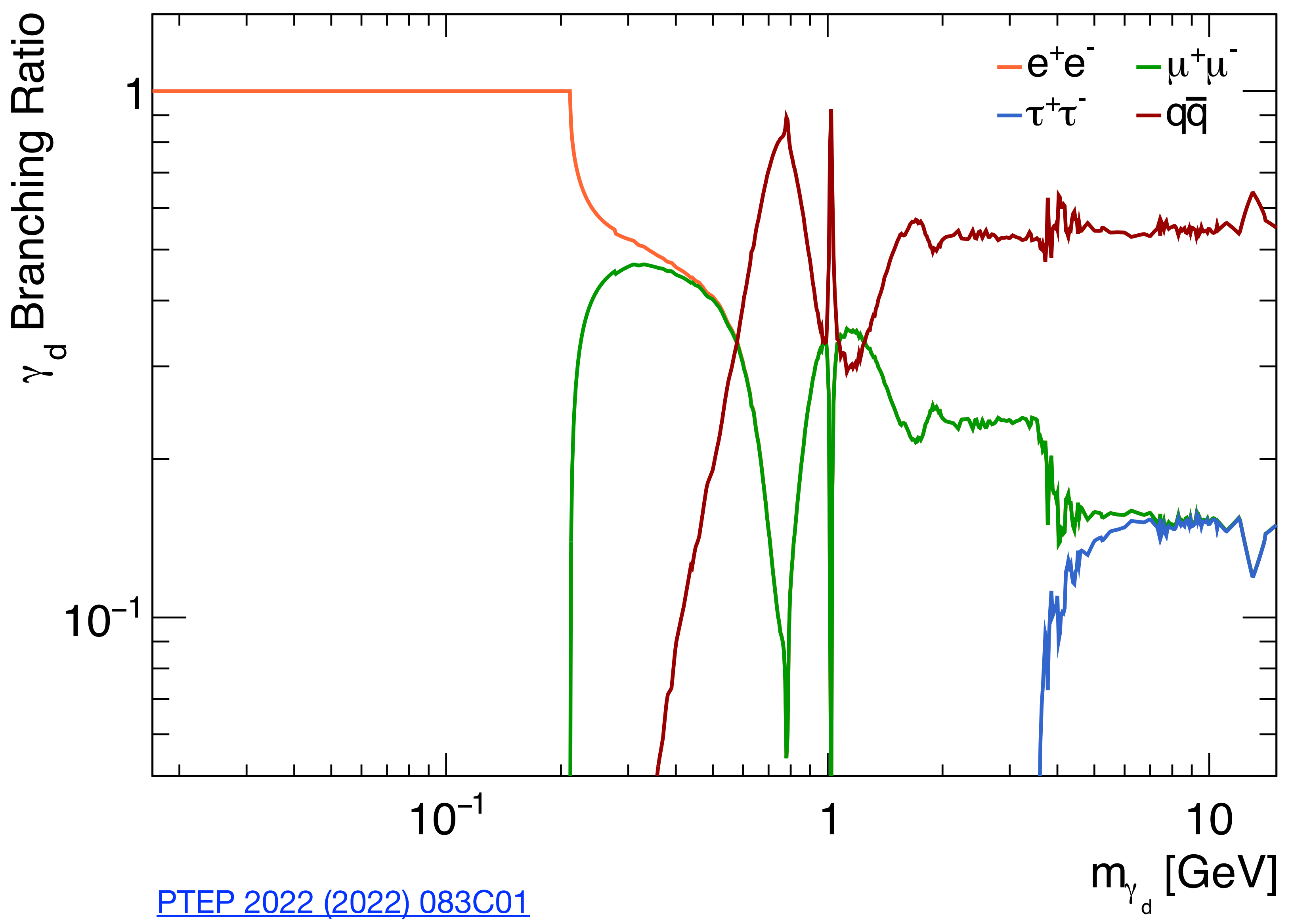


PTEP 2022 (2022) 083C01

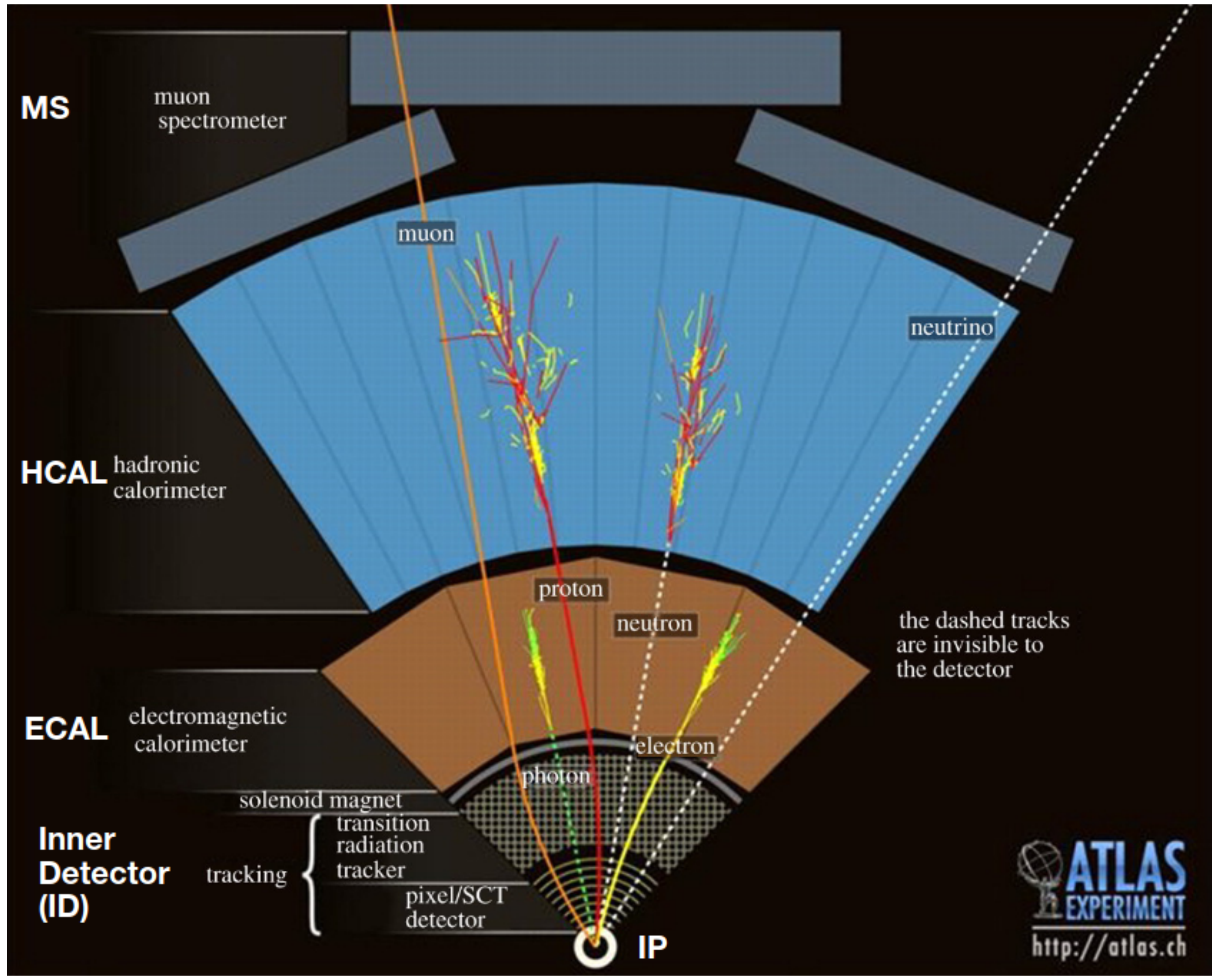

# Prompt decay of Dark Photon

Prompt decay —> The Dark Photon decays in the ID

Free Parameters of the Dark Sector:

- $BR(H \rightarrow und)$ affects the number of events
- $\epsilon$ affects where the Dark Photon decays ($\tau_{\gamma_d} \propto \epsilon^{-2}$)
- $m_{\gamma_d}$ determine the $BR$ of $\gamma_d$ in Standard Model particles

$$\tau_{\gamma_d} \propto \left(\frac{10^{-4}}{\epsilon}\right)^2 \left(\frac{100MeV}{m_{\gamma_d}}\right)$$

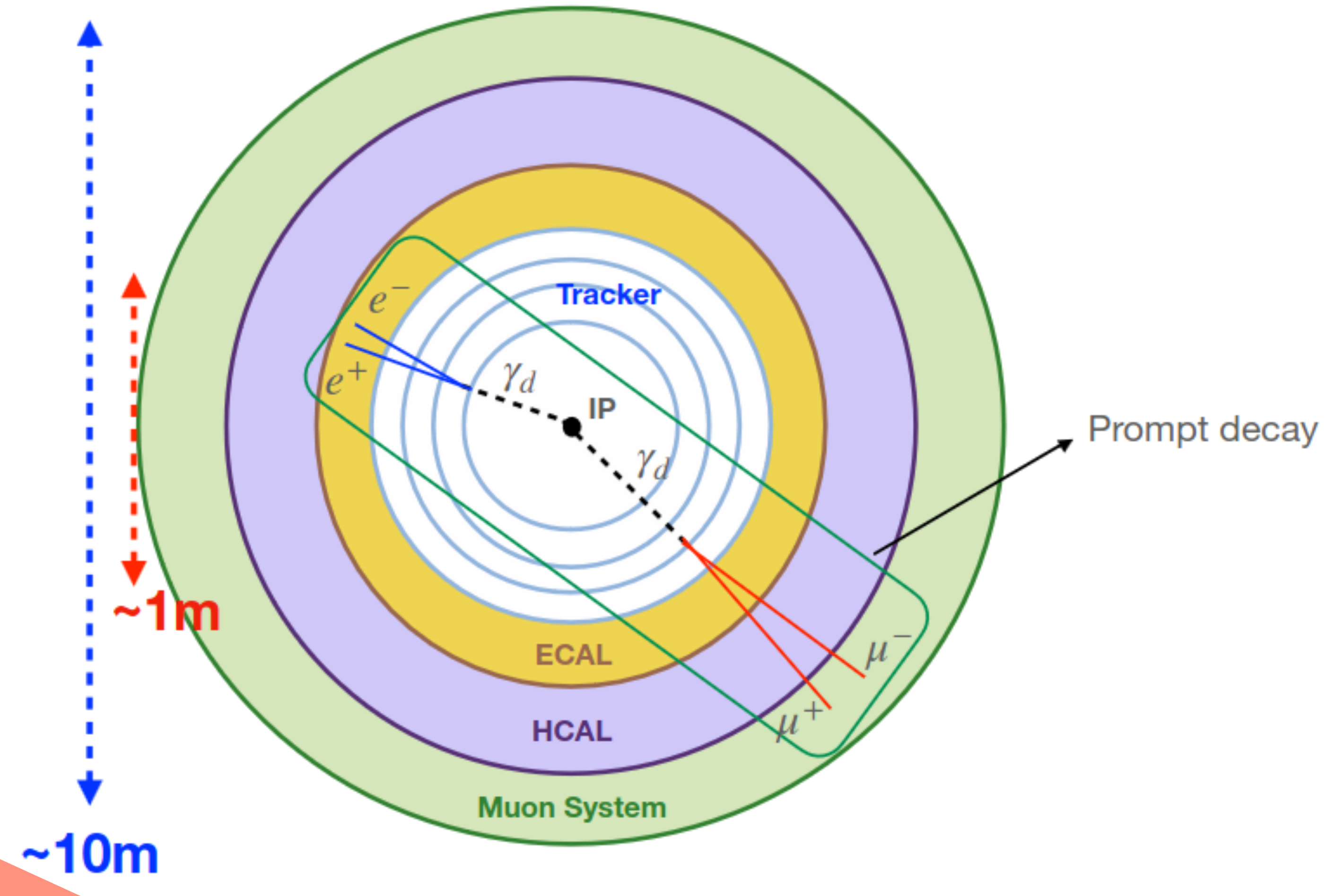


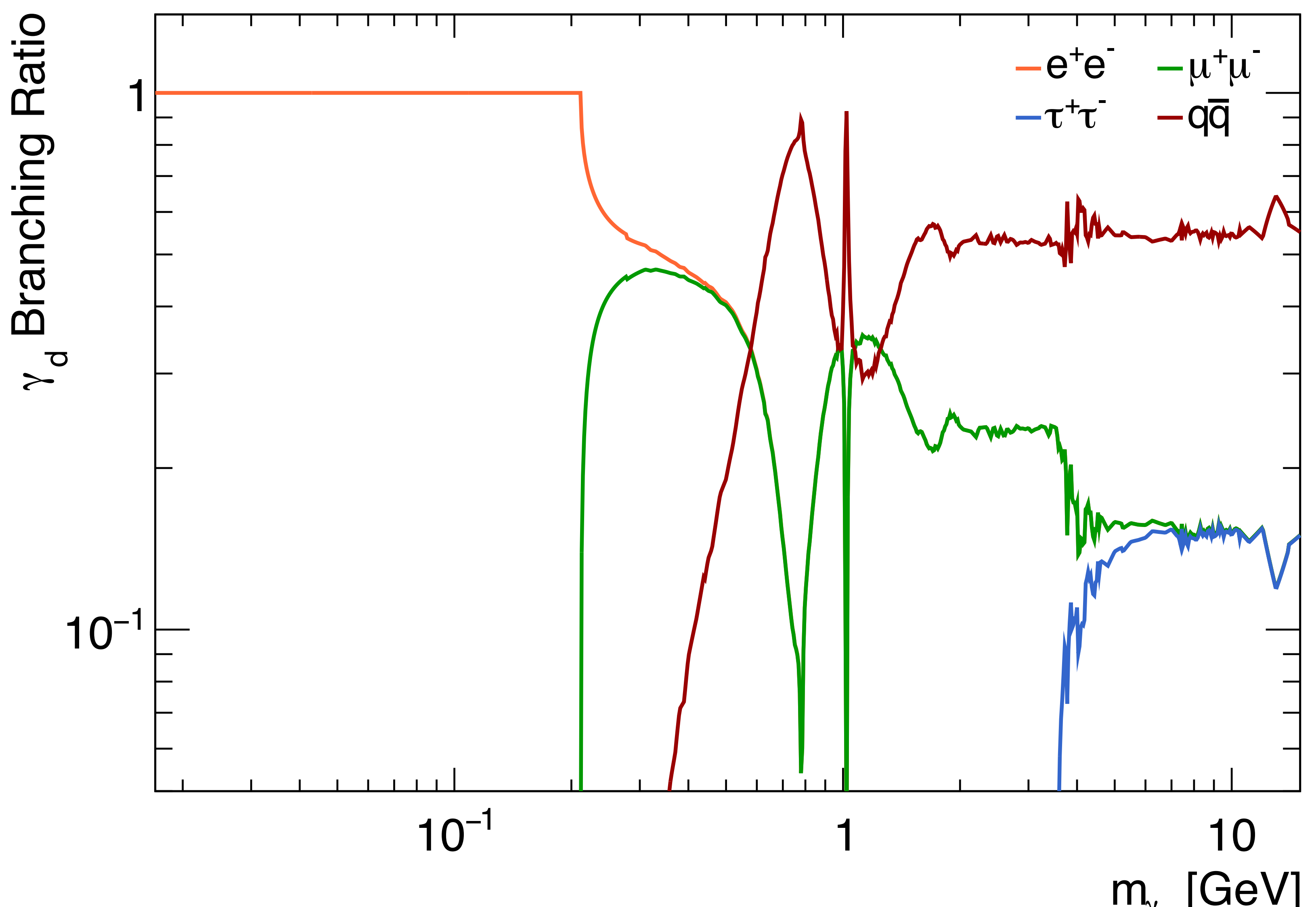


PTEP 2022 (2022) 083C01

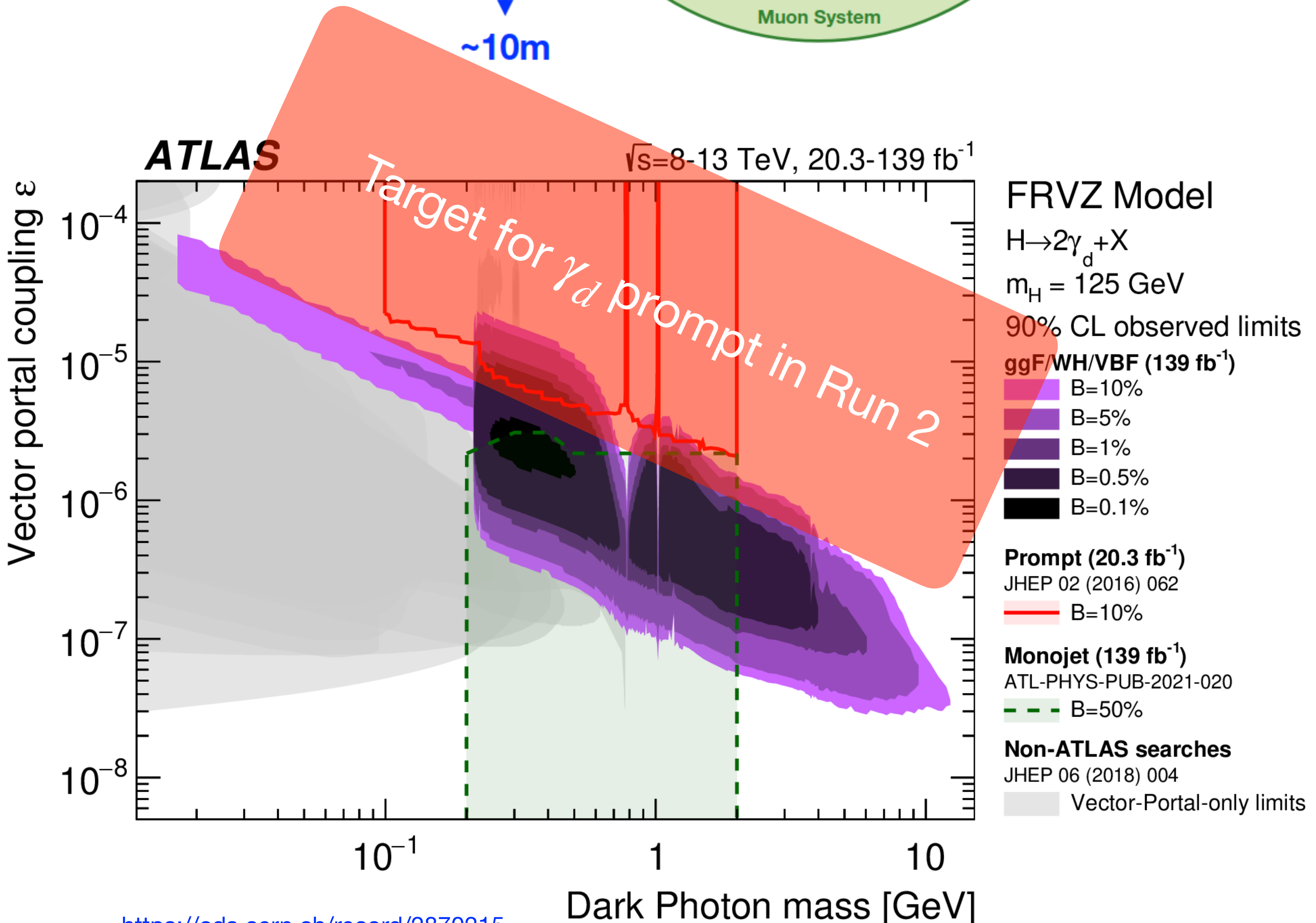


https://cds.cern.ch/record/2870215

# Benchmark models

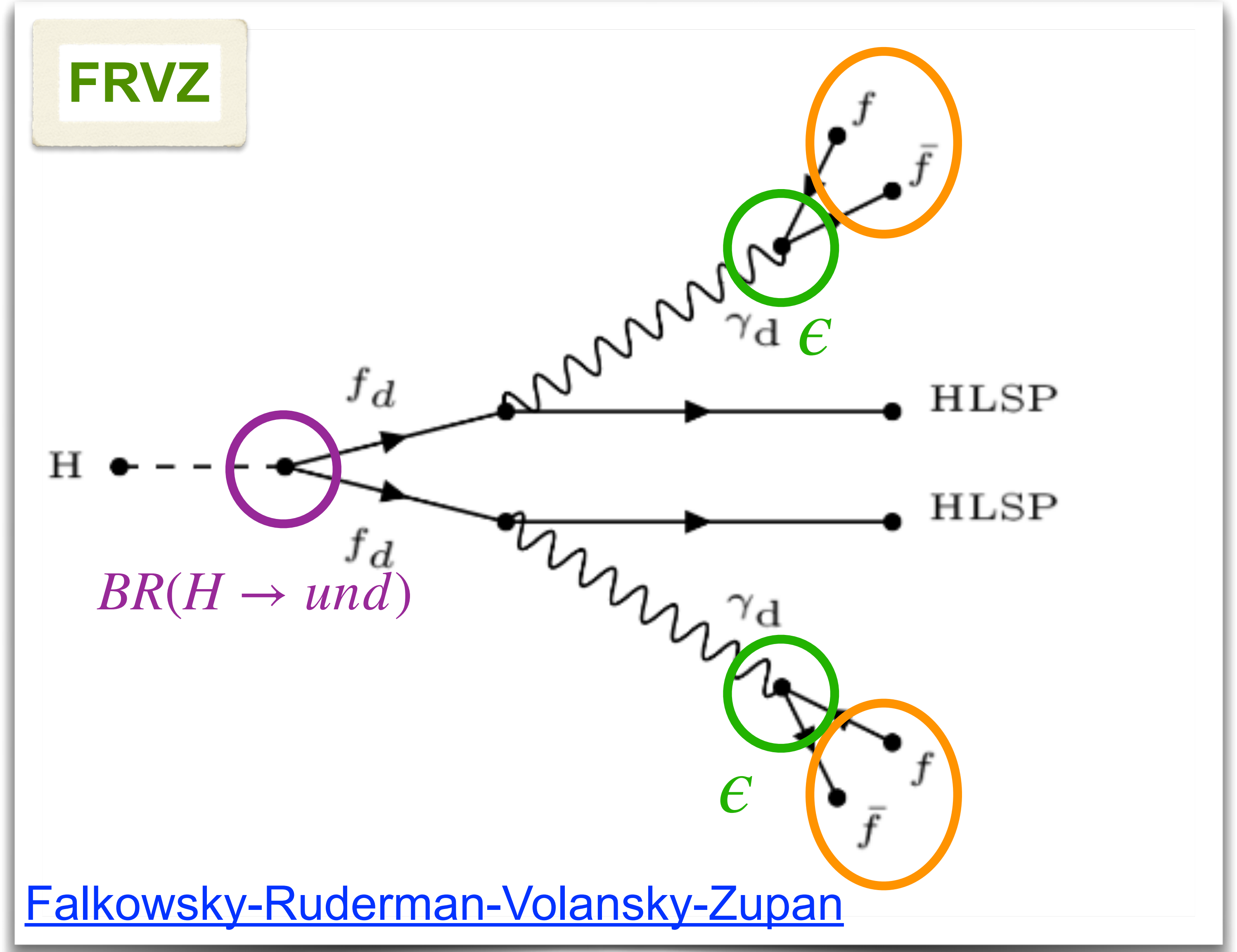


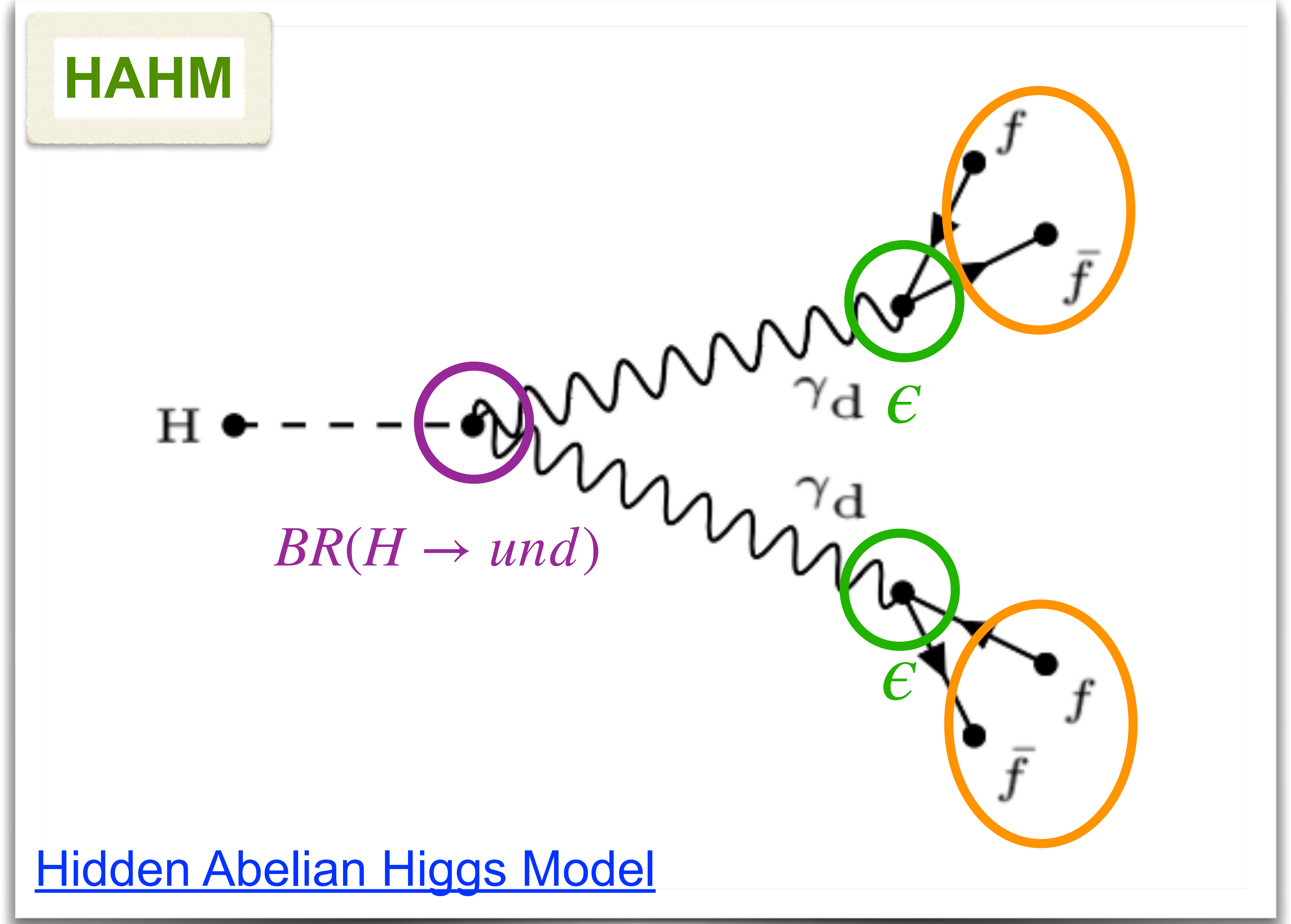


Considered only leptonic decays

$\gamma_d \to \mu^+\mu^-$ e $\gamma_d \to e^+e^-$

The decay products are extremely collimated —> **Lepton Jets (LJ)**

# Lepton Jets

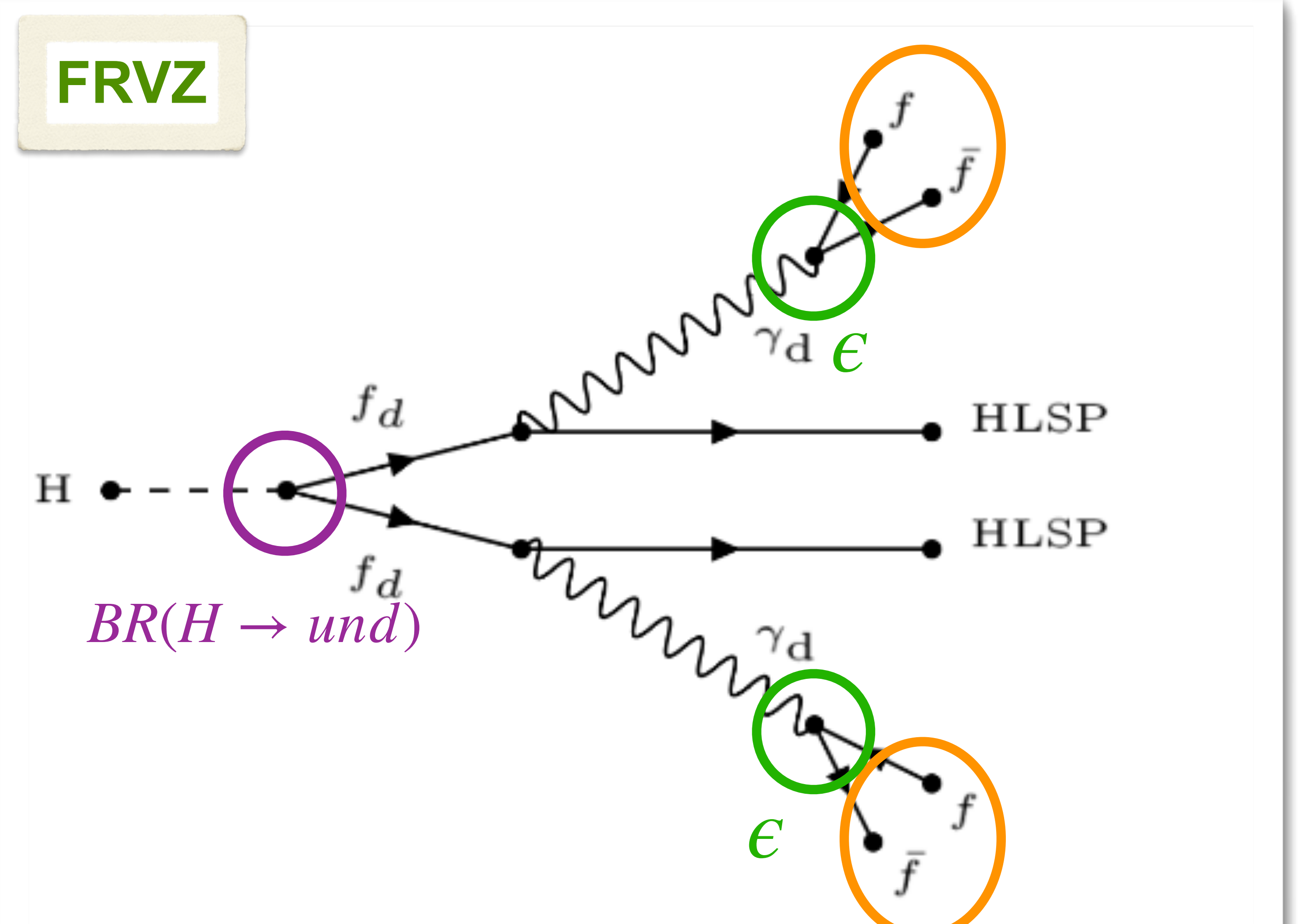


[Falkowsky-Ruderman-Volansky-Zupan]

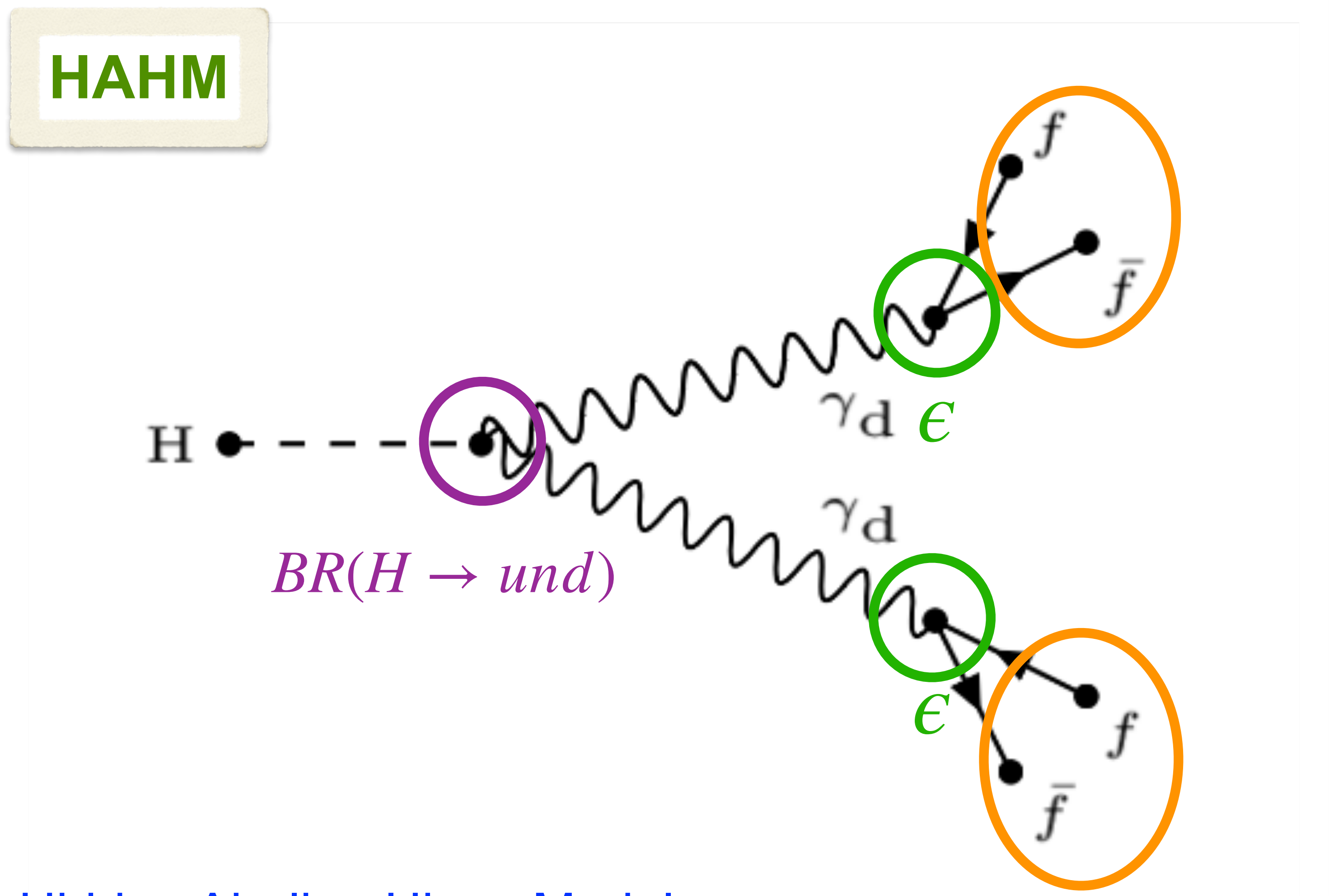


[Hidden Abelian Higgs Model]

Considered only leptonic decays

$\gamma_d \to \mu^+\mu^-$ e $\gamma_d \to e^+e^-$

The decay products are extremely collimated —> **Lepton Jets (LJ)**

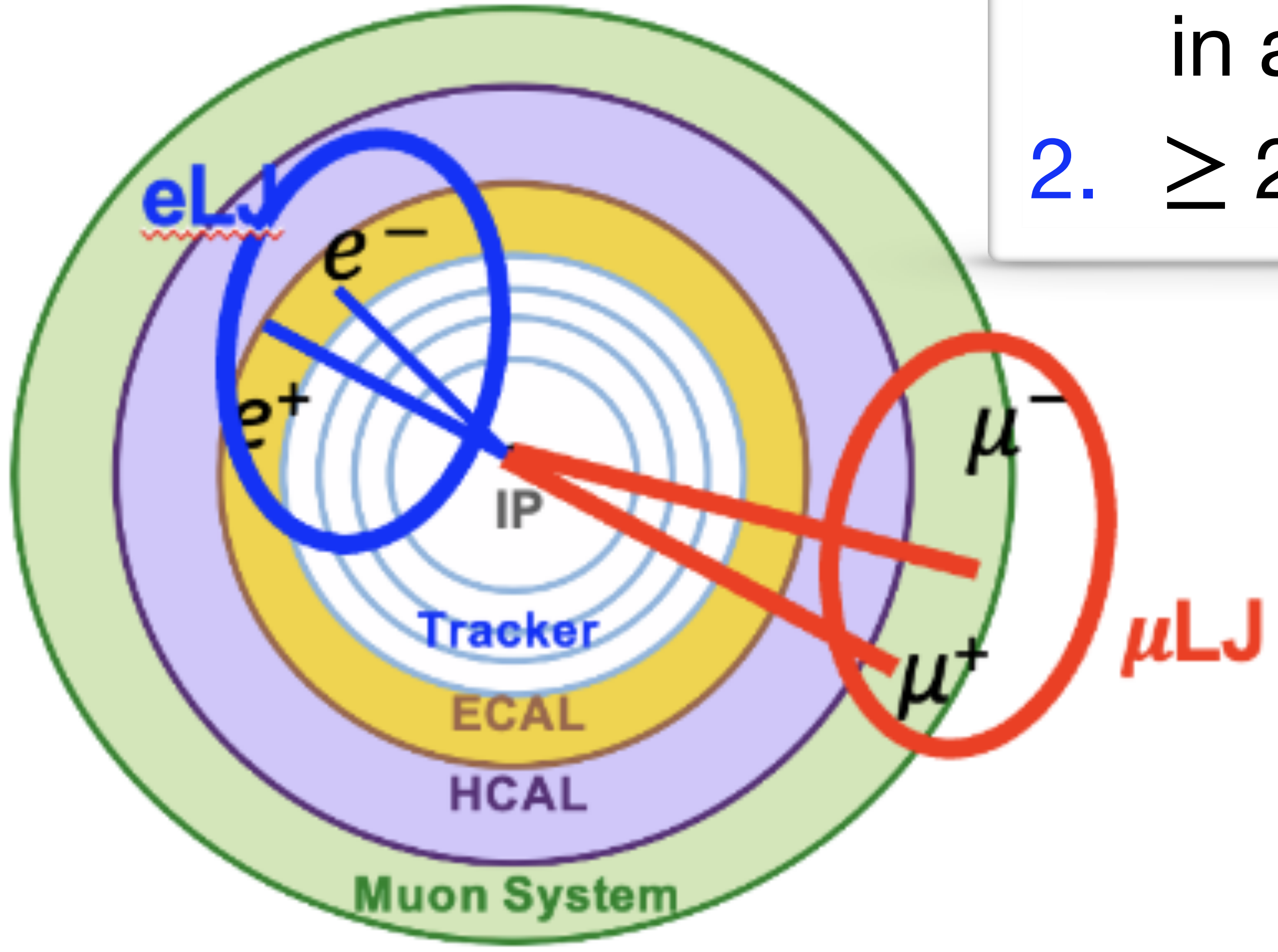


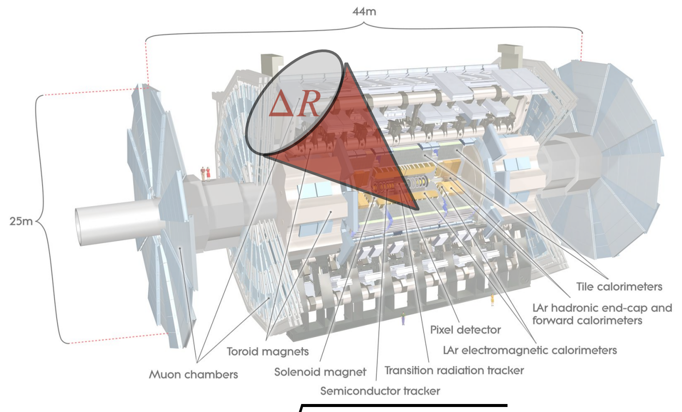


$\Delta R = \sqrt{\Delta\eta^2 + \Delta\phi^2}$

**eLJ**

1. $\geq 1$ reconstructed electron with $\geq 2$ associated tracks in a $\Delta R = 0.4$ cone
2. $\geq 2$ electrons reconstructed in a $\Delta R = 0.4$ cone

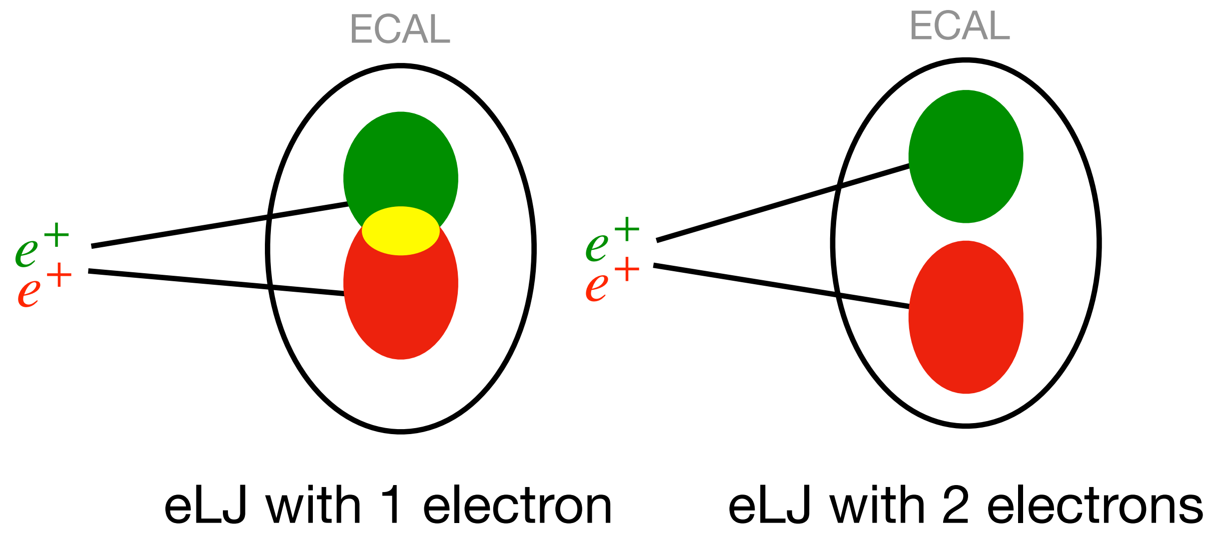


**$\mu$LJ**

$\geq 2$ muons and no electron in a $\Delta R = 0.4$ cone

# Analysis strategy

**Run-2** data-taking (2015-2018)

3 channels of study —> 3 **signal regions (SR)**
Background estimation —> 3 **control regions (CR)** —> **DATA DRIVEN**

2LJ

**Electronic channel**
2 eLJ

**Muonic channel**
2 $\mu$LJ

**Mixed channel**
1 eLJ + 1 $\mu$LJ

Background

- V + jets —> $e^+e^-$
- SM processes —> $e$ + tracks
- $\gamma^*$ —> $e^+e^-$

Resonances —> $\mu^+\mu^-$

- SM processes —> $e$ + tracks
- $\gamma^*$ —> $e^+e^-$
-Resonances —> $\mu^+\mu^-$

ABCD

Bump-hunting

Bump-hunting

$m_{\gamma_d}$ **< 240 MeV**

$m_{\gamma_d}$ **> 240 MeV**

$m_{\gamma_d}$ **> 240 MeV**

# Background estimation for $eLJ - eLJ$ channel

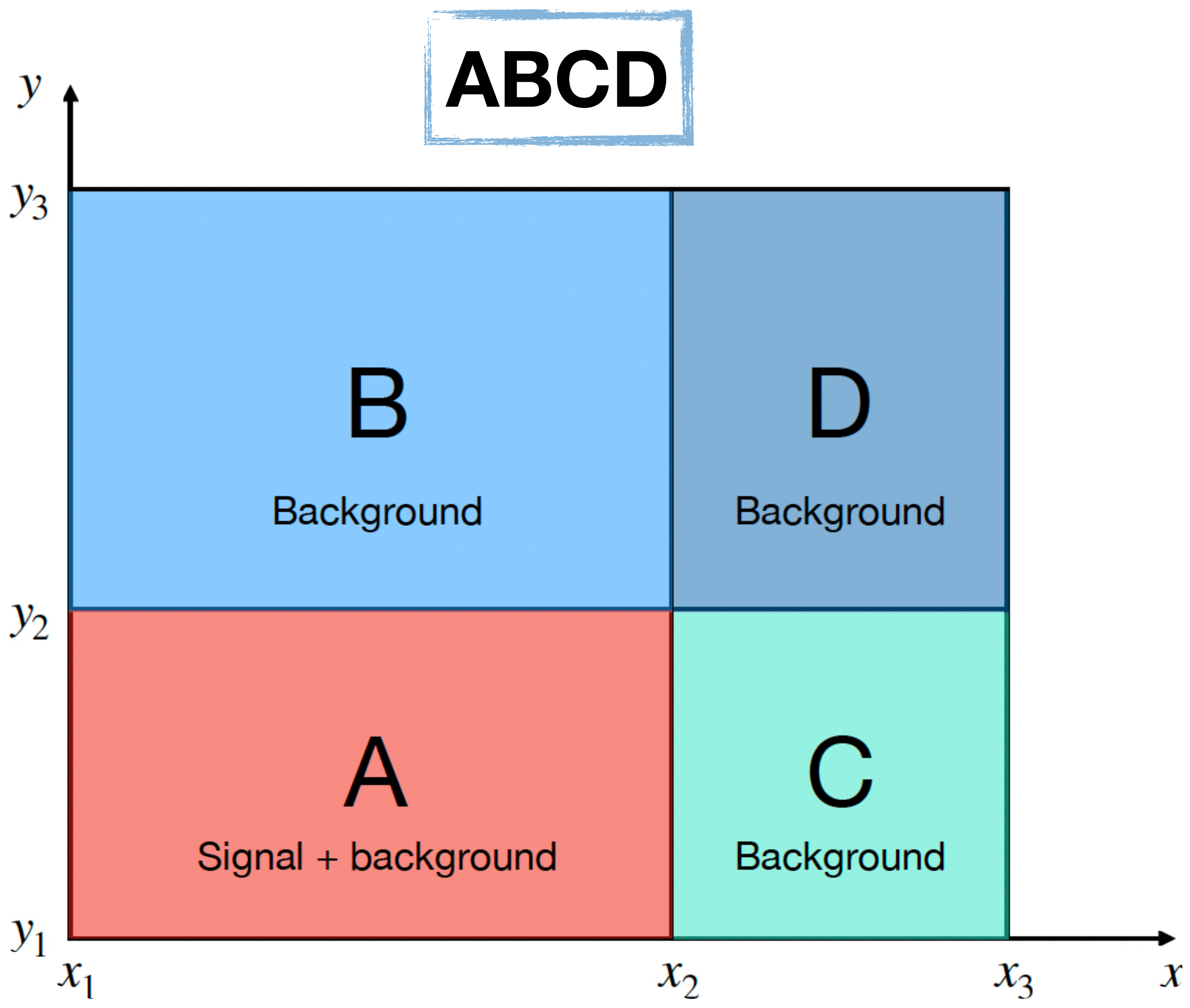


$x, y$ discriminating variables uncorrelated for the background(s)

→ defining **SR** and **CRs**

$$\rightarrow N_A = \frac{N_C}{N_D} N_B$$

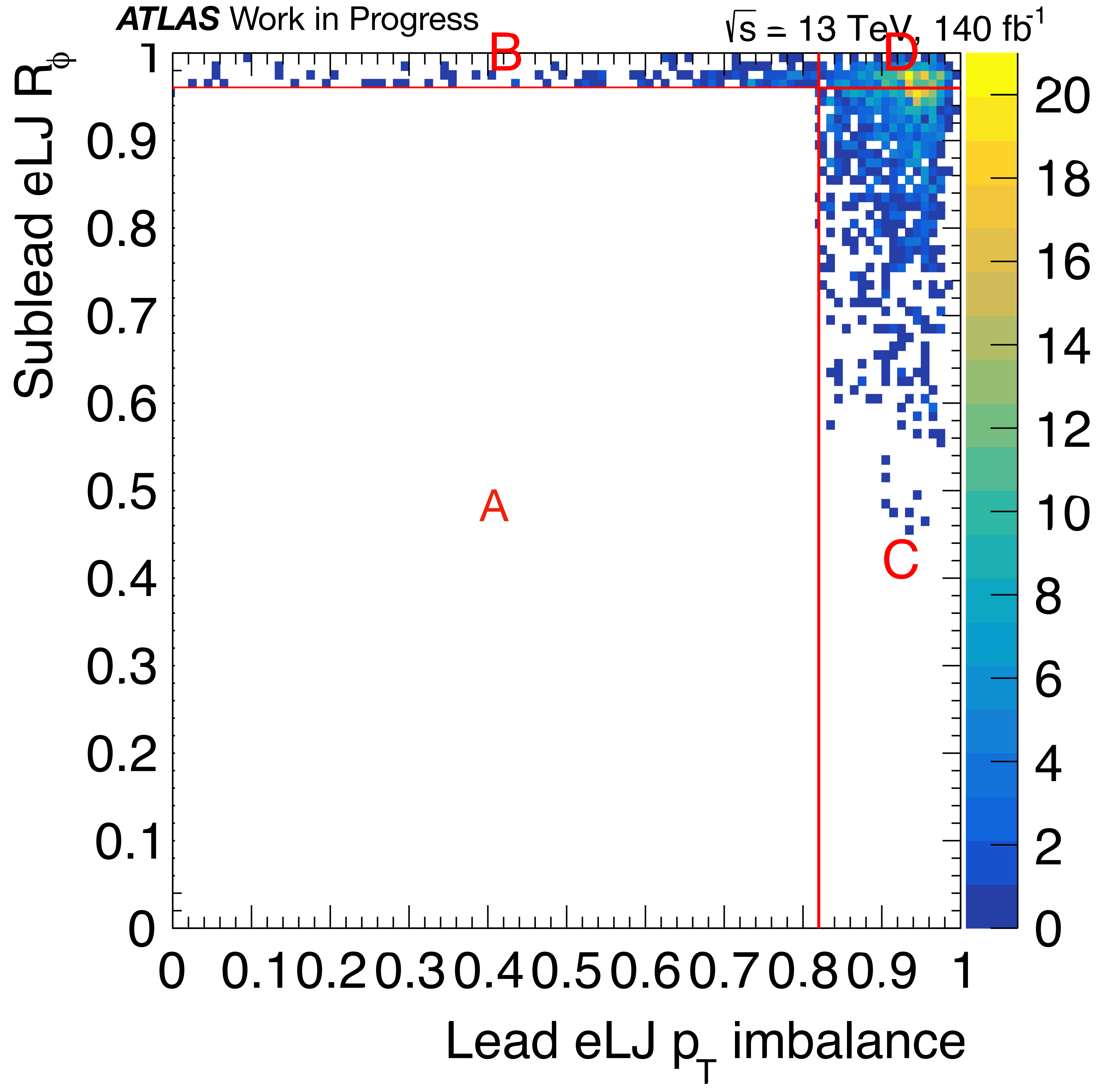


Background estimation validated in BD and DC sub-regions, and in the full ABCD plane in three additional VRs

# Background estimation for $\mu$LJ – $\mu$LJ and $\mu$LJ – $e$LJ channel

Bump hunting on $m_{\mu\mathrm{LJ}}$: looking for localised peaks (around $m_{\gamma_d}$) over a smoothly falling background

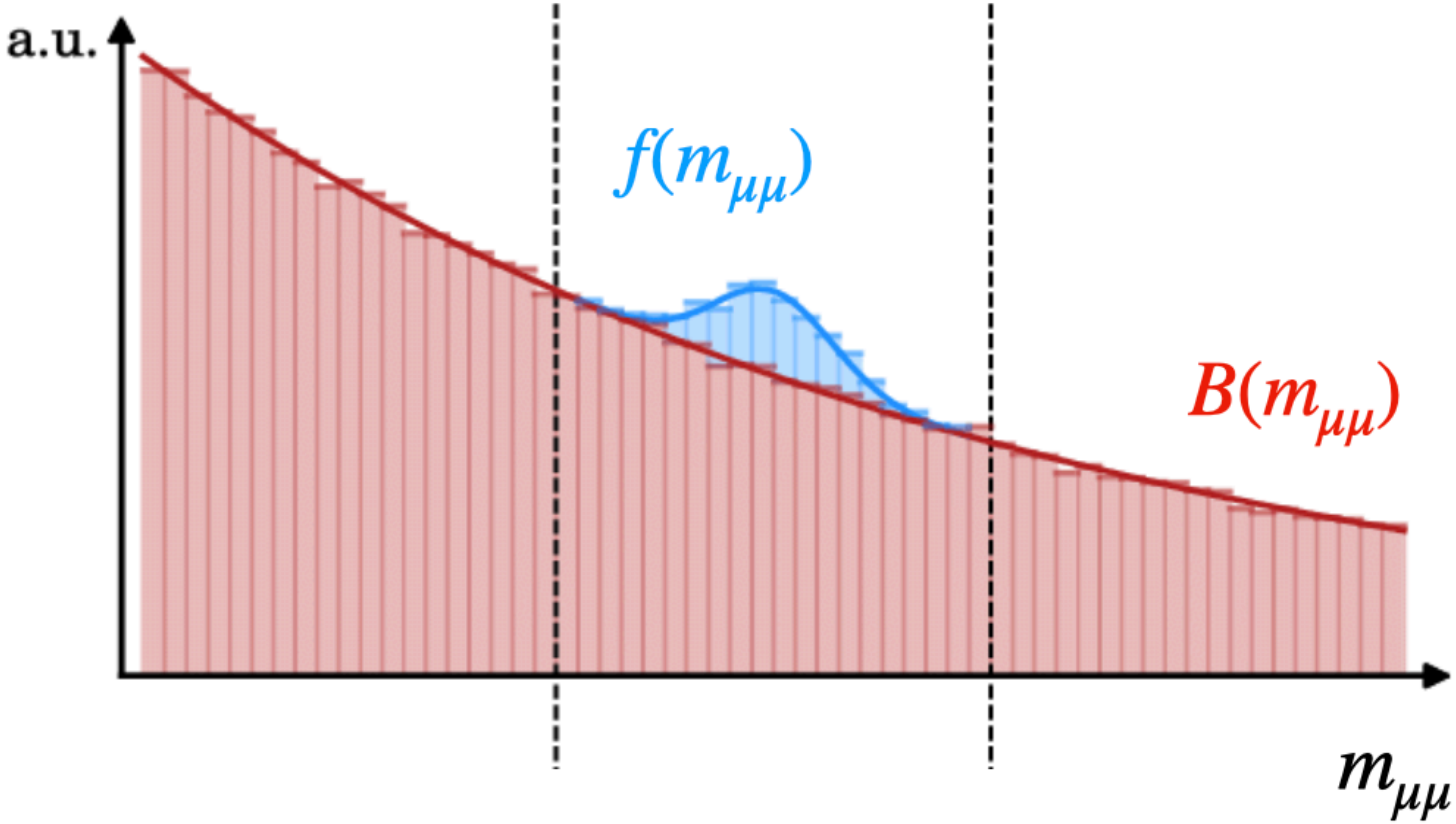


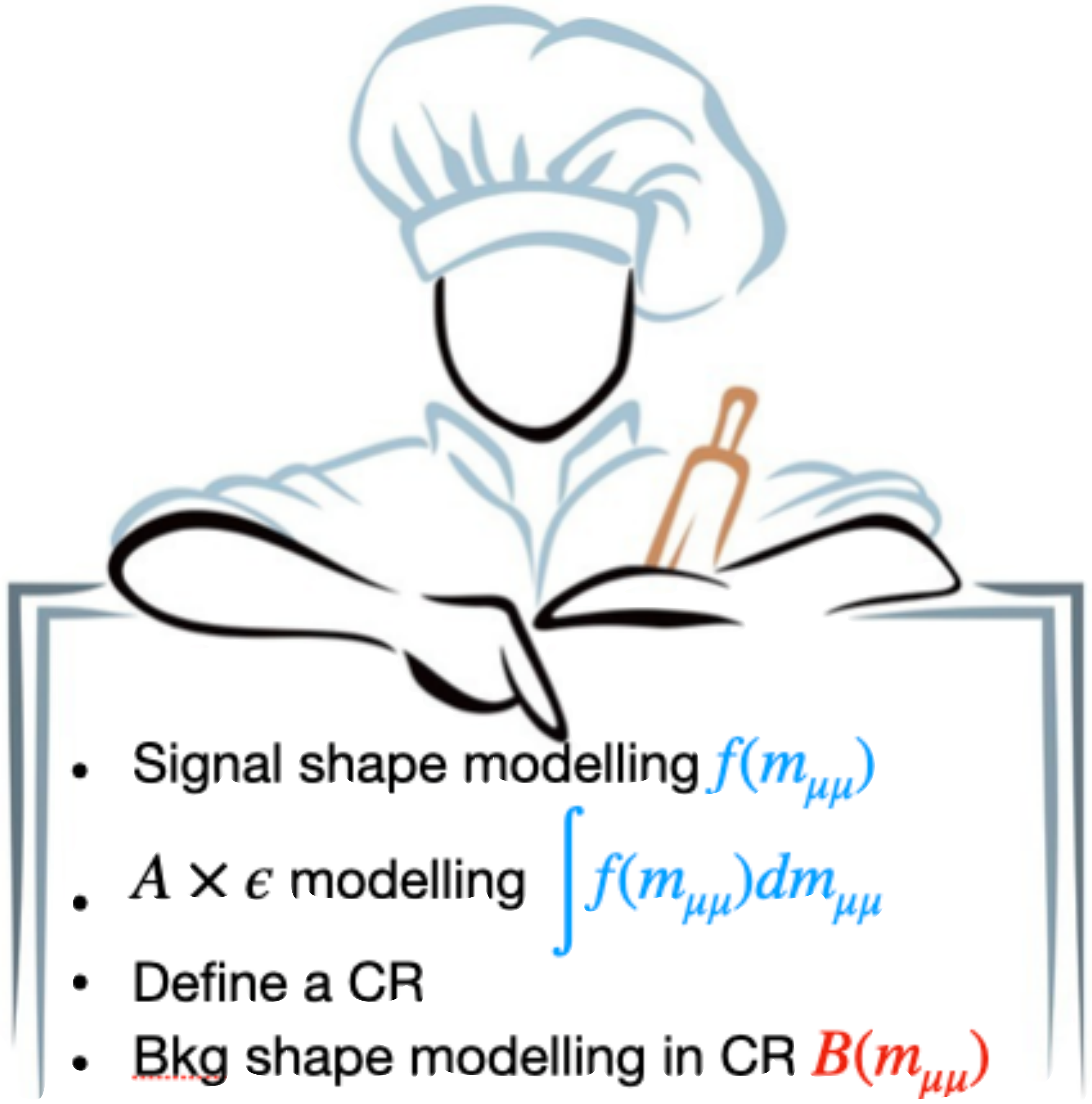

# CRs for $\mu$LJ $-$ $\mu$LJ and $\mu$LJ $-$ $e$LJ channel and background modelling

$2\mu$LJ CR:

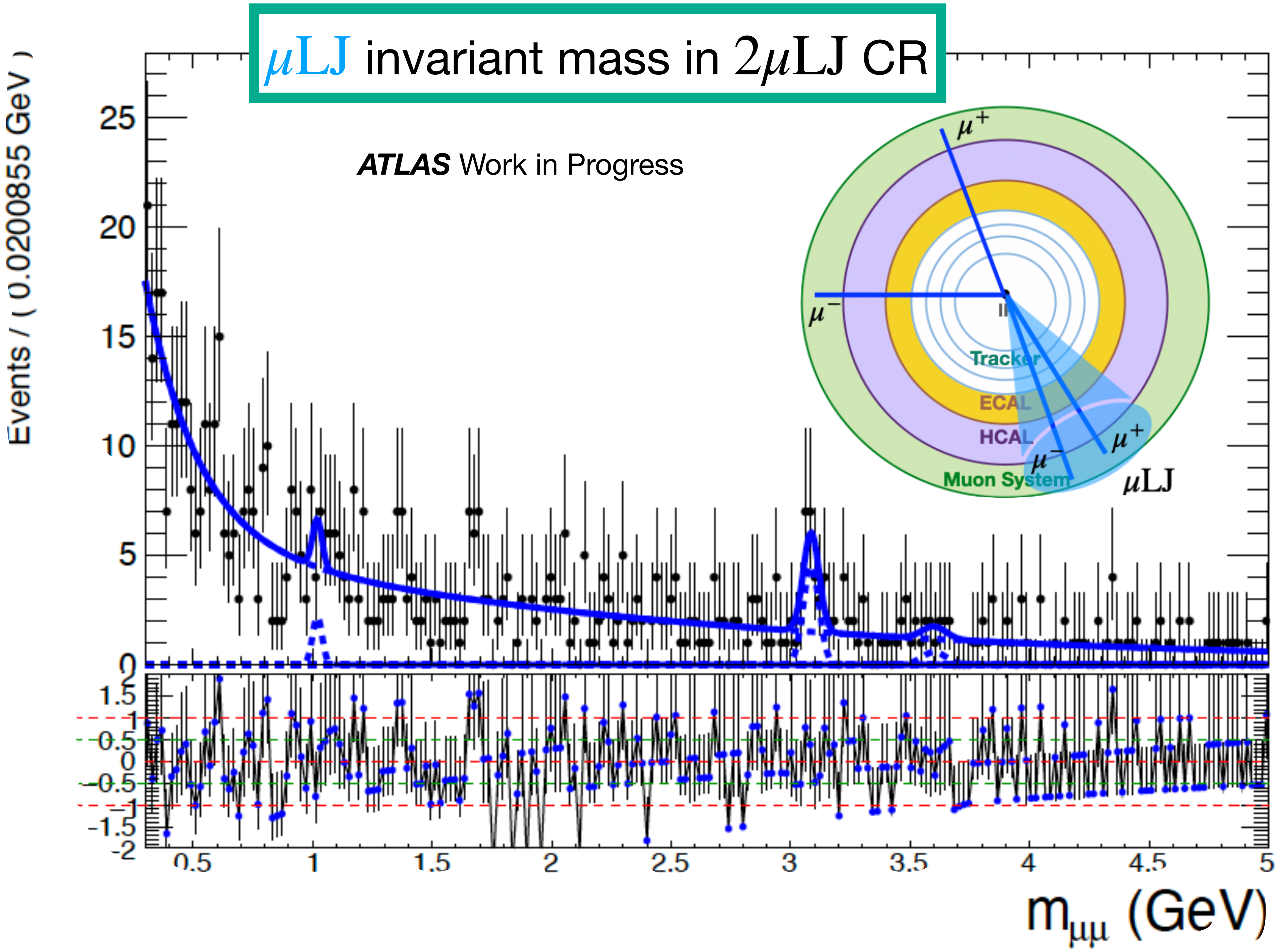


$1\mu$LJ-$1e$LJ CR:

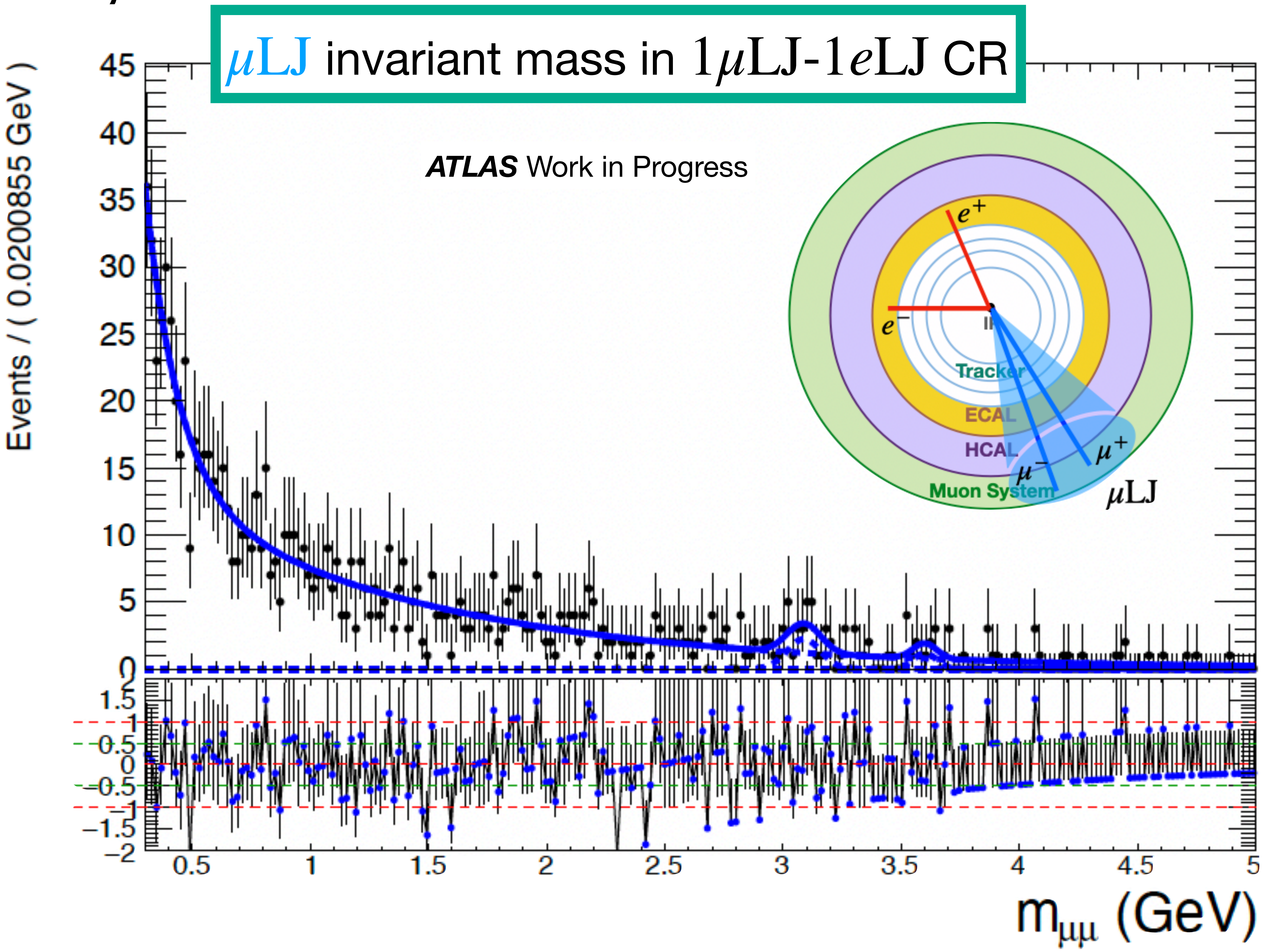


Un-binned likelihood fit using template:

$$B(m_{\mu\mu}) = \left(1 - f_{\exp} - f_{J/\psi} - f_{\phi(1020)} - f_{\psi(2S)}\right) e^{-m_{\mu\mu}/\tau_2} + f_{\exp} e^{-m_{\mu\mu}/\tau} + f_{J/\psi} e^{-\left(\frac{m_{\mu\mu}-\mu_{J/\psi}}{\sigma_{J/\psi}}\right)^2} + f_{\psi(2S)} e^{-\left(\frac{m_{\mu\mu}-\mu_{\psi(2S)}}{\sigma_{\psi(2S)}}\right)^2} + f_{\phi(1020)} e^{-\left(\frac{m_{\mu\mu}-\mu_{\phi(1020)}}{\sigma_{\phi(1020)}}\right)^2}$$

Functional form able to describe $m_{\mu\mathrm{LJ}}$ in the two orthogonal CRs

# Unblinded ABCD for $e\mathrm{LJ} - e\mathrm{LJ}$ channel

| Selection | CR B | CR C | CR D | SR expected | SR observed |
|---|---|---|---|---|---|
| *e*LJ–*e*LJ | 125 | 862 | 356 | 303 ± 33 | 351 |

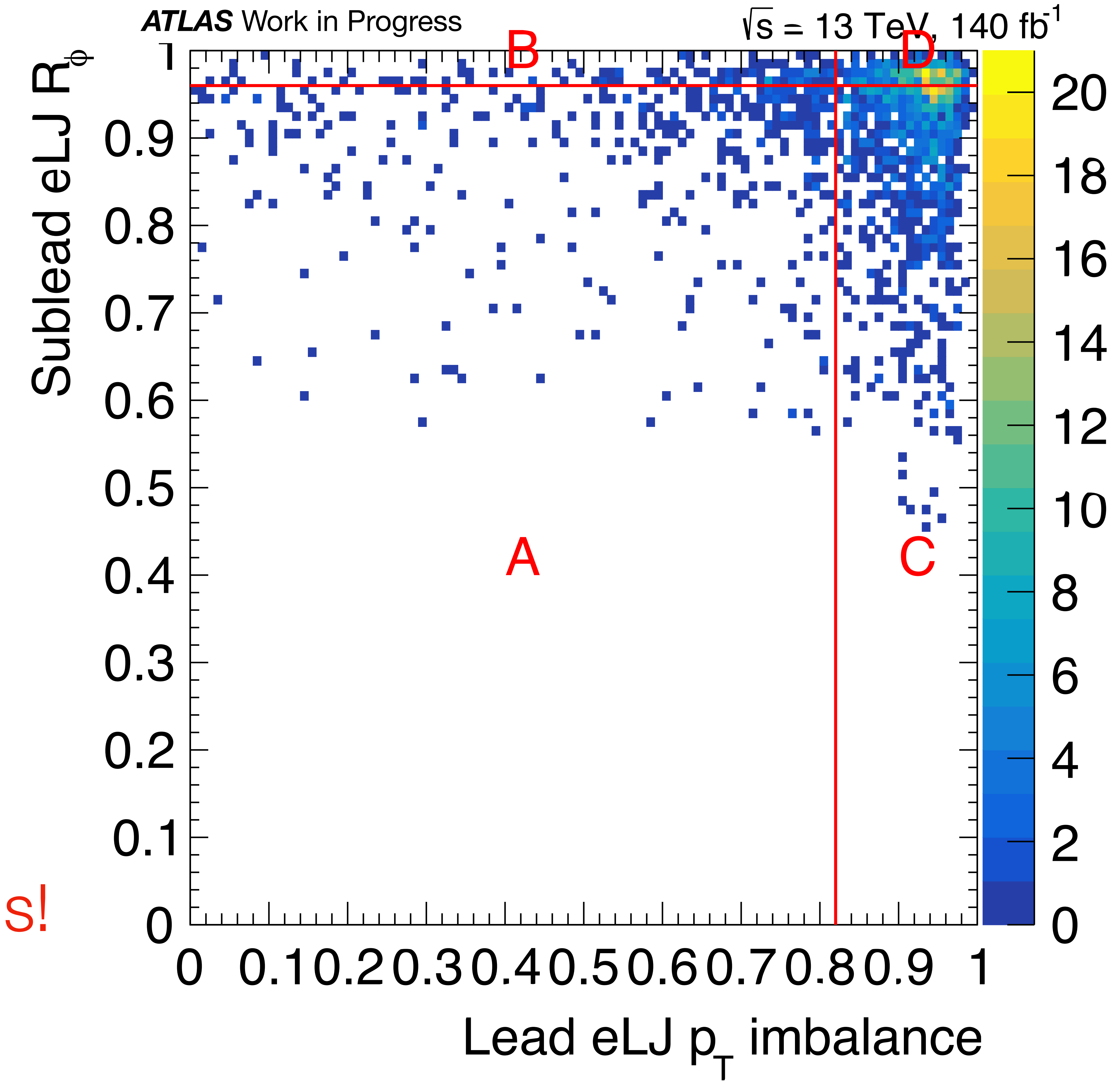


Compatible with SM expectation within $1.8\sigma$

→ constraints on free parameters of benchmark models!

# Unblinded distributions for $\mu$LJ – $\mu$LJ and $\mu$LJ – $e$LJ channel

$$B(m_{\mu\mu}) = \left(1 - f_{\exp} - f_{J/\psi} - f_{\phi(1020)} - f_{\psi(2S)}\right) e^{-m_{\mu\mu}/\tau_2} + f_{\exp} e^{-m_{\mu\mu}/\tau} +$$
$$+ f_{J/\psi} e^{-\left(\frac{m_{\mu\mu}-\mu_{J/\psi}}{\sigma_{J/\psi}}\right)^2} + f_{\psi(2S)} e^{-\left(\frac{m_{\mu\mu}-\mu_{\psi(2S)}}{\sigma_{\psi(2S)}}\right)^2} + f_{\phi(1020)} e^{-\left(\frac{m_{\mu\mu}-\mu_{\phi(1020)}}{\sigma_{\phi(1020)}}\right)^2}$$

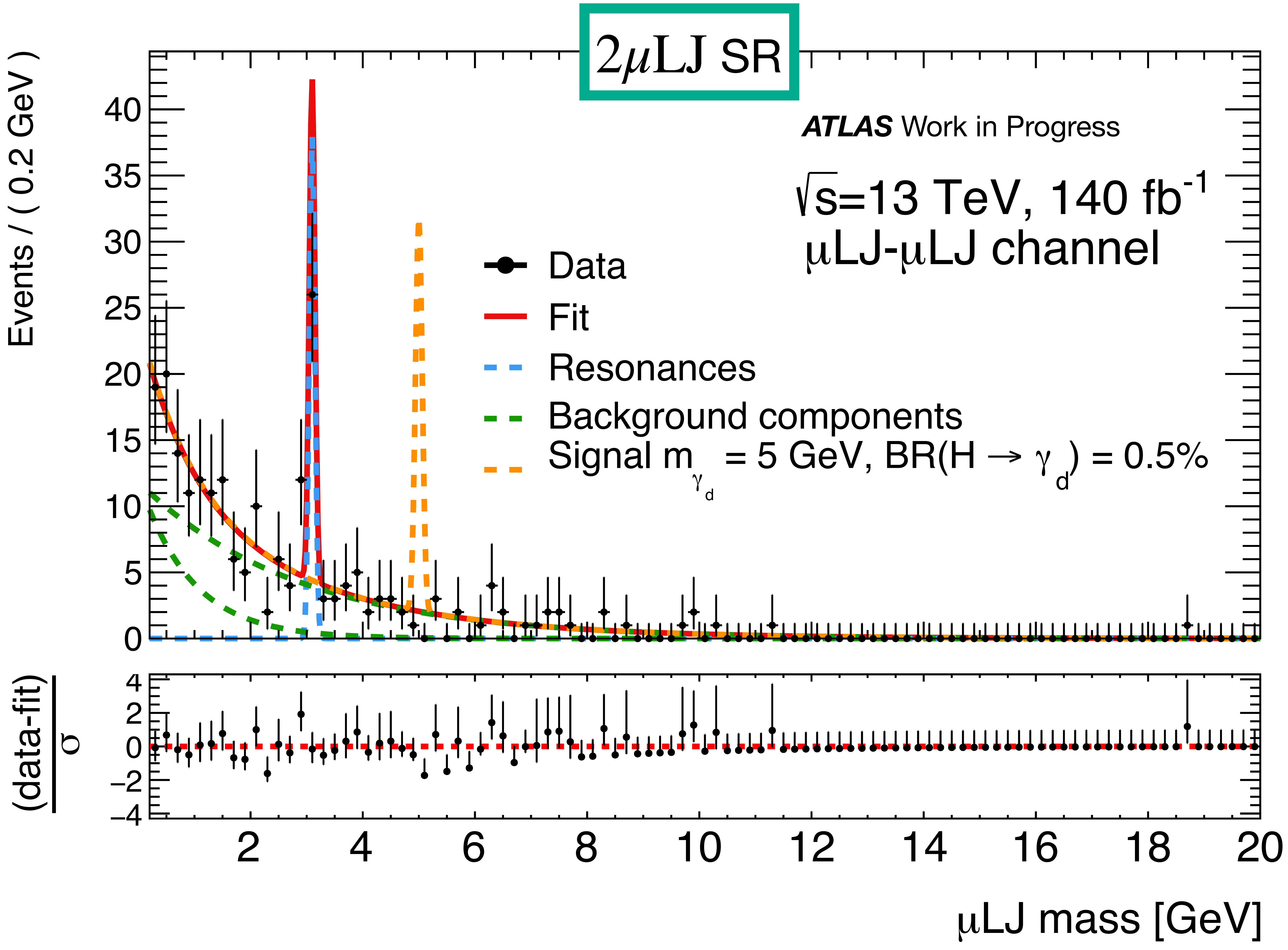


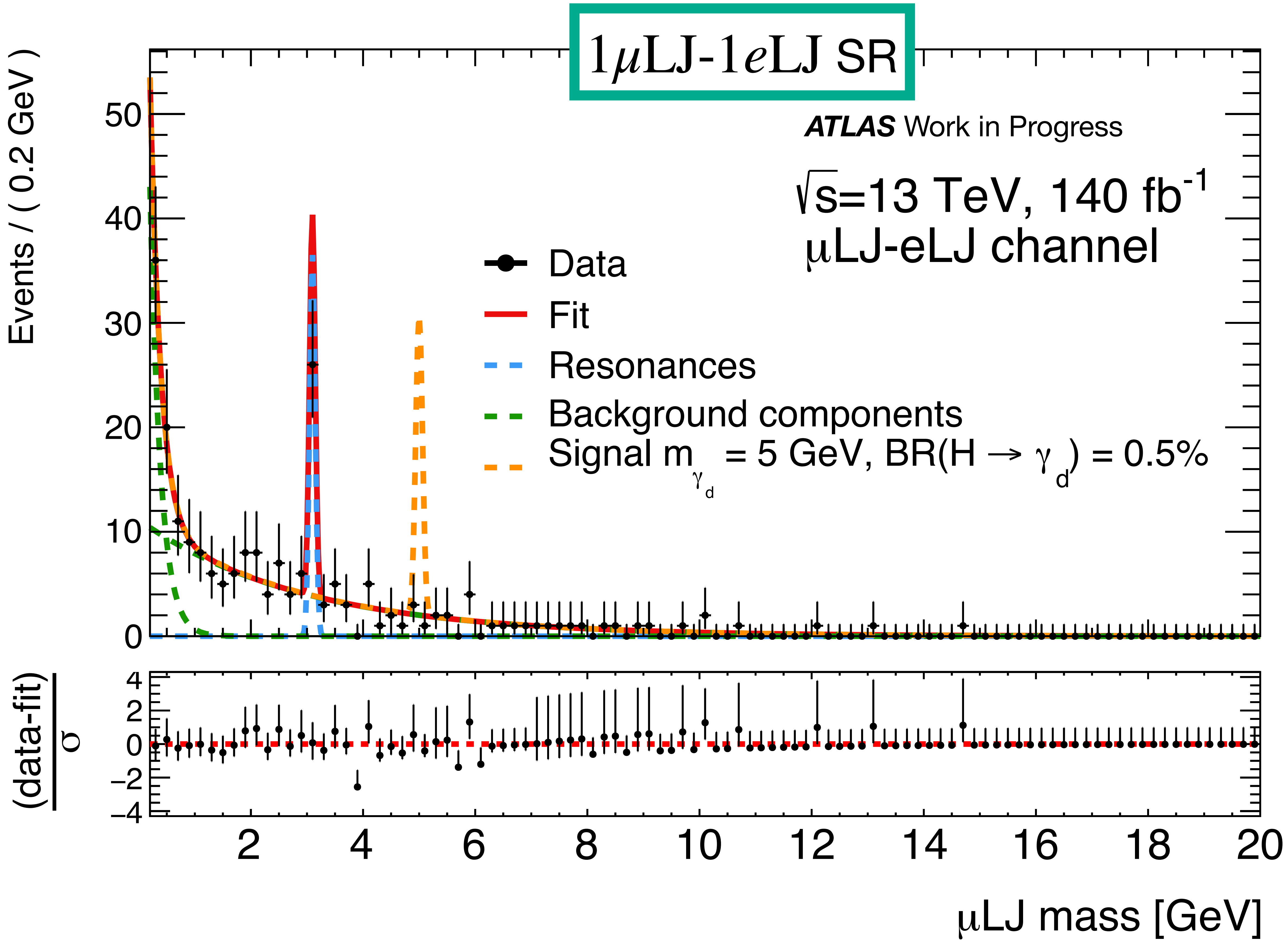


No excess over SM prediction compatible with $m_{\gamma_d}$ hypothesis
→ constraints on free parameters of benchmark models!

# Limits for all channels on $BR(H \to 2\gamma_d + X)$

- Known resonance regions ($\rho$, $\phi(1020)$, $J/\psi$) are vetoed
- $e$LJ-$e$LJ channel: $m_{\gamma_d}$ < 240 MeV — $\mu$LJ-$\mu$LJ and $\mu$LJ-$e$LJ: $m_{\gamma_d}$ > 240 MeV
- Combined fit for muonic and mixed channel

FRVZ

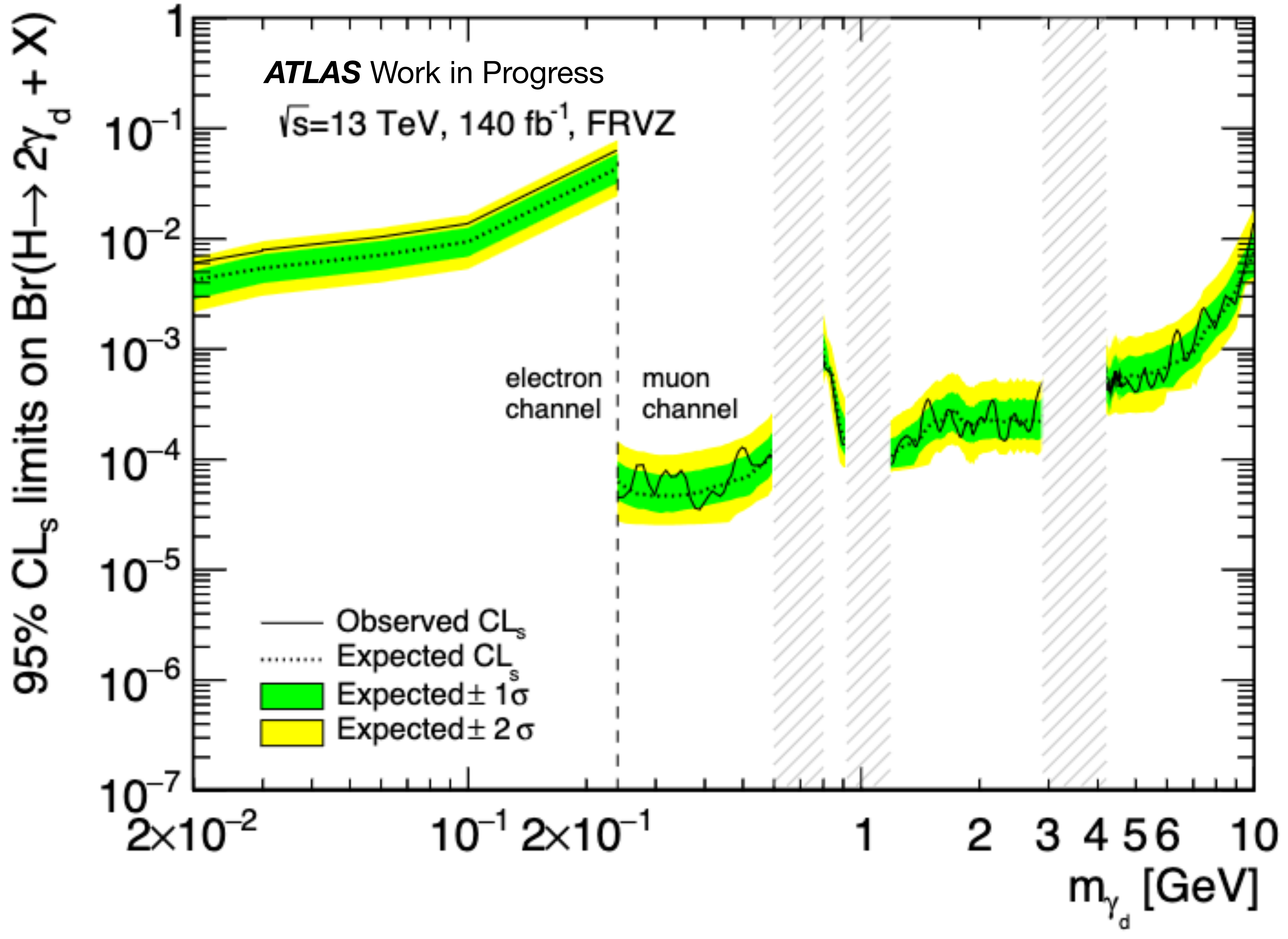


HAHM

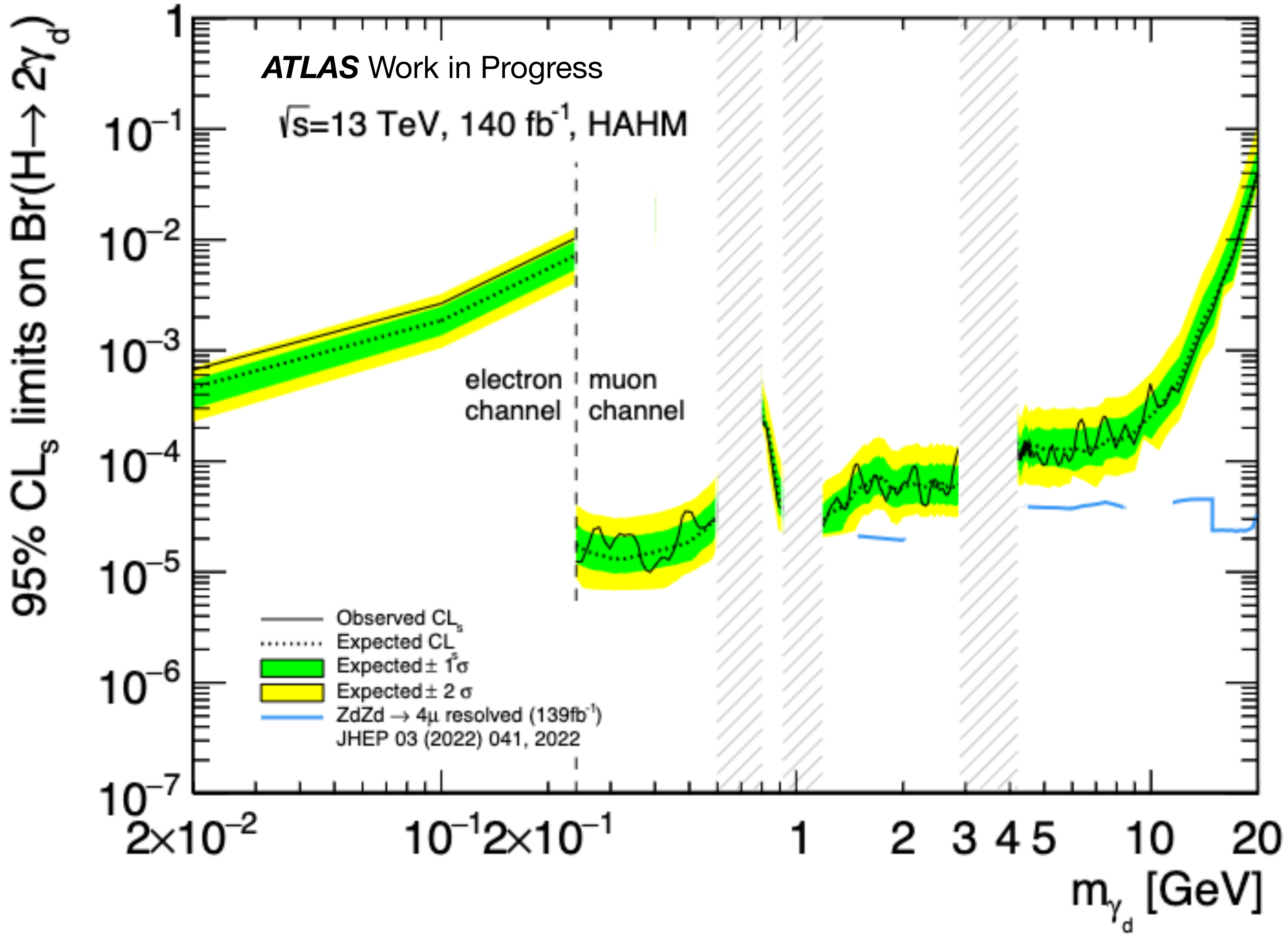

# Conclusions

Presented new result on a search for prompt Dark Photon decays with Lepton Jets

- Extension on $BR(H \to 2\gamma_d + X)$ upper limit
- First analysis in ATLAS for HAHM model

- First result with Run 2 (7x more stat compared to previous result)
- Extended mass range: from 17 MeV up to 20 GeV in Dark Photon masses.

# THANKS FOR THE ATTENTION


- A.F. et al., **Hidden Higgs Decaying to Lepton Jets** [https://arxiv.org/abs/1002.2952]
- D.C. et al., **Dark Photons with High-Energy Colliders** [https://arxiv.org/abs/1412.0018]
- P.I. et al., **Serendipity in dark photon searches** [https://arxiv.org/abs/1801.04847]
- Atlas Collaboration, **A search for prompt lepton-jets in pp collisions at $\sqrt{s} = 8$ TeV with the ATLAS detector** [https://arxiv.org/abs/1511.05542]
- R.L. Workman et al., **Review of Particle Physics** [PTEP 2022 (2022) 083C01]
- Tech. rep. Geneva: CERN, **Search for light long-lived neutral particles from Higgs boson decays via vector-boson-fusion production from pp collisions at $\sqrt{s} = 13$ TeV with the ATLAS detector** [https://cds.cern.ch/record/2870215]
- A. L. Read: **Presentation of search results: the CLs technique** [https://iopscience.iop.org/article/10.1088/0954-3899/28/10/313]
- G. Cowan, K. Cranmer, E. Gross, O. Vitells: **Asymptotic formulae for likelihood-based tests of new physics** [Eur. Phys. J. C **71** (2011) 1554]

# Backup

# Comparison with Run-1 search

FRVZ model excluded with a smaller $BR(H \rightarrow 2\gamma_d + X)$ wrt Run-1 search (e.g. for $m_{\gamma_d} = 0.4\mathrm{MeV}$ 100 times smaller!)

In the FRVZ model, $m_{\gamma_d} < 0.2\,\mathrm{GeV}$ and $m_{\gamma_d} \in [2,10]\,\mathrm{GeV}$ probed for the first time using the pLJ signature, excluding
$BR(H \rightarrow 2\gamma_d + X) \in [0.4\,\%\,,6\%]$ and
$BR(H \rightarrow 2\gamma_d + X) \in [0.005\,\%\,,1\%]$

HAHM model probed for the first time using the pLJ signature, excluding for $m_{\gamma_d} < 0.4\,\mathrm{GeV}$ $BR(H \rightarrow 2\gamma_d + X) \in [0.05\,\%\,,2\%]$ and for $m_{\gamma_d} \in [0.4,10]\,\mathrm{GeV}$
$BR(H \rightarrow 2\gamma_d + X) \in [0.0001\,\%\,,0.002\%]$!

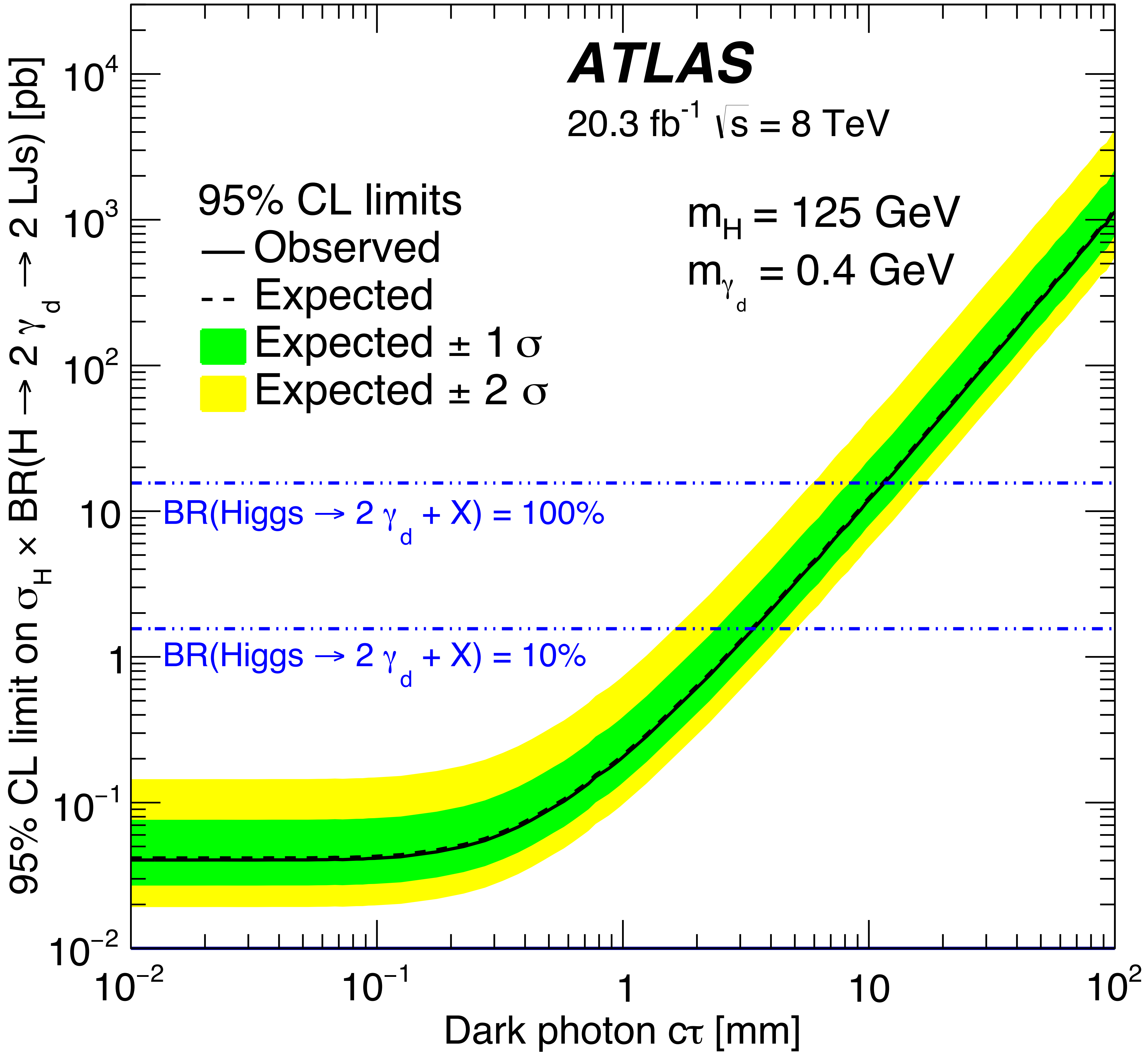

# MC

FRVZ

| $m_H$ [GeV] | number of $\gamma_D$ | $m_{\gamma_D}$ [GeV] | $m_{HLSP}$ [GeV] | $m_{f_d}$ [GeV] |
|---|---|---|---|---|
| 125 | 2 | 0.017 | 2 | 5 |
| 125 | 2 | 0.03 | 2 | 5 |
| 125 | 2 | 0.06 | 2 | 5 |
| 125 | 2 | 0.1 | 2 | 5 |
| 125 | 2 | 0.24 | 2 | 5 |
| 125 | 2 | 0.4 | 2 | 5 |
| 125 | 2 | 0.9 | 2 | 5 |
| 125 | 2 | 2 | 2 | 10 |
| 125 | 2 | 6 | 4 | 25 |
| 125 | 2 | 10 | 6 | 35 |
| 125 | 2 | 15 | 10 | 45 |
| 125 | 2 | 25 | 10 | 45 |
| 125 | 2 | 40 | 7 | 55 |

HAHM

| $m_H$ [GeV] | number of $\gamma_D$ | $m_{\gamma_D}$ [GeV] |
|---|---|---|
| 125 | 2 | 0.017 |
| 125 | 2 | 0.01 |
| 125 | 2 | 0.4 |
| 125 | 2 | 2 |
| 125 | 2 | 10 |
| 125 | 2 | 15 |
| 125 | 2 | 25 |
| 125 | 2 | 40 |

ATLAS is a multipurpose particle detector used at the Large Hadron Collider (LHC) at CERN

During Run 2 of LHC (2015-2018) ATLAS collected p-p collisions corresponding to an energy in the center of mass equal to $\sqrt{s}$= 13 TeV.

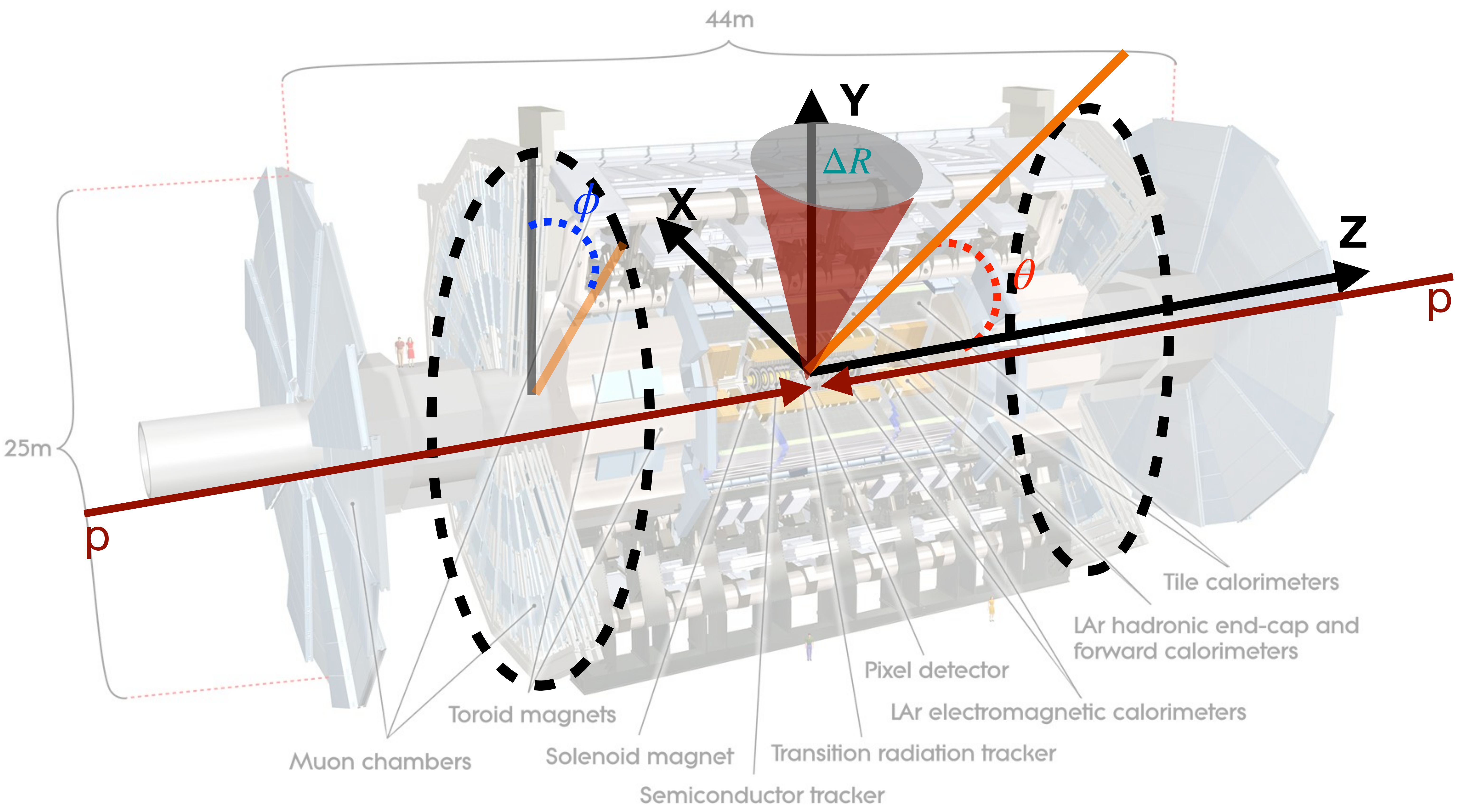


Pseudorapidity

$$\eta = -\ln(\tan\frac{\theta}{2})$$

$$\Delta R = \sqrt{\Delta\eta^2 + \Delta\phi^2}$$

$$p_{\mathrm{T}} = \sqrt{p_x^2 + p_y^2}$$

# ATLAS

ATLAS is a multipurpose particle detector used at the Large Hadron Collider (LHC) at CERN
During Run 2 of LHC (2015-2018) ATLAS collected p-p collisions corresponding to an energy in the center of mass equal to $\sqrt{s}$= 13 TeV.

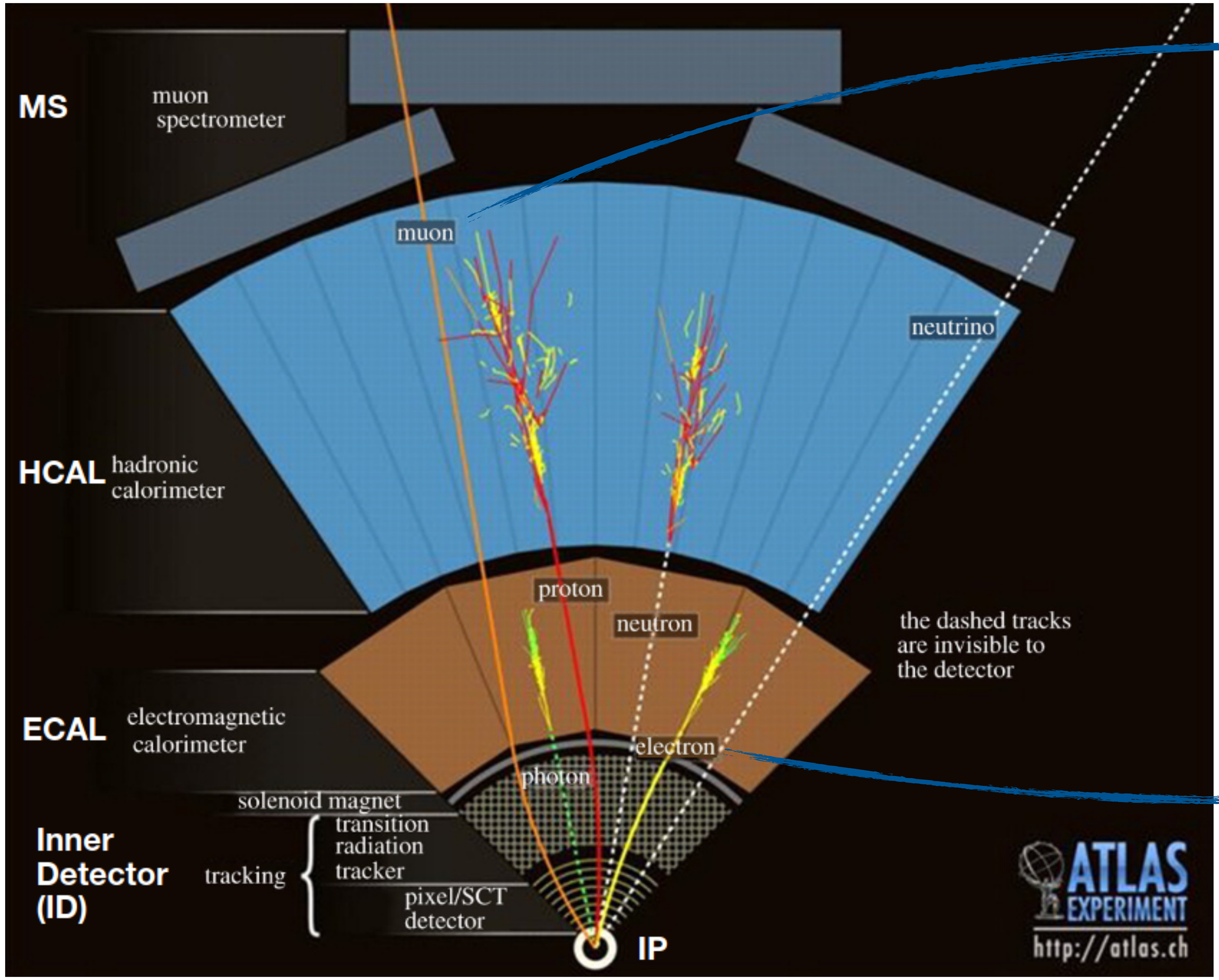


Muons: ID + MS

Electrons: ID + ECAL

# FRVZ and HAHM

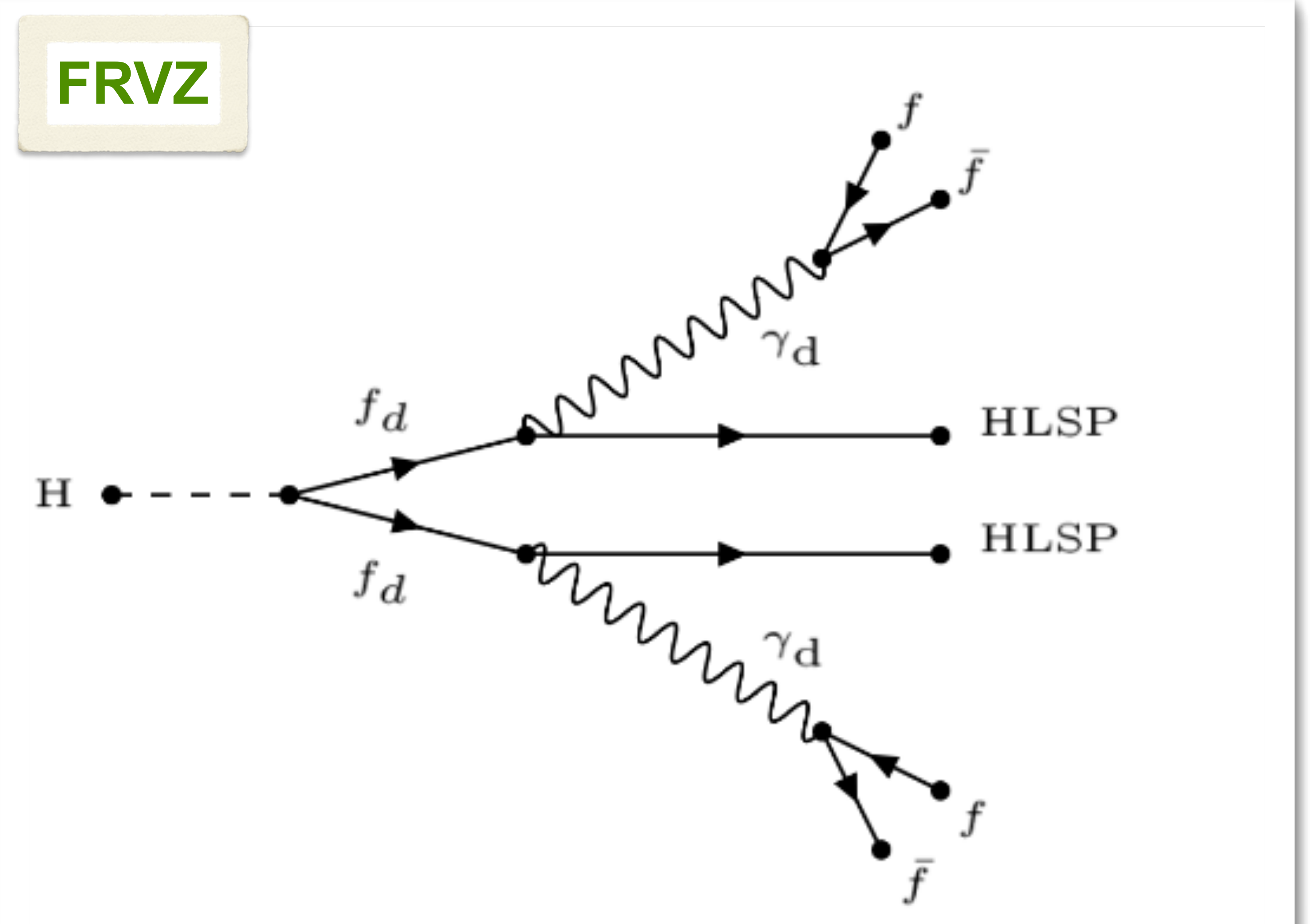


[Falkowsky-Ruderman-Volansky-Zupan]

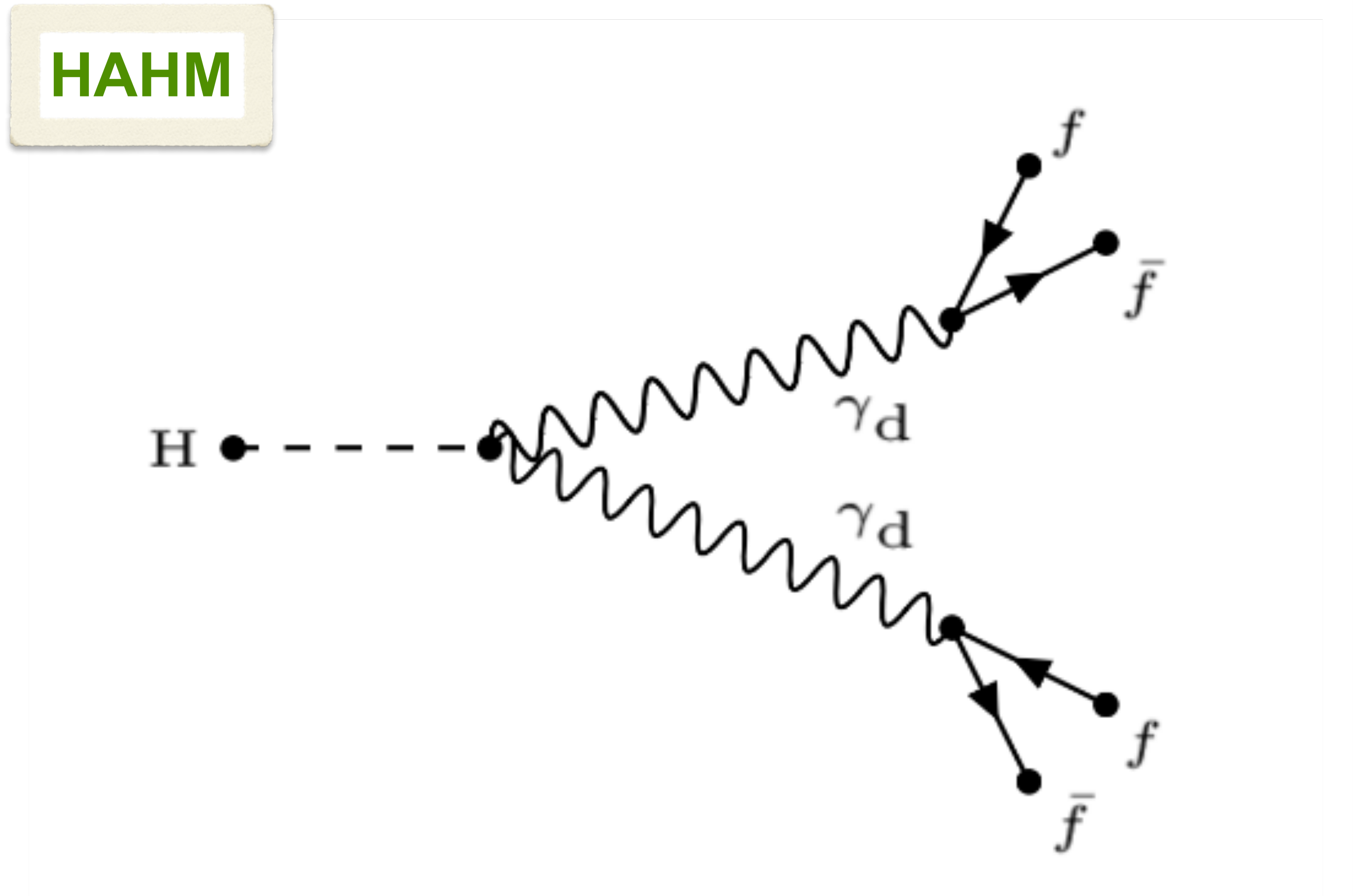


[Hidden Abelian Higgs Model]

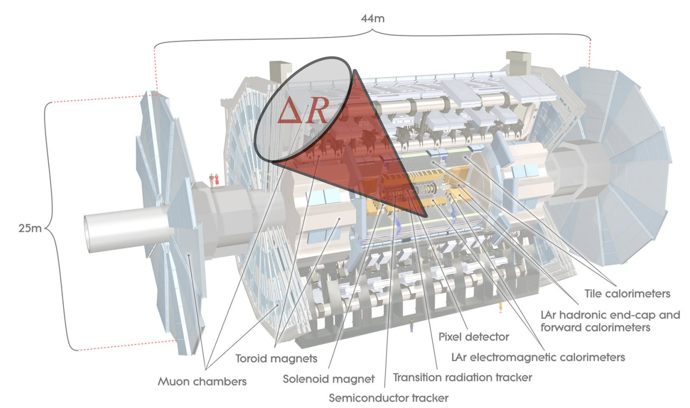


$\Delta R = \sqrt{\Delta\eta^2 + \Delta\phi^2}$

In HAHM $\gamma_d$ are more *boosted* with respect to FRVZ model → decay products are more collimated → in HAHM more signal efficiency!

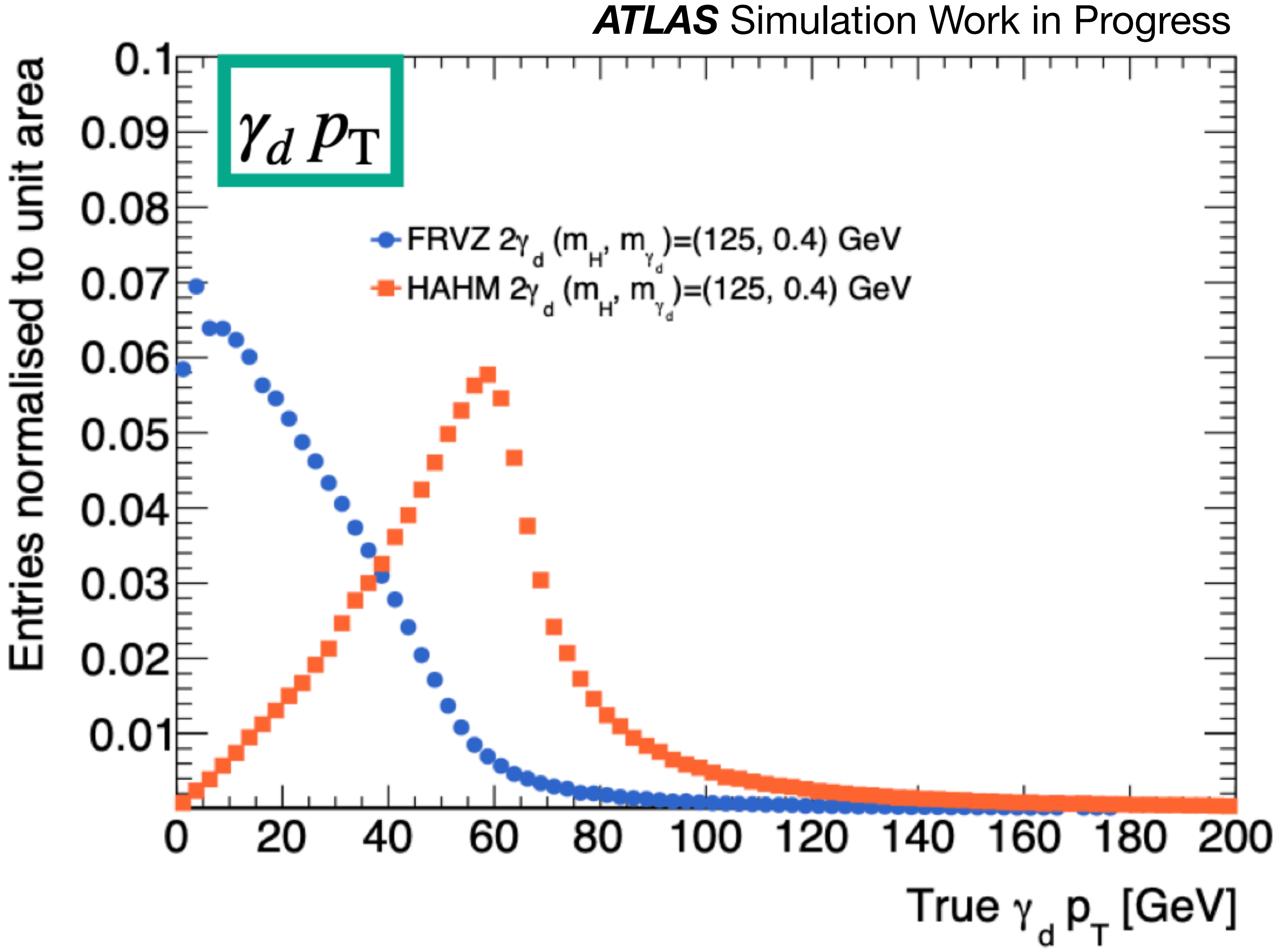


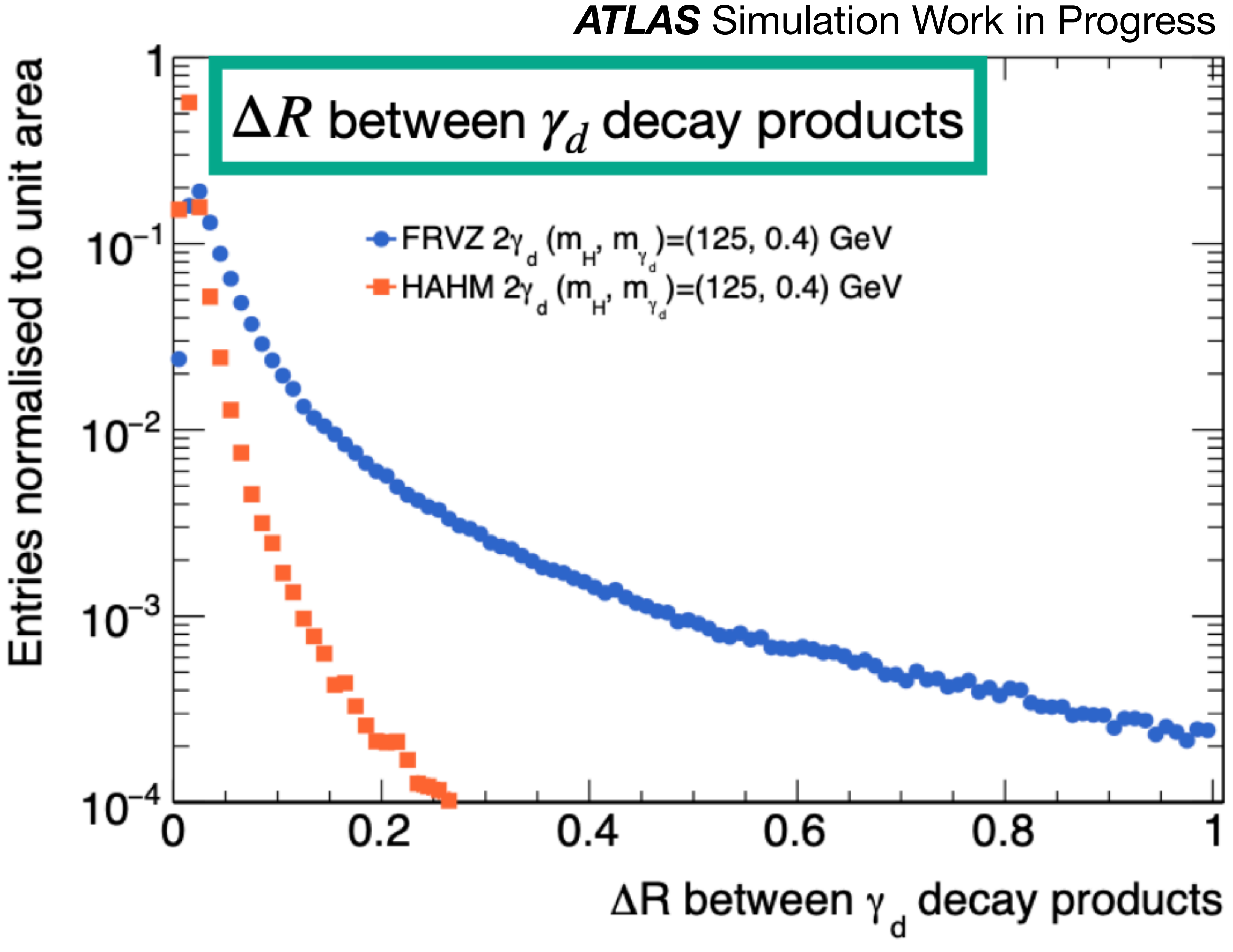

# Reconstruction efficiency $\mu$LJ

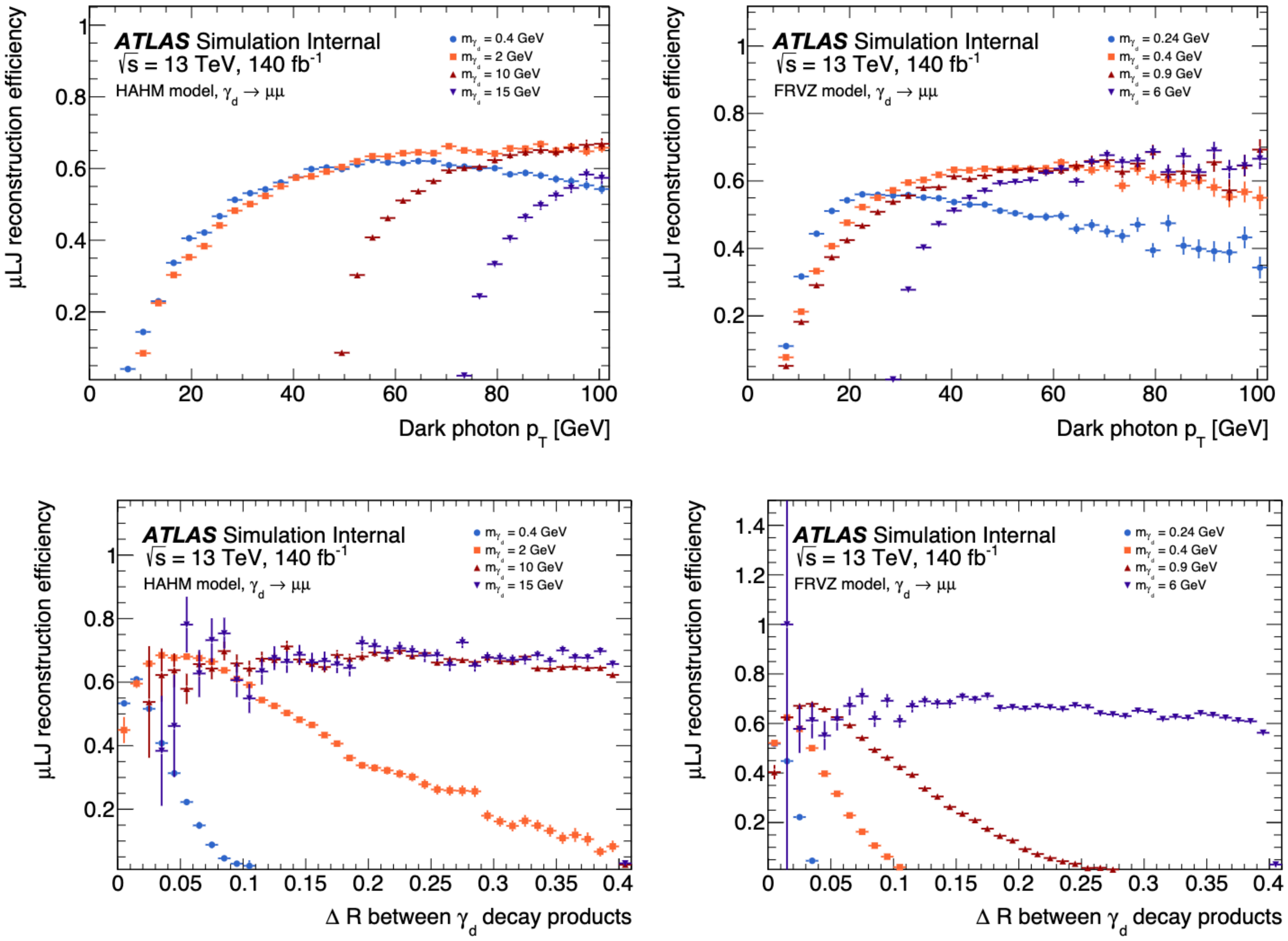

# Reconstruction efficiency eLJ

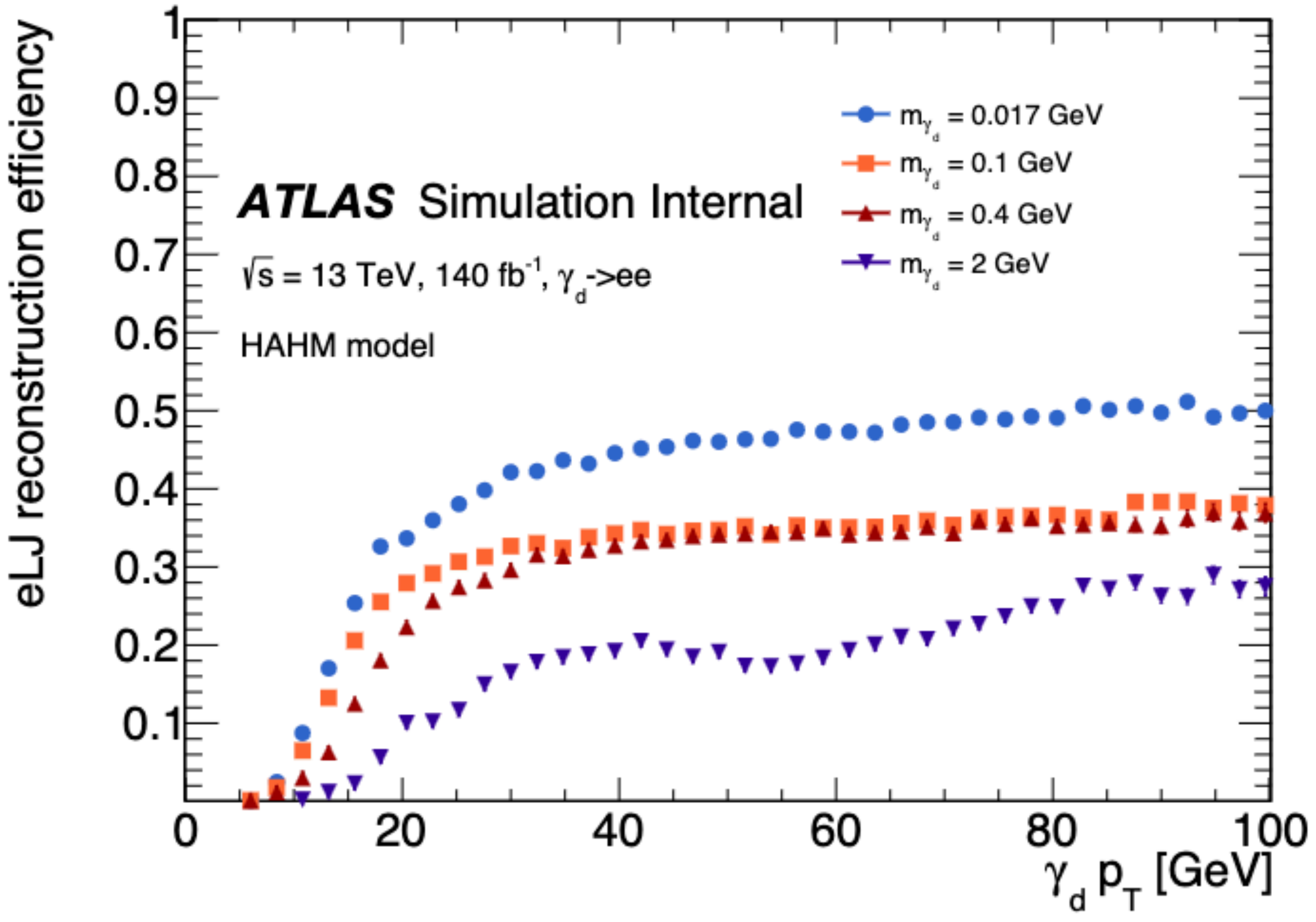


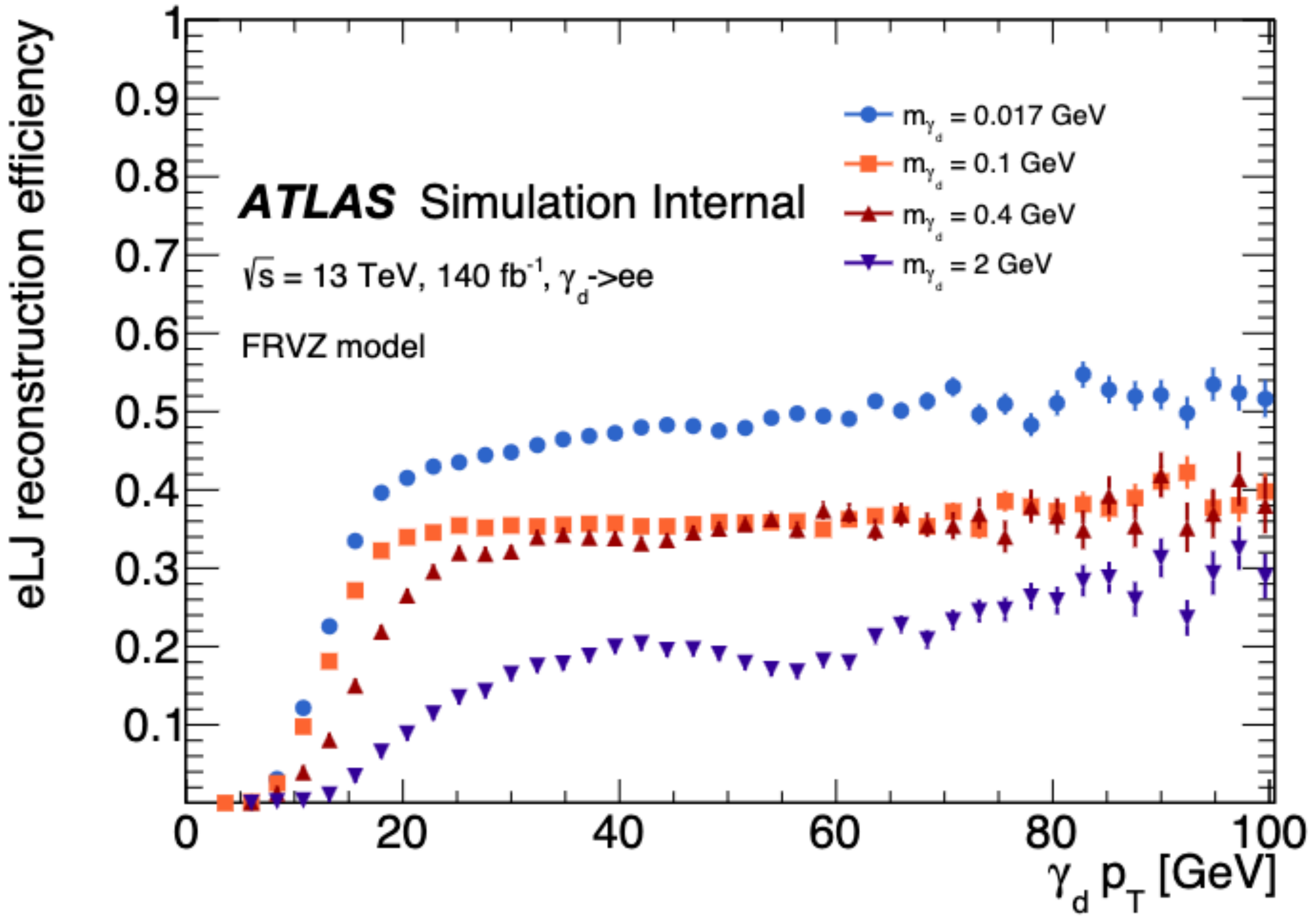


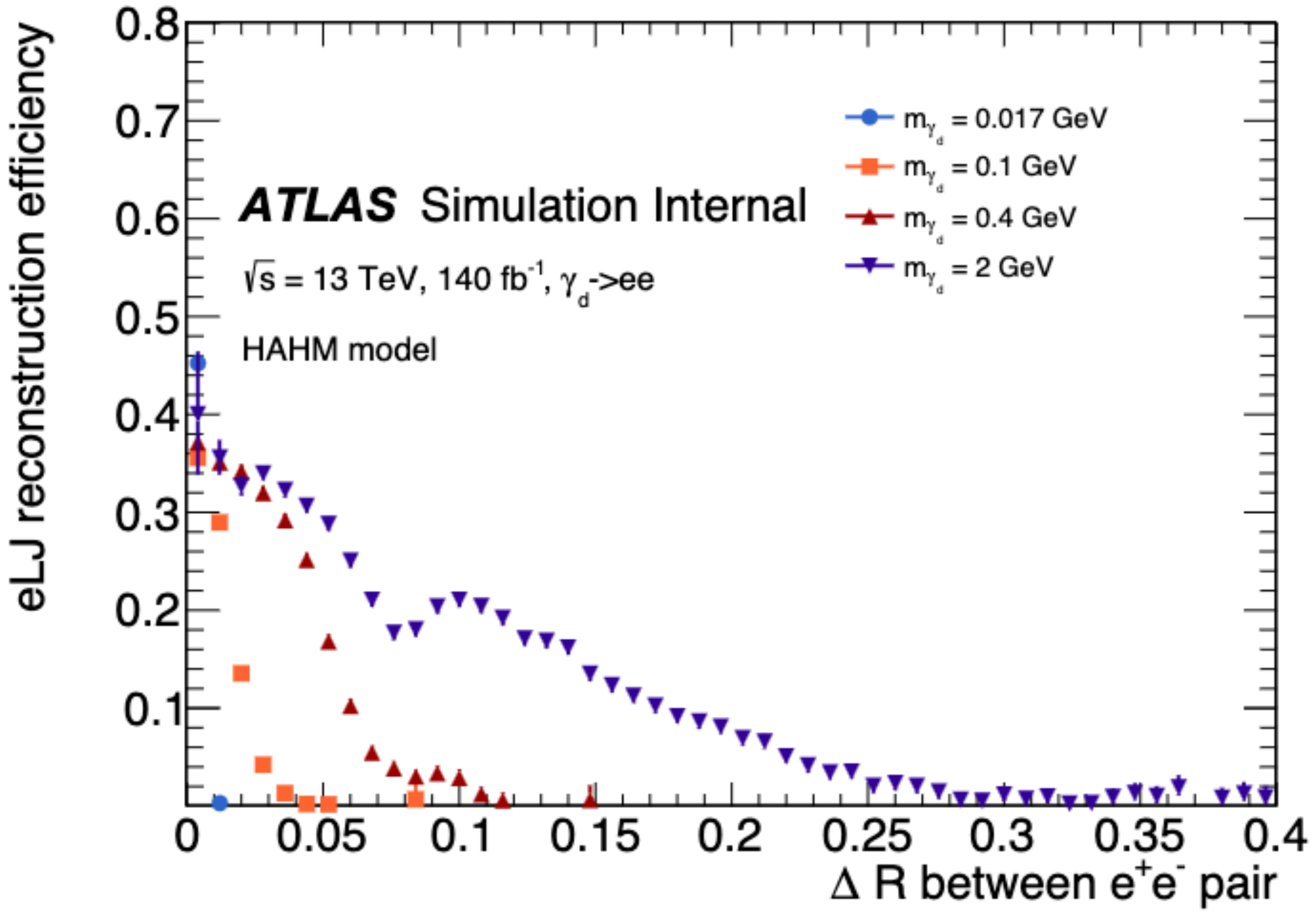


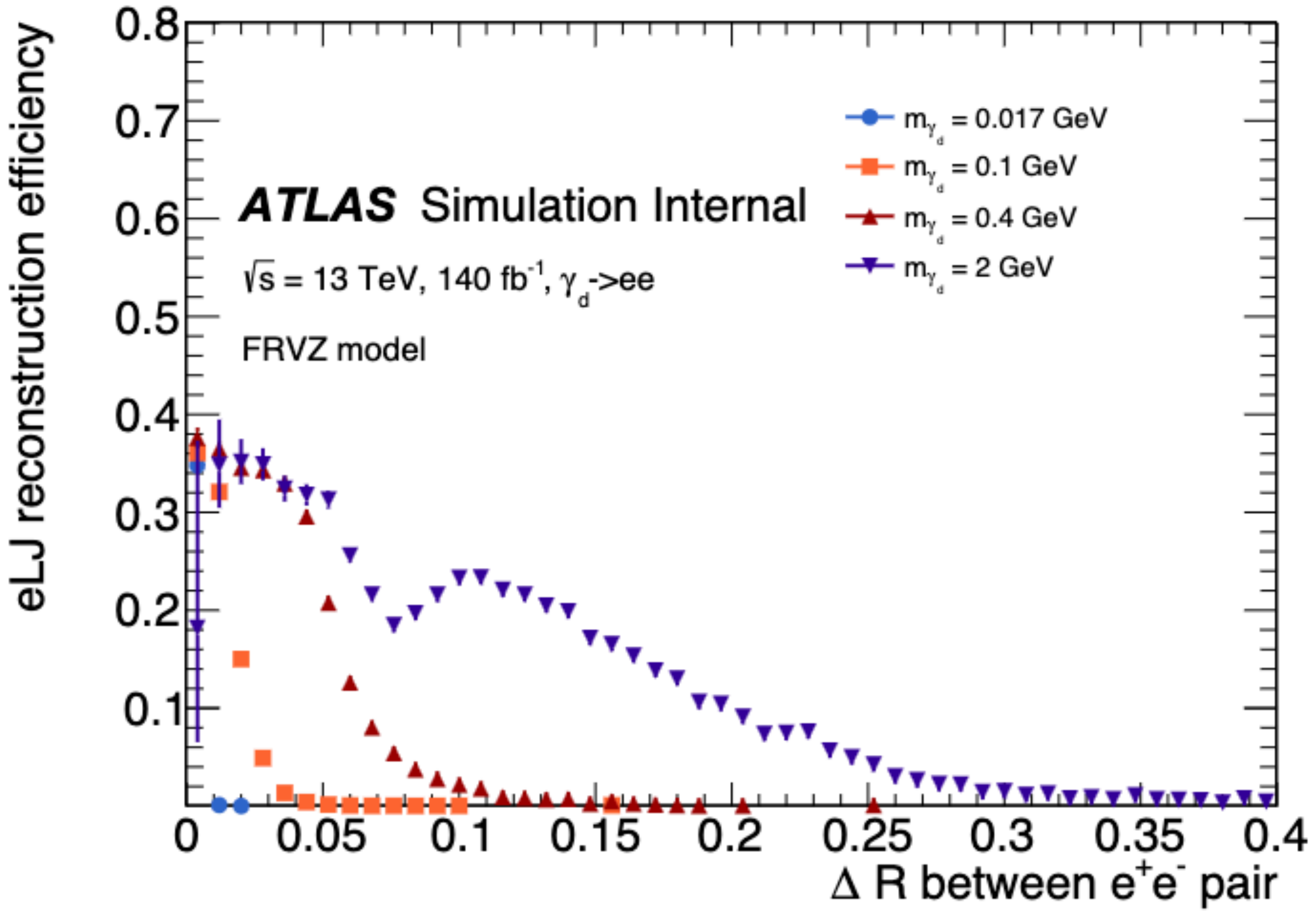

# Number of electrons in eLJ

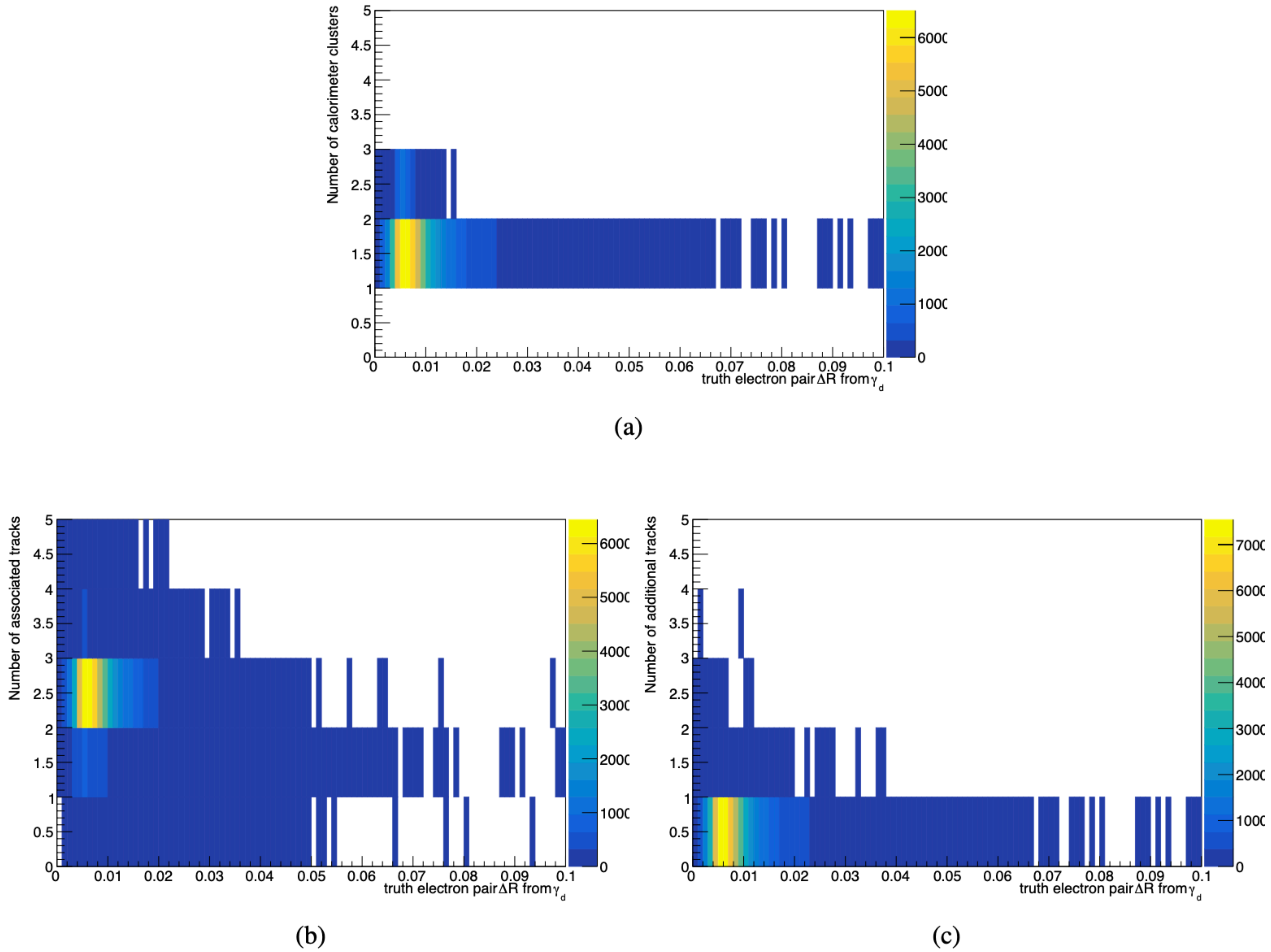


Figure 5.4: (a) Number of calorimeter clusters in $e$LJ as a function of $\Delta R$ between truth electrons. Number of (b) associated and (c) non-associated tracks in $e$LJ, as a function of $\Delta R$ between truth electrons. These plots are produced from a signal sample with a dark photon mass of 0.1 GeV.

# FRVZ and HAHM

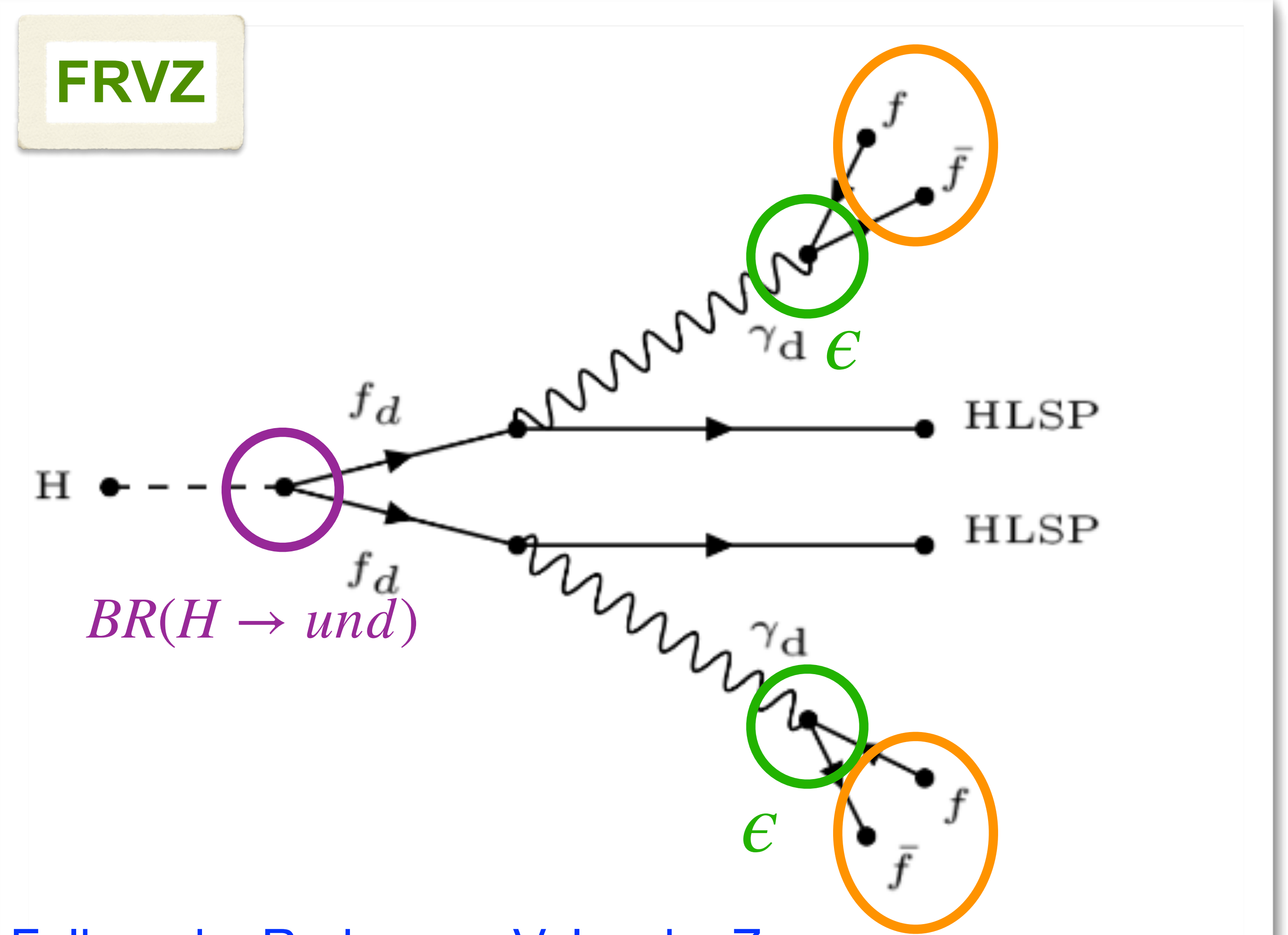


[Falkowsky-Ruderman-Volansky-Zupan]

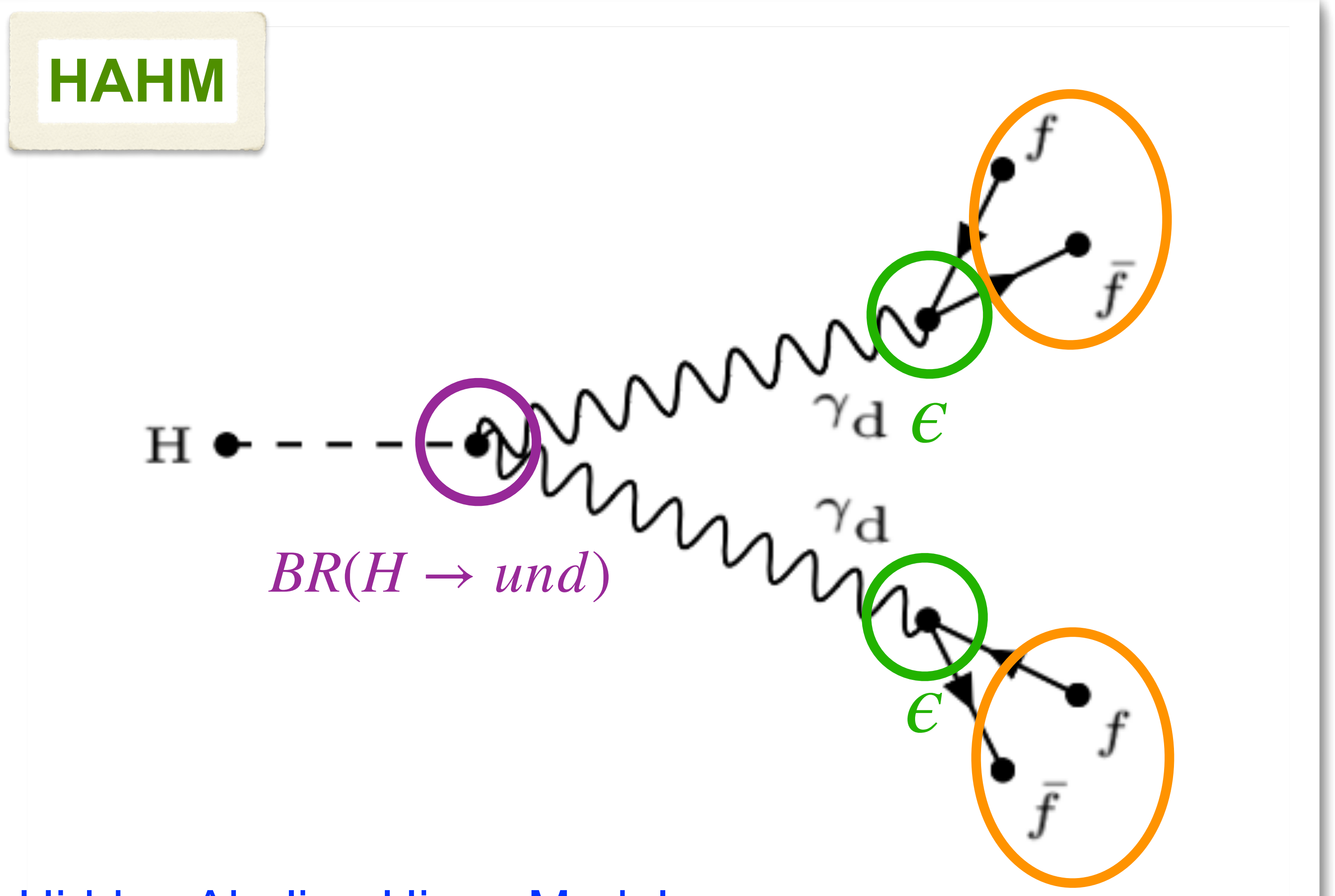


[Hidden Abelian Higgs Model]

Considered only leptonic decays

$\gamma_d \to \mu^+\mu^-$ e $\gamma_d \to e^+e^-$

The decay products are extremely collimated —> **Lepton Jets (LJ)**

**$\Delta$R between decay products**

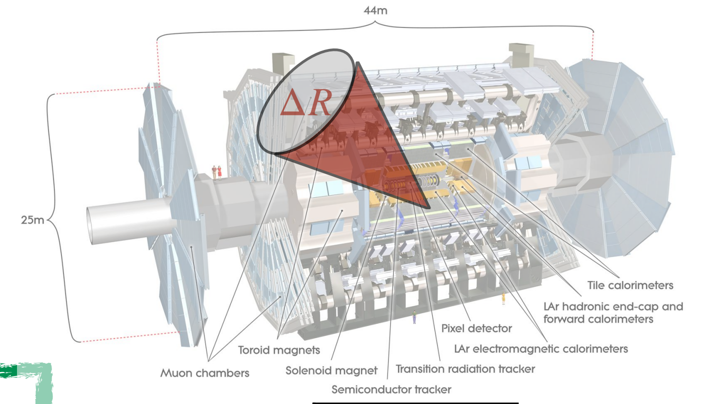

$$\Delta R = \sqrt{\Delta\eta^2 + \Delta\phi^2}$$

FRVZ

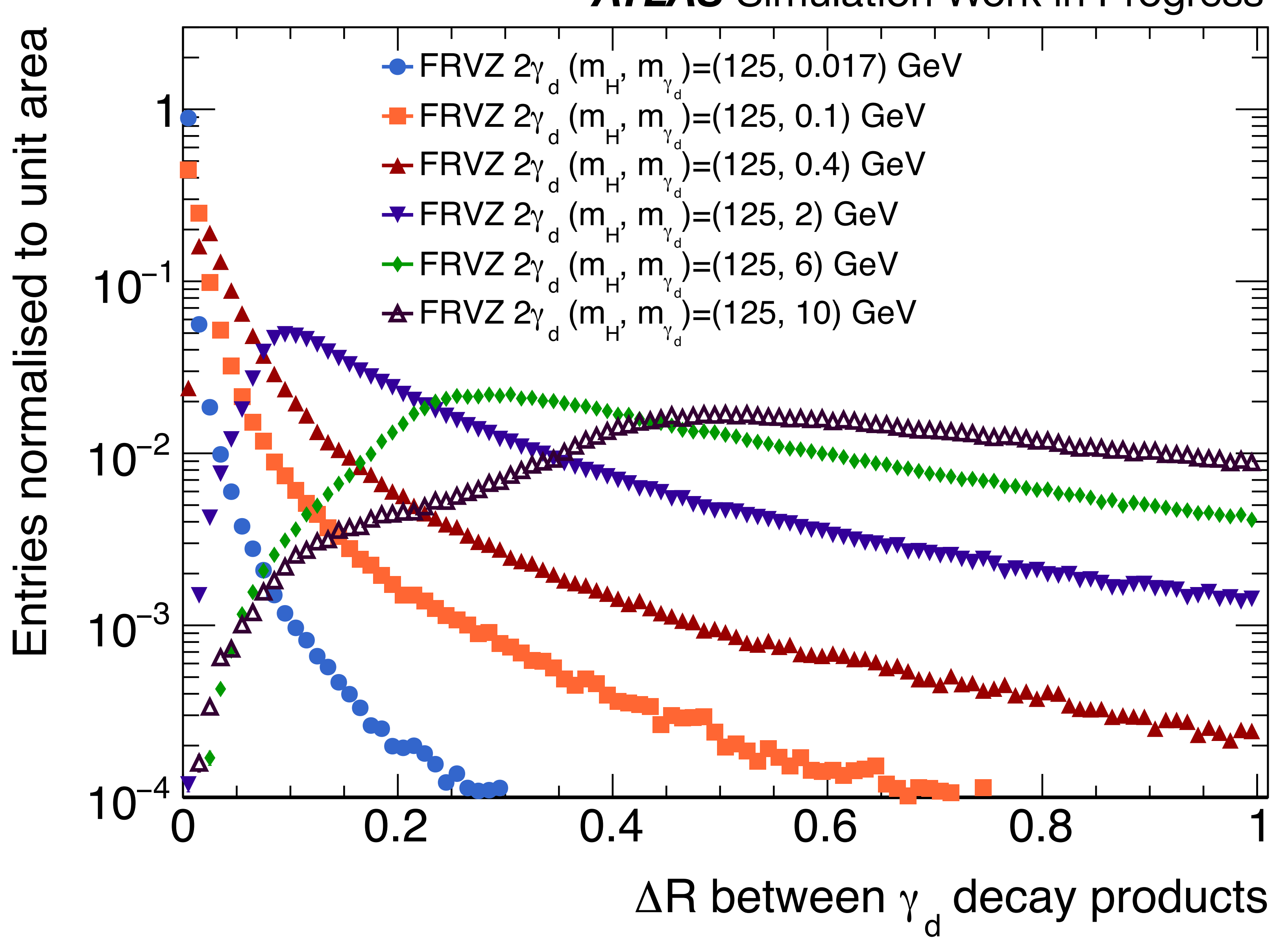


HAHM

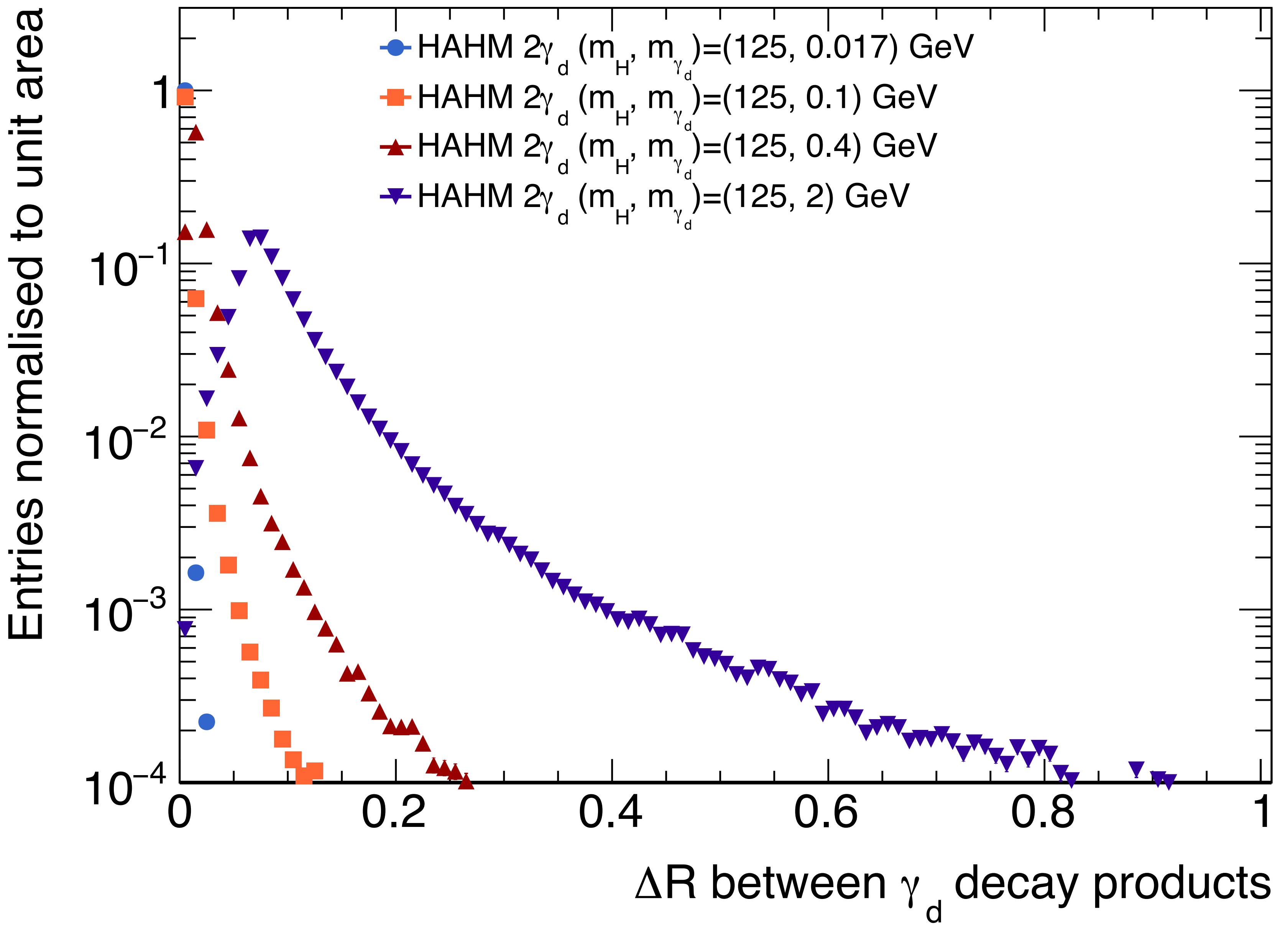

# Trigger strategy

$2e$LJ channel: 2 resolved electrons (one per each $e$LJ) → single and di-electron triggers

$1e$LJ – $1\mu$LJ channel: at most 2 collimated electrons and 2 collimated muons→ single electron, di-muon and 1electron-1muon triggers

$2\mu$LJ channel: at most two pairs of collimated muons → di-muon and tri-muon trigger

| Requirement / Region | $2\mu\mathrm{LJ}^{\mathrm{high}-p_{\mathrm{T}}}$ | $2\mu\mathrm{LJ}^{\mathrm{low}-p_{\mathrm{T}}}$ | $\mu$LJ–$e$LJ |
|---|---|---|---|
| Number of $\mu$LJs | 2 | 2 | 1 |
| Number of $e$LJs | 0 | 0 | 1 |
| di-muon trigger | yes | – | yes |
| tri-muon trigger | – | yes | – |
| electron-muon trigger | – | – | yes |
| electron trigger | – | – | yes |

# Signal Regions

| Selection | $2\mu$LJ SR | $1\mu$LJ–$1e$LJ SR | $2e$LJ SR |
|---|---|---|---|
| $q_{\text{LJ}} = 0$ | ✓ | ✓ | ✓ |
| $\Delta\phi(\text{LJ}, \text{LJ})$ | ✗ | $\geq 2$ | $\geq 2.5$ |
| $e$LJ $\|\eta\| \leq 1.37$ | ✗ | ✓ | ✓ |
| $e$LJ leading track $p_{\text{T}} \geq 5\,\text{GeV}$ | ✗ | ✓ | ✓ |
| $e$LJ $p_{\text{T}}^{\text{imb}}$ | ✗ | $< 0.8$ | $< 0.82$ (leading $e$LJ) |
| $e$LJ $R_{\phi} < 0.96$ | ✗ | ✗ | sub-leading $e$LJ |
| $m^{\text{imb}} < 0.8$ | ✗ | ✗ | ✓ |
| Z mass veto | ✗ | ✗ | ✓ |
| $N_{\text{jet40}} = 0$ | ✗ | ✗ | ✓ |

Suppressing combinatorial background

Suppressing Z+jets background

Suppressing $t\bar{t}$ background

After these requirements, dominating backgrounds:

- $2\mu$LJ channel: di-boosted resonances (decaying into muons) production
- $e$LJ – $\mu$LJ channel: single boosted resonance (decaying into muons) production
- $2e$LJ channel: Z+jets

# Preselection and trigger strategy

- Preselection of events:
  - Event in GRL + presence of at least one “good primary vertex”
  - Reconstruction of at least 2 LJ
  - Pass trigger strategy
  - Trigger matching
- 1$\mu$LJ + 1eLJ —> OR ff **single electron**, **di-muon** and **mixed triggers** e-$\mu$

| Type | Data-taking periods | Trigger |
|---|---|---|
| Single-electron | 2015 | HLT_e24_lhmedium_L1EM20VH |
| | | HLT_e60_lhmedium |
| | | HLT_e120_lhloose |
| | 2016 A-end | HLT_e26_lhtight_nod0_ivarloose |
| | | HLT_e60_lhmedium_nod0 |
| | | HLT_e140_lhloose_nod0 |
| Di-muon | 2015 | HLT_mu18_mu8noL1 |
| | 2015 - 2016 A | HLT_2mu10 |
| | 2016 A - E | HLT_mu20_mu8noL1 |
| | 2016 B - end - 2017 - 2018 | HLT_2mu14 |
| | 2016 F - end - 2017 -2018 | HLT_mu22_mu8noL1 |
| Electron-muon | 2015 | HLT_e7_lhmedium_mu24 |
| | | HLT_e17_lhloose_mu14 |
| | 2016 - 2017 -2018 | HLT_e17_lhloose_nod0_mu14 |
| | 2016 A | HLT_e24_lhmedium_nod0_L1EM20VHI_mu8noL1 |
| | 2016 B-E | HLT_e7_lhmedium_nod0_mu24 |
| | 2016 F-end | HLT_e26_lhmedium_nod0_L1EM22VHI_mu8noL1 |
| | 2017-2018 | HLT_e26_lhmedium_nod0_mu8noL1 |

# Invariant mass $\mu$LJ

- $\mu$LJ always with 2 muons: mass unchanged with reconstructed muons
- Good resolution of invariant mass (as in the muonic channel)

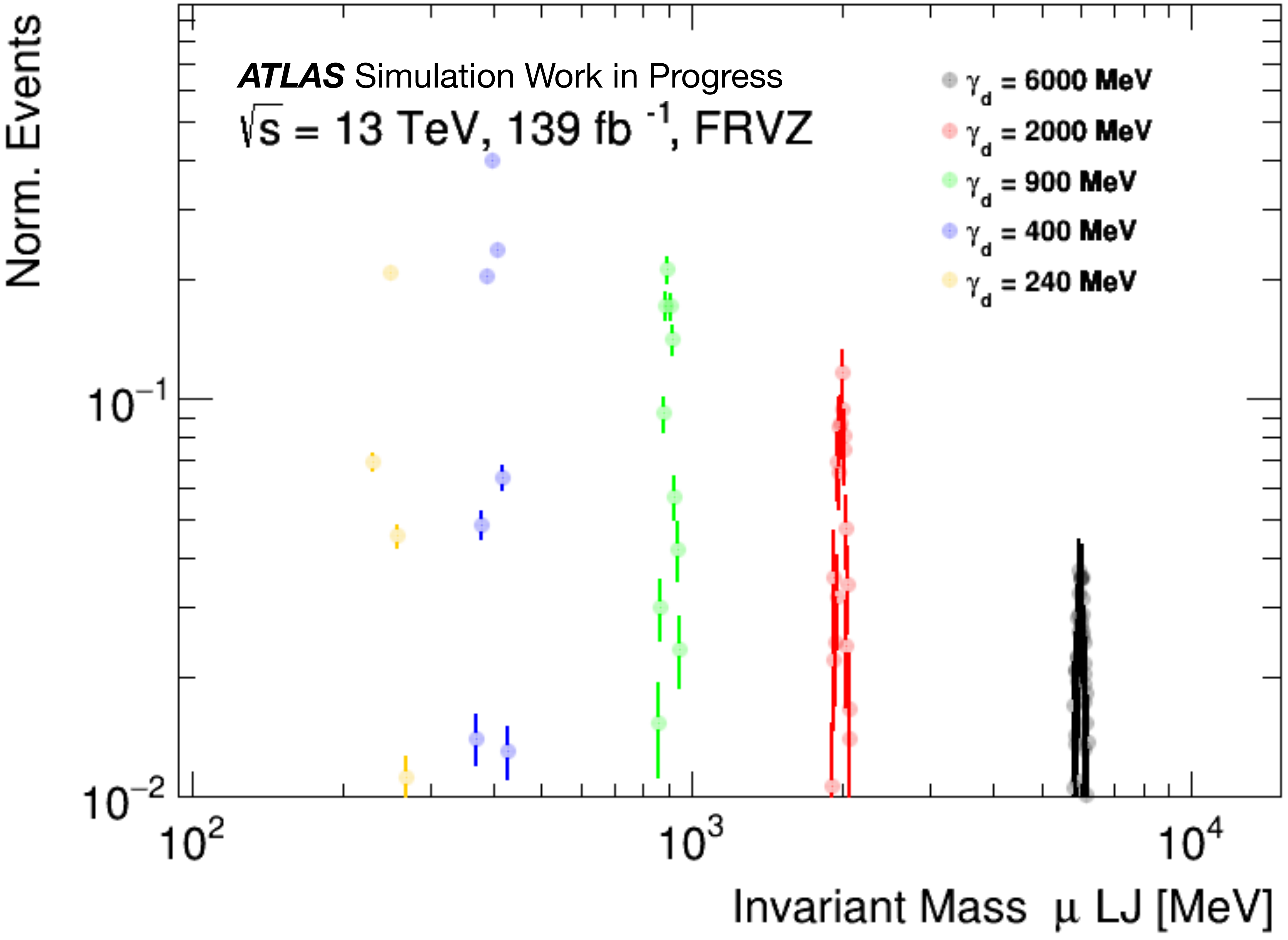

# Invariant mass eLJ

- eLJ with 1 electron: unchanged mass reconstructed from tracks:
  - Best-matched track with same charge as the electron
  - Track with opposite charge with higher $p_T$
- eLJ with 2 electrons: mass unchanged from reconstructed electrons

eLJ con 2 elettroni

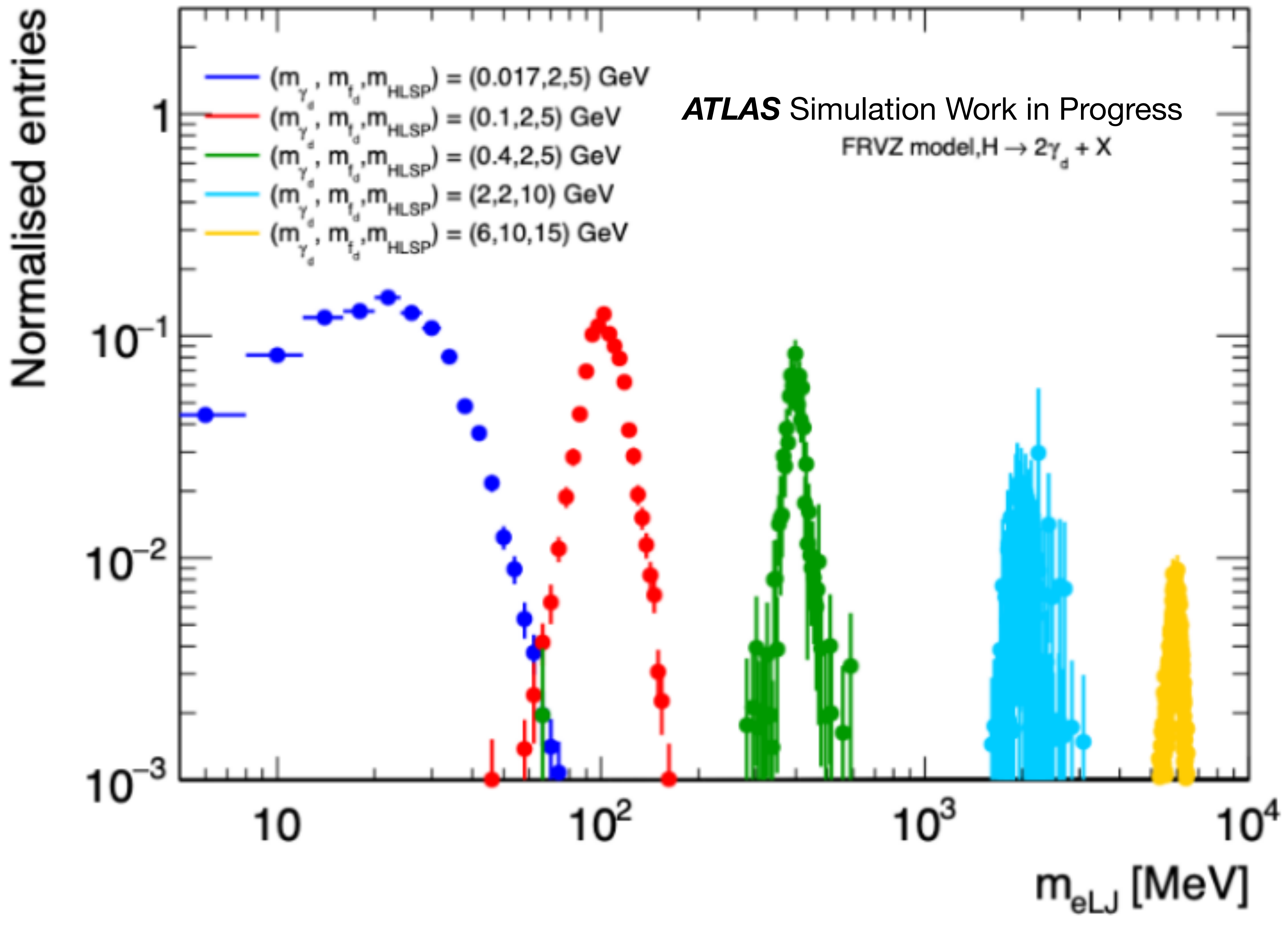


eLJ con 1 elettrone

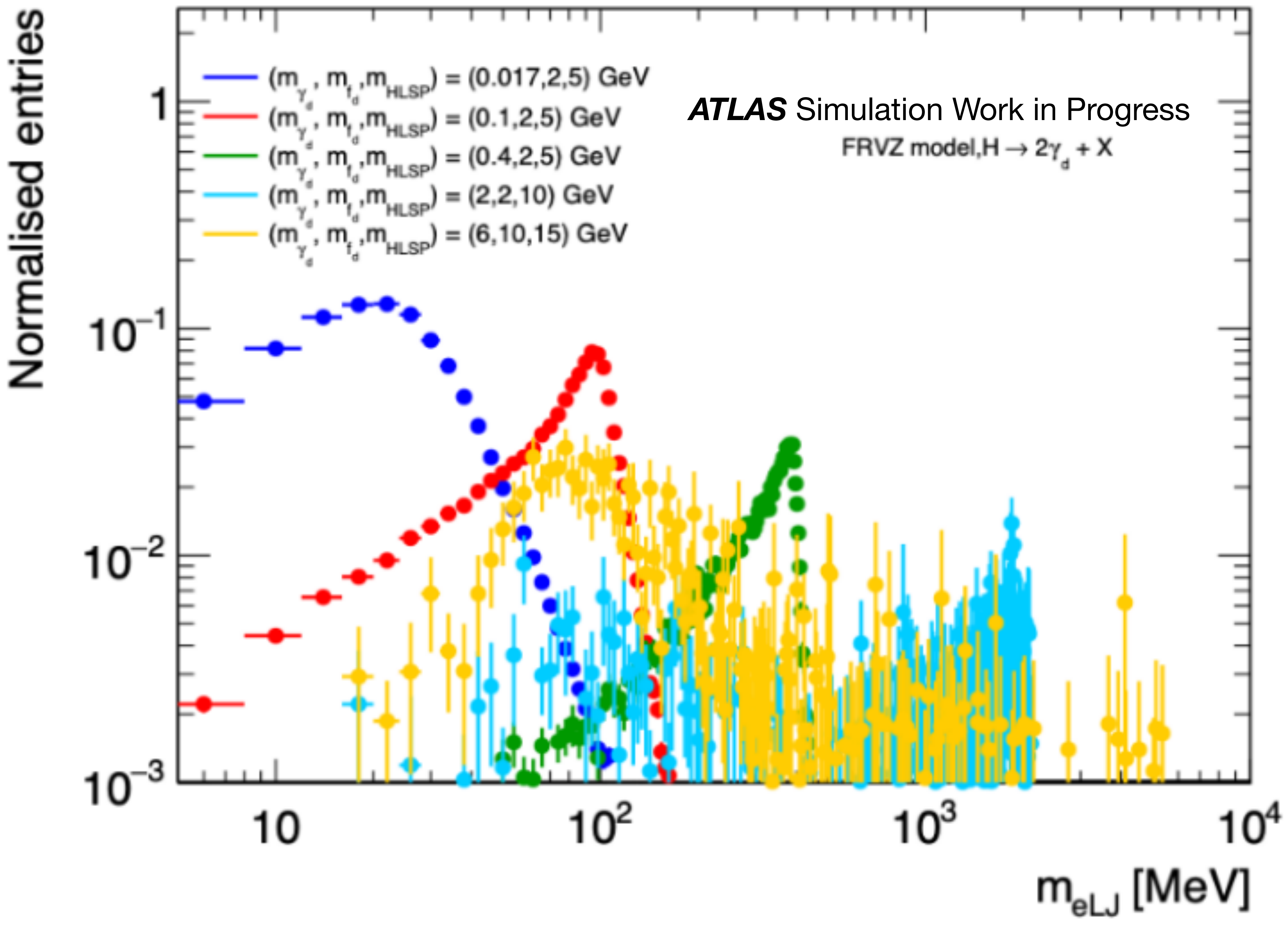

# Invariant mass eLJ: 1 electron VS 2 electrons

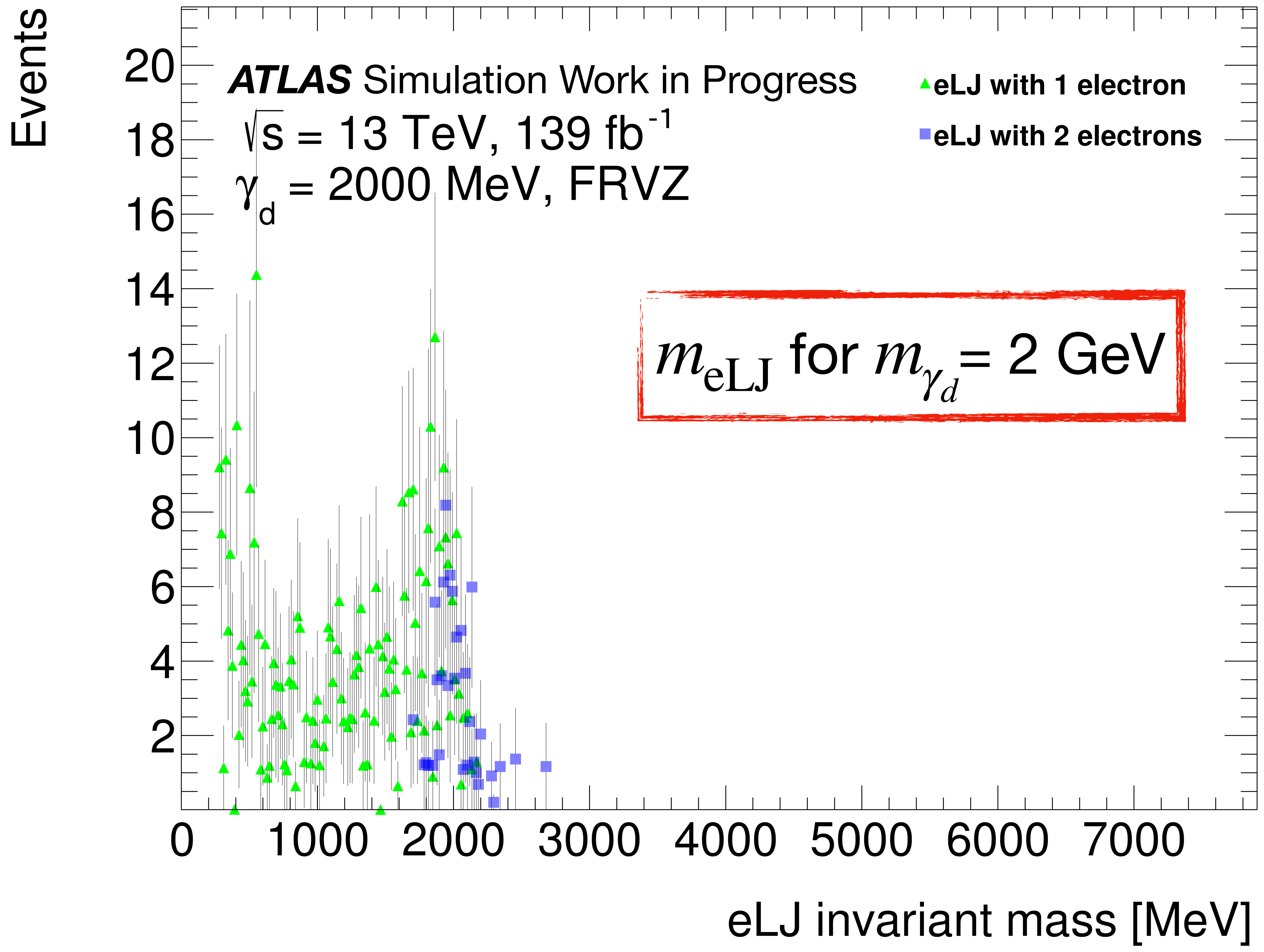


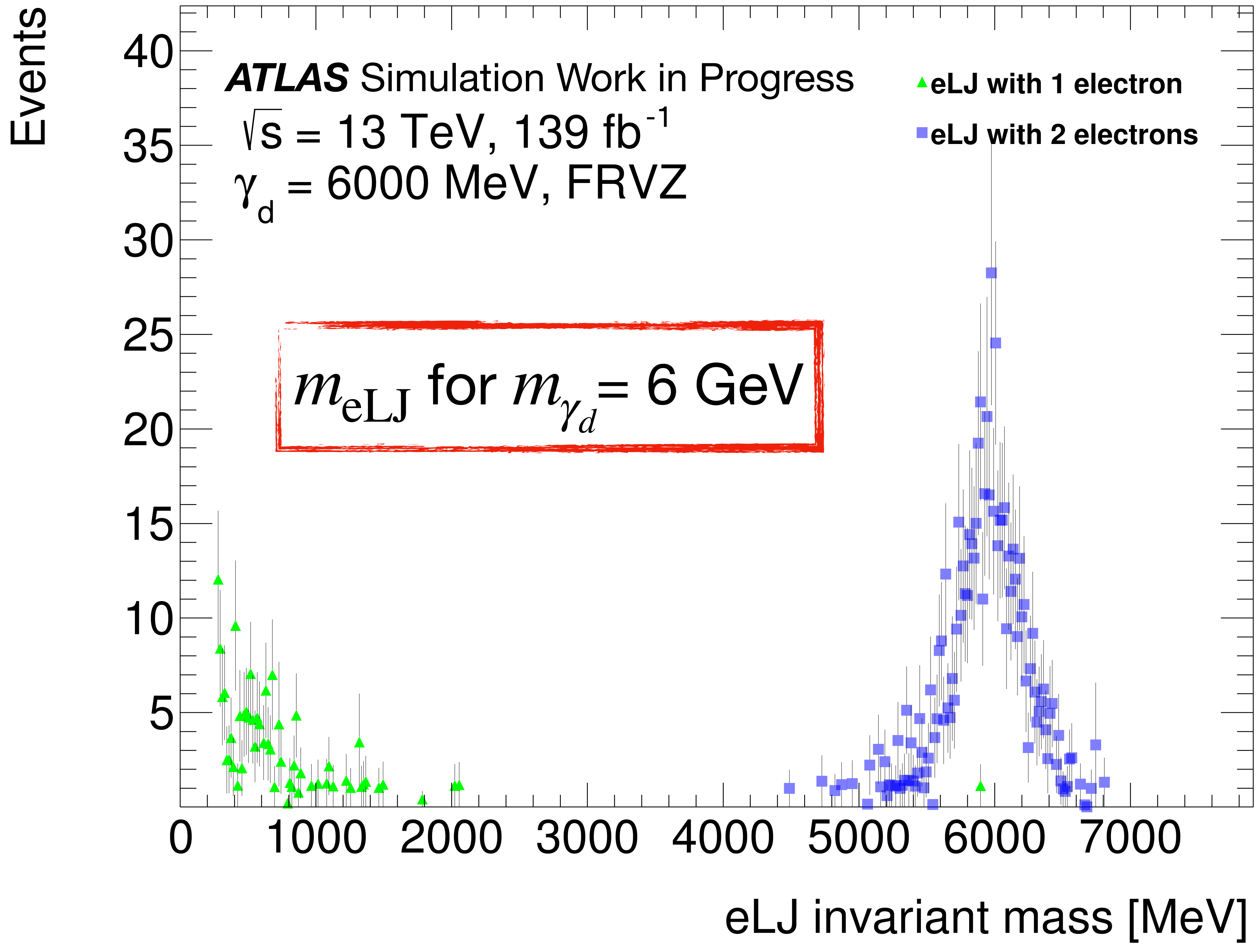


eLJ reconstructed with 1 electron for high $m_{\gamma_d}$:

- Two electrons too far away to reconstruct an eLJ
- Two electrons are quite close, but one fails requirements of the WP and ISO —> eLJ reconstructed with an electron + random track

# Trigger efficiencies and trigger-matching

| Type | Data-taking periods | Trigger |
|---|---|---|
| Single-electron | 2015 | HLT_e24_lhmedium_L1EM20VH |
| | | HLT_e60_lhmedium |
| | | HLT_e120_lhloose |
| | 2016 A-end | HLT_e26_lhtight_nod0_ivarloose |
| | | HLT_e60_lhmedium_nod0 |
| | | HLT_e140_lhloose_nod0 |
| Di-muon | 2015 | HLT_mu18_mu8noL1 |
| | 2015 - 2016 A | HLT_2mu10 |
| | 2016 A - E | HLT_mu20_mu8noL1 |
| | 2016 B - end - 2017 - 2018 | HLT_2mu14 |
| | 2016 F - end - 2017 -2018 | HLT_mu22_mu8noL1 |
| Electron-muon | 2015 | HLT_e7_lhmedium_mu24 |
| | | HLT_e17_lhloose_mu14 |
| | 2016 - 2017 -2018 | HLT_e17_lhloose_nod0_mu14 |
| | 2016 A | HLT_e24_lhmedium_nod0_L1EM20VHI_mu8noL1 |
| | 2016 B-E | HLT_e7_lhmedium_nod0_mu24 |
| | 2016 F-end | HLT_e26_lhmedium_nod0_L1EM22VHI_mu8noL1 |
| | 2017-2018 | HLT_e26_lhmedium_nod0_mu8noL1 |

FRVZ

| | 240 MeV | 400 MeV | 900 MeV | 2 GeV | 6 GeV |
|---|---|---|---|---|---|
| 2015 | $0.64 \pm 0.04$ | $0.65 \pm 0.06$ | $0.83 \pm 0.08$ | $0.86 \pm 0.13$ | $0.94 \pm 0.06$ |
| 2016 A | $0.70 \pm 0.09$ | $0.69 \pm 0.19$ | $1.00^{+0.00}_{-0.35}$ | $0.67 \pm 0.27$ | $1.00^{+0.00}_{-0.48}$ |
| 2016 B-E | $0.505 \pm 0.021$ | $0.500 \pm 0.029$ | $0.63 \pm 0.05$ | $0.60 \pm 0.08$ | $0.926 \pm 0.032$ |
| 2016 F-end | $0.497 \pm 0.015$ | $0.575 \pm 0.020$ | $0.681 \pm 0.034$ | $0.56 \pm 0.06$ | $0.830 \pm 0.032$ |
| 2017 | $0.600 \pm 0.013$ | $0.679 \pm 0.016$ | $0.733 \pm 0.028$ | $0.65 \pm 0.05$ | $0.863 \pm 0.028$ |
| 2018 | $0.615 \pm 0.010$ | $0.681 \pm 0.013$ | $0.741 \pm 0.022$ | $0.653 \pm 0.034$ | $0.907 \pm 0.017$ |

HAHM

| | 400 MeV | 2 GeV | 10 GeV |
|---|---|---|---|
| 2015 | $0.939 \pm 0.015$ | $0.86 \pm 0.07$ | $0.987 \pm 0.013$ |
| 2016 A | $0.90 \pm 0.04$ | $1.00^{+0.00}_{-0.34}$ | $1.00^{0.00}_{-0.14}$ |
| 2016 B-E | $0.824 \pm 0.012$ | $0.79 \pm 0.04$ | $0.934 \pm 0.015$ |
| 2016 F-end | $0.863 \pm 0.008$ | $0.832 \pm 0.023$ | $0.988 \pm 0.004$ |
| 2017 | $0.926 \pm 0.005$ | $0.917 \pm 0.014$ | $0.9939 \pm 0.0025$ |
| 2018 | $0.911 \pm 0.004$ | $0.869 \pm 0.014$ | $0.9882 \pm 0.0030$ |

- Trigger matching:
- If single electron trigger: trigger matching with at least one electron in the eLJ
- If di-muon trigger: trigger matching with both muons in the $\mu$LJ
- If e-$\mu$ trigger: trigger matching both the electron and the muon

# Signal Regions

| Selection | 2$\mu$LJ SR | 1$\mu$LJ–1$e$LJ SR | 2$e$LJ SR |
|---|---|---|---|
| $q_{\mathrm{LJ}} = 0$ | ✓ | ✓ | ✓ |
| $\Delta\phi(\mathrm{LJ}, \mathrm{LJ})$ | ✗ | $\geq 2$ | $\geq 2.5$ |
| $e$LJ $\lvert\eta\rvert \leq 1.37$ | ✗ | ✓ | ✓ |
| $e$LJ leading track $p_{\mathrm{T}} \geq 5\,\mathrm{GeV}$ | ✗ | ✓ | ✓ |
| $e$LJ $p_{\mathrm{T}}^{\mathrm{imb}}$ | ✗ | $< 0.8$ | $< 0.82$ (leading $e$LJ) |
| $e$LJ $R_{\phi} < 0.96$ | ✗ | ✗ | sub-leading $e$LJ |
| | | ✗ | ✓ |
| | | ✗ | ✓ |
| | | ✗ | ✓ |

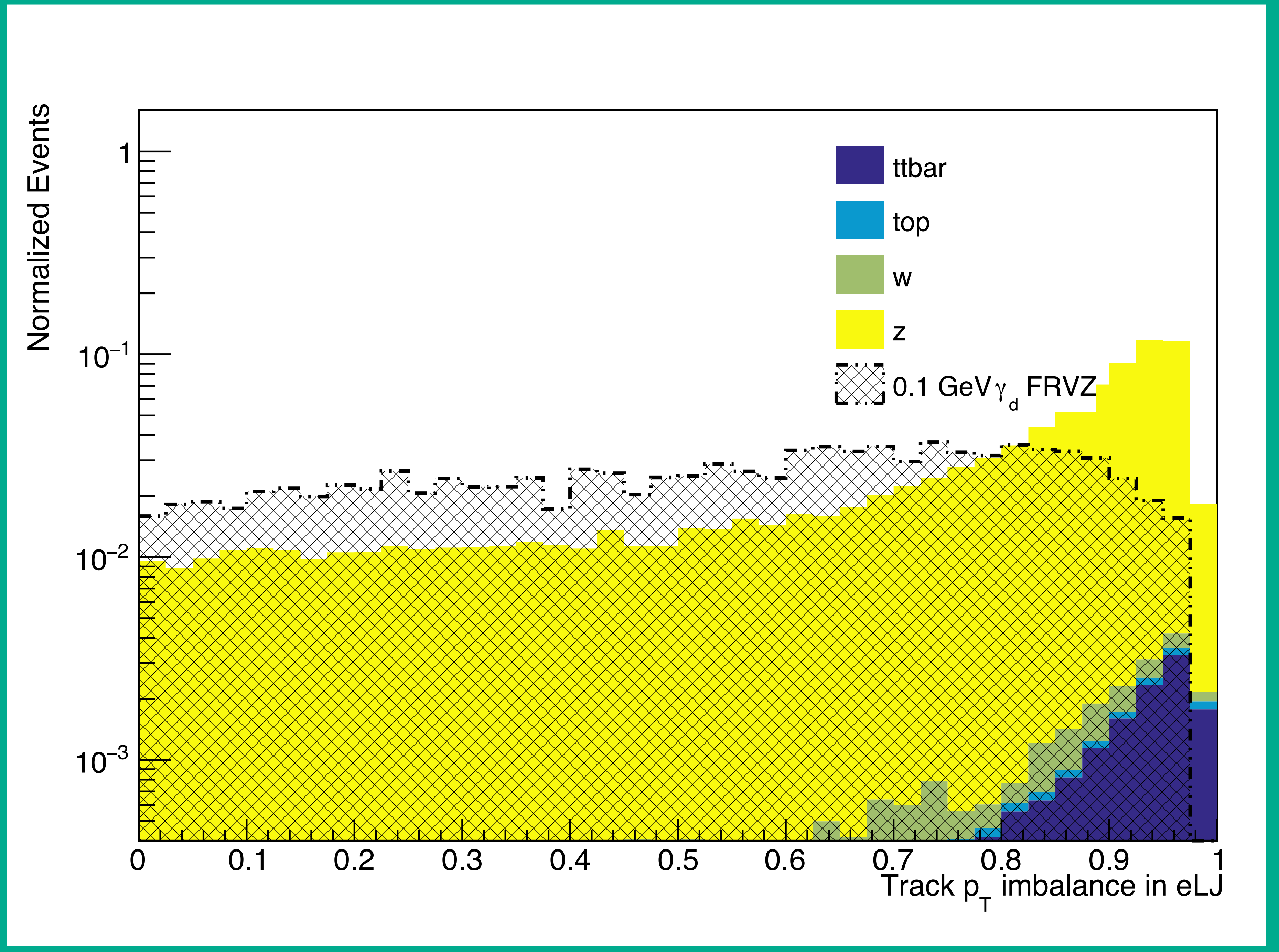

| Selection | $2\mu$LJ SR | $1\mu$LJ–$1e$LJ SR | $2e$LJ SR |
|---|---|---|---|
| $q_{\mathrm{LJ}} = 0$ | ✓ | ✓ | ✓ |
| $\Delta\phi(\mathrm{LJ}, \mathrm{LJ})$ | ✗ | $\geq 2$ | $\geq 2.5$ |
| $e$LJ $\lvert\eta\rvert \leq 1.37$ | ✗ | ✓ | ✓ |
| $e$LJ leading track $p_{\mathrm{T}} \geq 5\,\mathrm{GeV}$ | ✗ | ✓ | ✓ |
| $e$LJ $p_{\mathrm{T}}^{\mathrm{imb}}$ | ✗ | $< 0.8$ | $< 0.82$ (leading $e$LJ) |
| $e$LJ $R_\phi < 0.96$ | ✗ | ✗ | sub-leading $e$LJ |
| | | ✗ | ✓ |
| | | ✗ | ✓ |
| | | ✗ | ✓ |

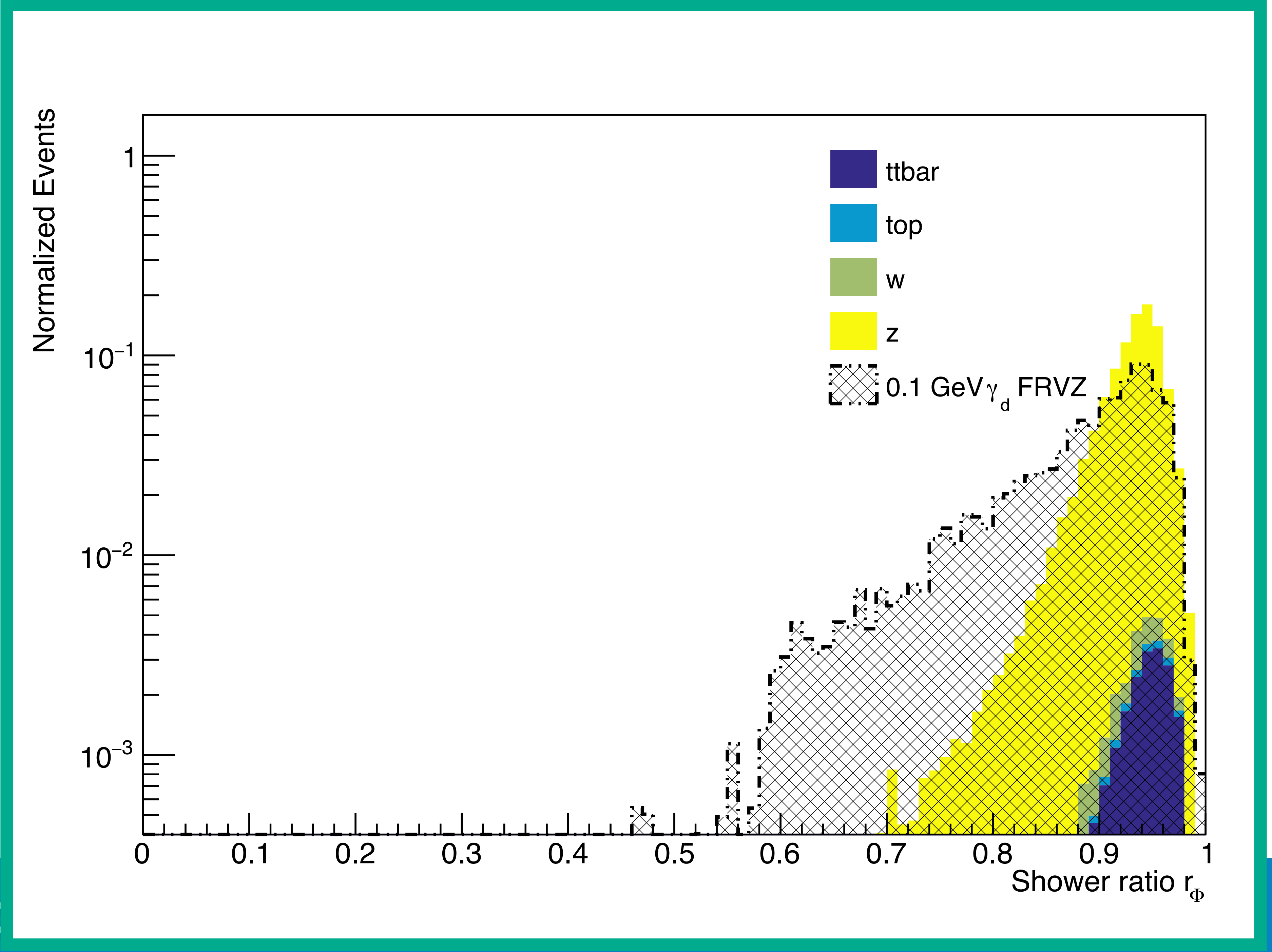

# Signal Regions

| Selection | $2\mu$LJ SR | $1\mu$LJ–$1e$LJ SR | |
|---|---|---|---|
| $q_{\mathrm{LJ}} = 0$ | ✓ | ✓ | |
| $\Delta\phi(\mathrm{LJ}, \mathrm{LJ})$ | ✗ | $\geq 2$ | |
| $e$LJ $\lvert\eta\rvert \leq 1.37$ | ✗ | ✓ | |
| $e$LJ leading track $p_{\mathrm{T}} \geq 5\,\mathrm{GeV}$ | ✗ | ✓ | |
| $e$LJ $p_{\mathrm{T}}^{\mathrm{imb}}$ | ✗ | $< 0.8$ | |
| $e$LJ $R_{\phi} < 0.96$ | ✗ | ✗ | |
| $m^{\mathrm{imb}} < 0.8$ | ✗ | ✗ | |
| Z mass veto | ✗ | ✗ | ✓ |
| $N_{\mathrm{jet40}} = 0$ | ✗ | ✗ | ✓ |

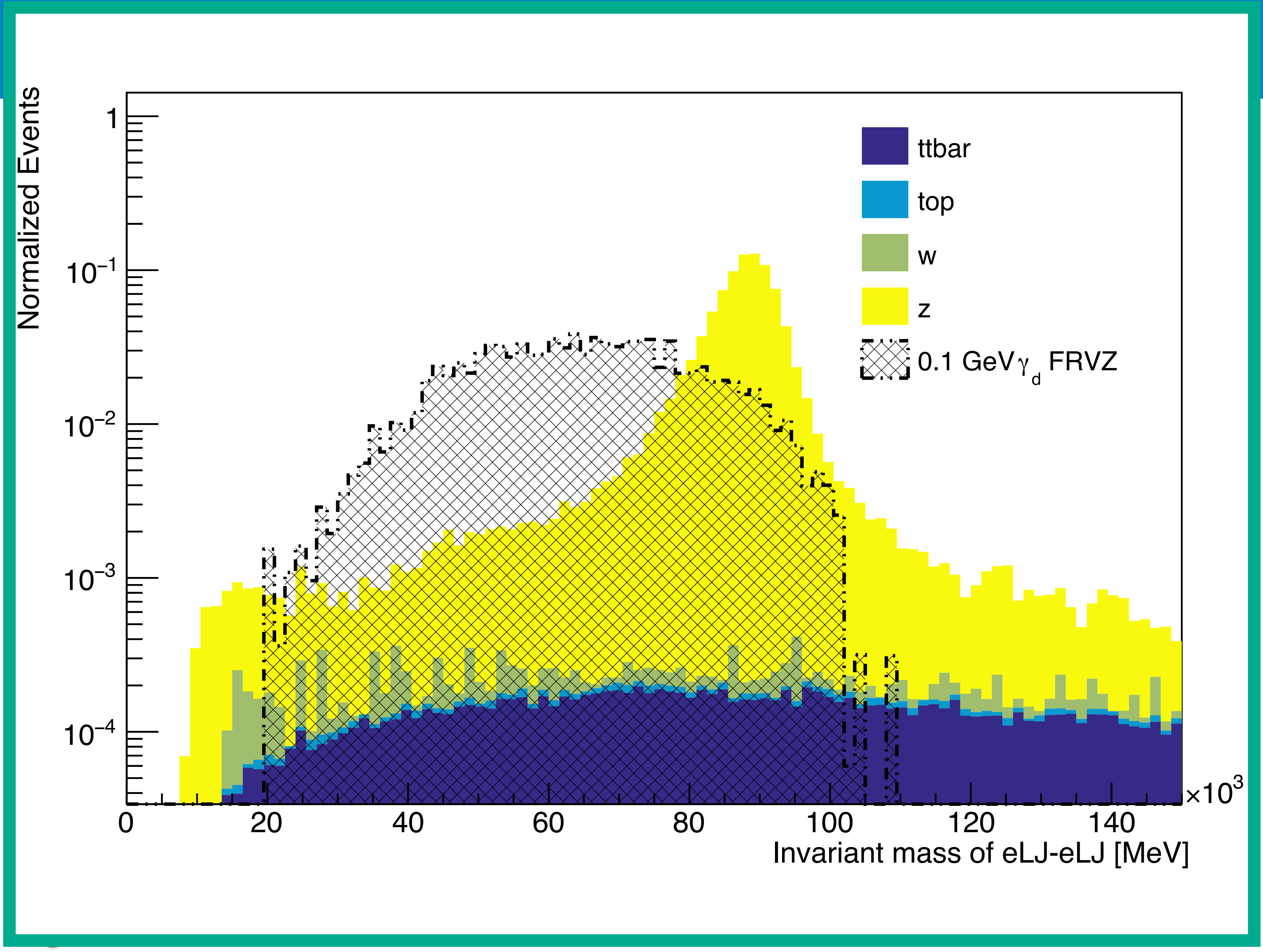


Suppressing Z+jets background

# Signal Regions

| Selection | $2\mu$LJ SR | $1\mu$LJ–$1e$LJ SR | |
|---|---|---|---|
| $q_{\mathrm{LJ}} = 0$ | ✓ | ✓ | |
| $\Delta\phi(\mathrm{LJ}, \mathrm{LJ})$ | ✗ | $\geq 2$ | |
| $e$LJ $\lvert\eta\rvert \leq 1.37$ | ✗ | ✓ | |
| $e$LJ leading track $p_{\mathrm{T}} \geq 5\,\mathrm{GeV}$ | ✗ | ✓ | |
| $e$LJ $p_{\mathrm{T}}^{\mathrm{imb}}$ | ✗ | $< 0.8$ | |
| $e$LJ $R_{\phi} < 0.96$ | ✗ | ✗ | |
| $m^{\mathrm{imb}} < 0.8$ | ✗ | ✗ | |
| Z mass veto | ✗ | ✗ | ✓ |
| $N_{\mathrm{jet40}} = 0$ | ✗ | ✗ | ✓ |

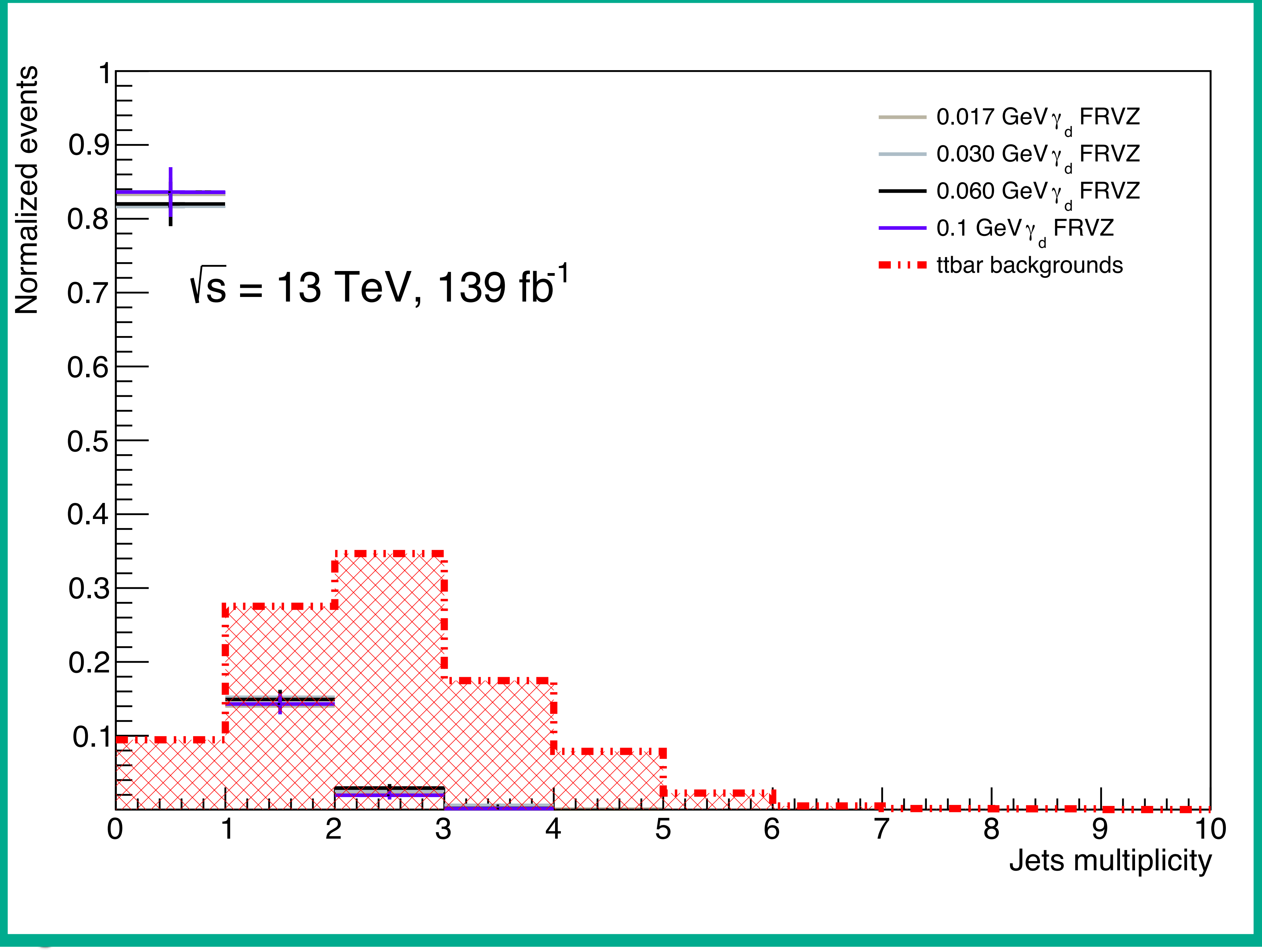


Suppressing $t\bar{t}$ background

# Background estimation for $e\mathrm{LJ} - e\mathrm{LJ}$ channel

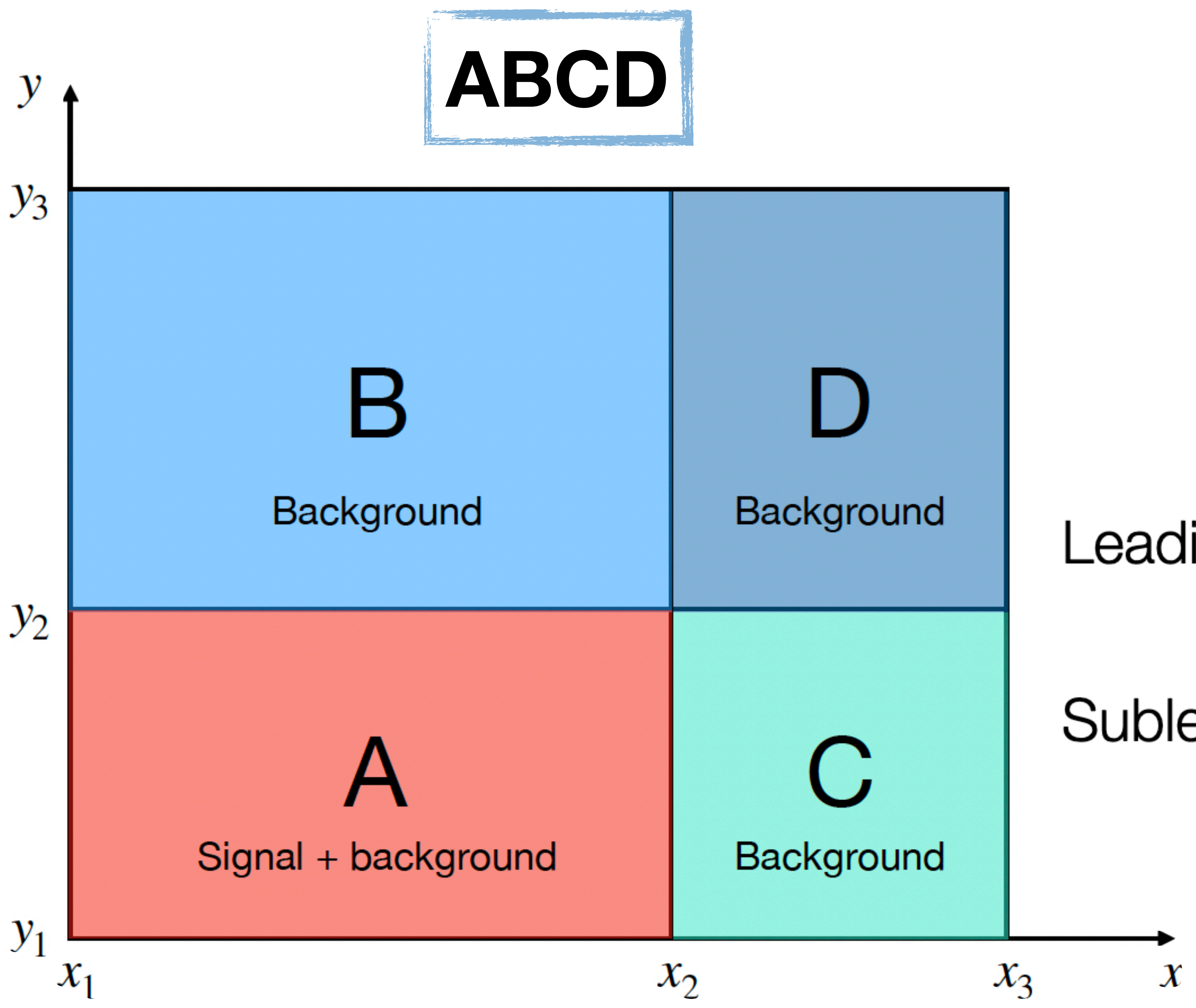


Leading eLJ $p_T$ imbalance $\left( = \left| \frac{p_T^{trk2} - p_T^{trk1}}{p_T^{trk1} + p_T^{trk2}} \right| \right) < 0.8$

Subleading eLJ $R_\phi$ $\left( = \frac{E_{3\times3}}{E_{3\times7}} \right) < 0.96$

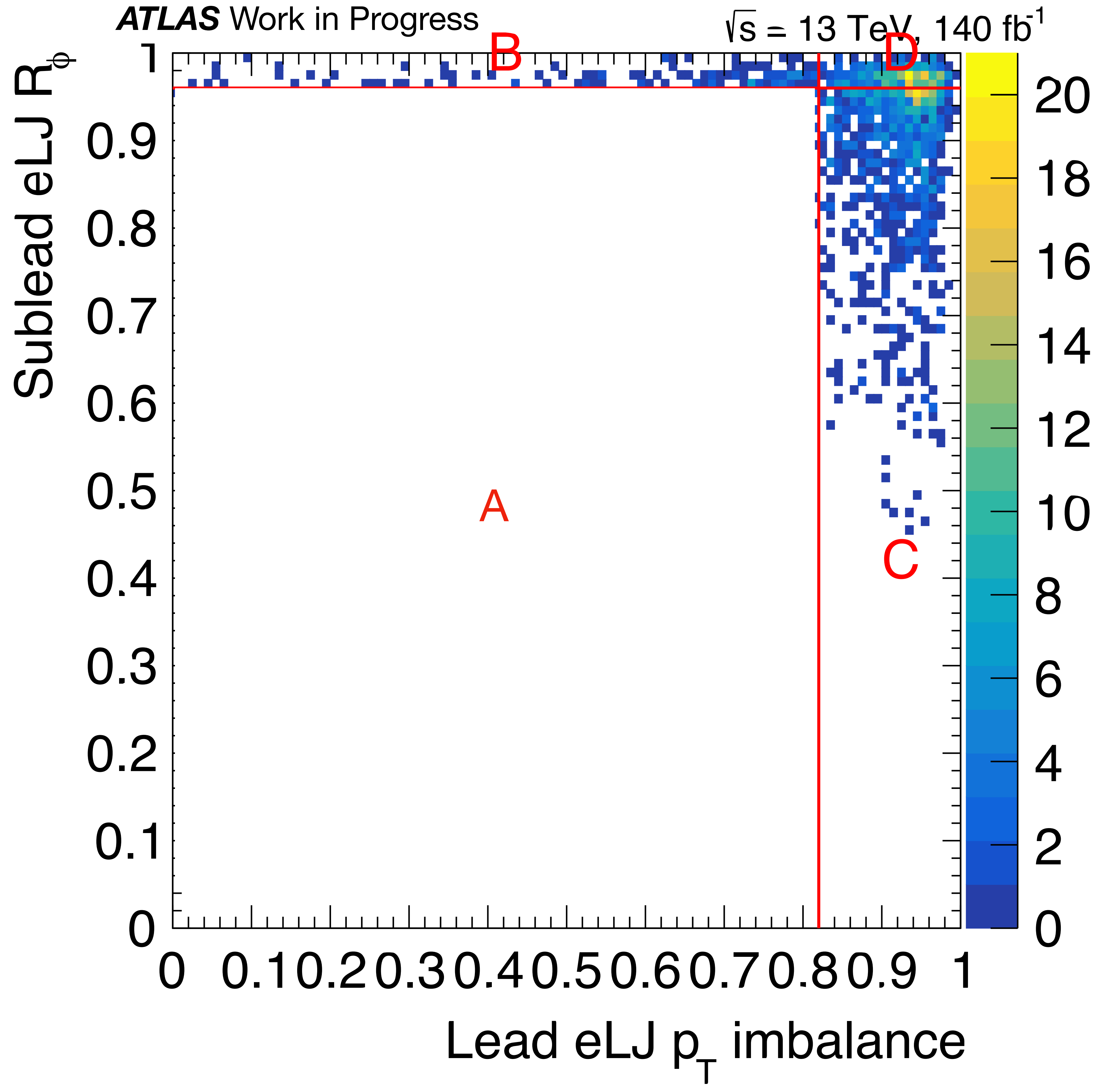


$x, y$ discriminating variables uncorrelated for the background(s)

→ defining SR and CRs

$$\rightarrow N_A = \frac{N_C}{N_D} N_B$$

Background estimation validated in BD and DC sub-regions, and in the full ABCD plane in three additional VRs

# Signal Region

FRVZ

| $m_{\gamma_d}$ | 240 MeV | 400 MeV | 900 MeV | 2 GeV | 6 GeV |
|---|---|---|---|---|---|
| Triggers | 44210 ± 240 | 41150 ± 230 | 35090 ± 210 | 45380 ± 240 | 49680 ± 250 |
| 1 $\mu$LJ, 1 $e$LJ | 3880 ± 70 | 2470 ± 50 | 834 ± 32 | 331 ± 20 | 711 ± 29 |
| Trigger matching | 3650 ± 70 | 2370 ± 50 | 802 ± 31 | 324 ± 20 | 698 ± 29 |
| $e$LJ $p_{\mathrm{T}}$ track > 5 GeV | 3630 ± 70 | 2340 ± 50 | 795 ± 31 | 315 ± 20 | 689 ± 28 |
| $e$LJ $\|\eta\| < 1.37$ | 2500 ± 60 | 1670 ± 50 | 613 ± 27 | 203 ± 16 | 501 ± 24 |
| $\|\Delta\phi\|(\mu\mathrm{LJ},e\mathrm{LJ}) > 2$ | 1750 ± 50 | 1080 ± 40 | 354 ± 21 | 100 ± 11 | 361 ± 21 |
| $q_{eLJ} = 0$ | 1700 ± 50 | 1070 ± 40 | 341 ± 21 | 88 ± 10 | 341 ± 20 |
| $q_{\mu\mathrm{LJ}} = 0$ | 1700 ± 50 | 1070 ± 40 | 341 ± 21 | 88 ± 10 | 341 ± 20 |
| $\|p_{\mathrm{T}}^{imb}\| < 0.8$ | 1320 ± 40 | 793 ± 31 | 275 ± 19 | 54 ± 8 | 323 ± 19 |

HAHM

| $m_{\gamma_d}$ | 400 MeV | 2 GeV | 10 GeV |
|---|---|---|---|
| Triggers | 126600 ± 400 | 98570 ± 350 | 150100 ± 400 |
| 1 $\mu$LJ, 1 $e$LJ | 12400 ± 120 | 1500 ± 40 | 3710 ± 70 |
| Trigger matching | 12310 ± 120 | 1480 ± 40 | 3700 ± 70 |
| $e$LJ $p_{\mathrm{T}}$ track > 5 GeV | 12270 ± 120 | 1470 ± 40 | 3670 ± 70 |
| $e$LJ $\|\eta\| < 1.37$ | 8840 ± 110 | 1080 ± 40 | 2610 ± 60 |
| $\|\Delta\phi\|(\mu\mathrm{LJ},e\mathrm{LJ}) > 2$ | 6810 ± 90 | 625 ± 27 | 2260 ± 50 |
| $q_{eLJ} = 0$ | 6630 ± 90 | 581 ± 26 | 2190 ± 50 |
| $q_{\mu\mathrm{LJ}} = 0$ | 6630 ± 90 | 581 ± 26 | 2190 ± 50 |
| $\|p_{\mathrm{T}}^{imb}\| < 0.8$ | 5470 ± 80 | 425 ± 22 | 2130 ± 50 |

$\sigma_{\mathrm{ggF}} = 48.51$ pb, L = 139 fb$^{-1}$, BR$(H \rightarrow 2\gamma_d + X) = 5\,\%$

# Control Region

FRVZ

| Selection cuts | 240 MeV | 400 MeV | 900 MeV | 2 GeV | 6 GeV |
|---|---|---|---|---|---|
| Triggers | 44210 ± 240 | 41150 ± 230 | 35090 ± 210 | 45380 ± 240 | 49680 ± 250 |
| 1 $\mu$LJ, 0 $e$LJ, 0 $\mu$, $e \geq 2$ | 9.5 ± 3.4 | 5.5 ± 2.5 | 12 ± 4 | 21 ± 5 | 650 ± 28 |
| Trigger matching | 6.1 ± 2.7 | 3.4 ± 2.0 | 7.0 ± 2.9 | 17 ± 4 | 579 ± 26 |
| $ee$ $p_{\mathrm{T}}$ track > 5 GeV | 6.1 ± 2.7 | 3.4 ± 2.0 | 7.0 ± 2.9 | 15 ± 4 | 579 ± 26 |
| $\lvert\Delta\phi\rvert(\mu\mathrm{LJ},ee) > 2$ | 2.4 ± 1.7 | 2.2 ± 1.6 | 2.4 ± 1.7 | 11.2 ± 3.5 | 433 ± 22 |
| $q_{\mu\mathrm{LJ}} = 0$ | 2.4 ± 1.7 | 2.2 ± 1.6 | 2.4 ± 1.7 | 11.2 ± 3.5 | 433 ± 22 |
| $m_{imb} > 0.6$ | 2.4 ± 1.7 | 2.2 ± 1.6 | 2.4 ± 1.7 | 6.4 ± 2.6 | 1.3 ± 0.9 |

HAHM

| Selection cuts | 400 MeV | 2 GeV | 10 GeV |
|---|---|---|---|
| Triggers | 126600 ± 400 | 98570 ± 350 | 150100 ± 400 |
| 1 $\mu$LJ, 0 $e$LJ, 0 $\mu$, $e \geq 2$ | 23 ± 5 | 14 ± 4 | 3320 ± 60 |
| Trigger matching | 22 ± 5 | 10.2 ± 3.4 | 3250 ± 60 |
| $ee$ $p_{\mathrm{T}}$ track > 5 GeV | 22 ± 5 | 10.2 ± 3.4 | 3250 ± 60 |
| $\lvert\Delta\phi\rvert(\mu\mathrm{LJ},ee) > 2$ | 18 ± 5 | 4.4 ± 2.2 | 2730 ± 60 |
| $q_{\mu\mathrm{LJ}} = 0$ | 18 ± 5 | 4.4 ± 2.2 | 2730 ± 60 |
| $m_{imb} > 0.6$ | 12 ± 4 | 4.4 ± 2.2 | 3.9 ± 2.1 |

$\sigma_{\mathrm{ggF}} = 48.51$ pb, L = 139 fb$^{-1}$, BR($H \rightarrow 2\gamma_d + X$) = 5 %

# Signal shape modelling

Double-Sided Crystal Ball

$$
N \cdot \begin{cases} e^{-t^2/2} & \text{if } -\alpha_{\text{low}} \le t \le \alpha_{\text{high}} \\ \dfrac{e^{-0.5\alpha_{\text{low}}^2}}{\left[\frac{\alpha_{\text{low}}}{n_{\text{low}}}\left(\frac{n_{\text{low}}}{\alpha_{\text{low}}} - \alpha_{\text{low}} - t\right)\right]^{n_{\text{low}}}} & \text{if } t < -\alpha_{\text{low}} \\ \dfrac{e^{-0.5\alpha_{\text{high}}^2}}{\left[\frac{\alpha_{\text{high}}}{n_{\text{high}}}\left(\frac{n_{\text{high}}}{\alpha_{\text{high}}} - \alpha_{\text{high}} + t\right)\right]^{n_{\text{high}}}} & \text{if } t > \alpha_{\text{high}}, \end{cases}
$$

$$t = (m_{\mu\mu} - \mu_{\text{CB}})/\sigma_{\text{CB}}$$

$n_h$ = const = 6

$n_l$ = const = 3

Muonic channel parameterization
Also good for the mixed channel

Poor statistics for $m_{\gamma_d}$ = 2 GeV —> excluded from the extrapolation of parameters

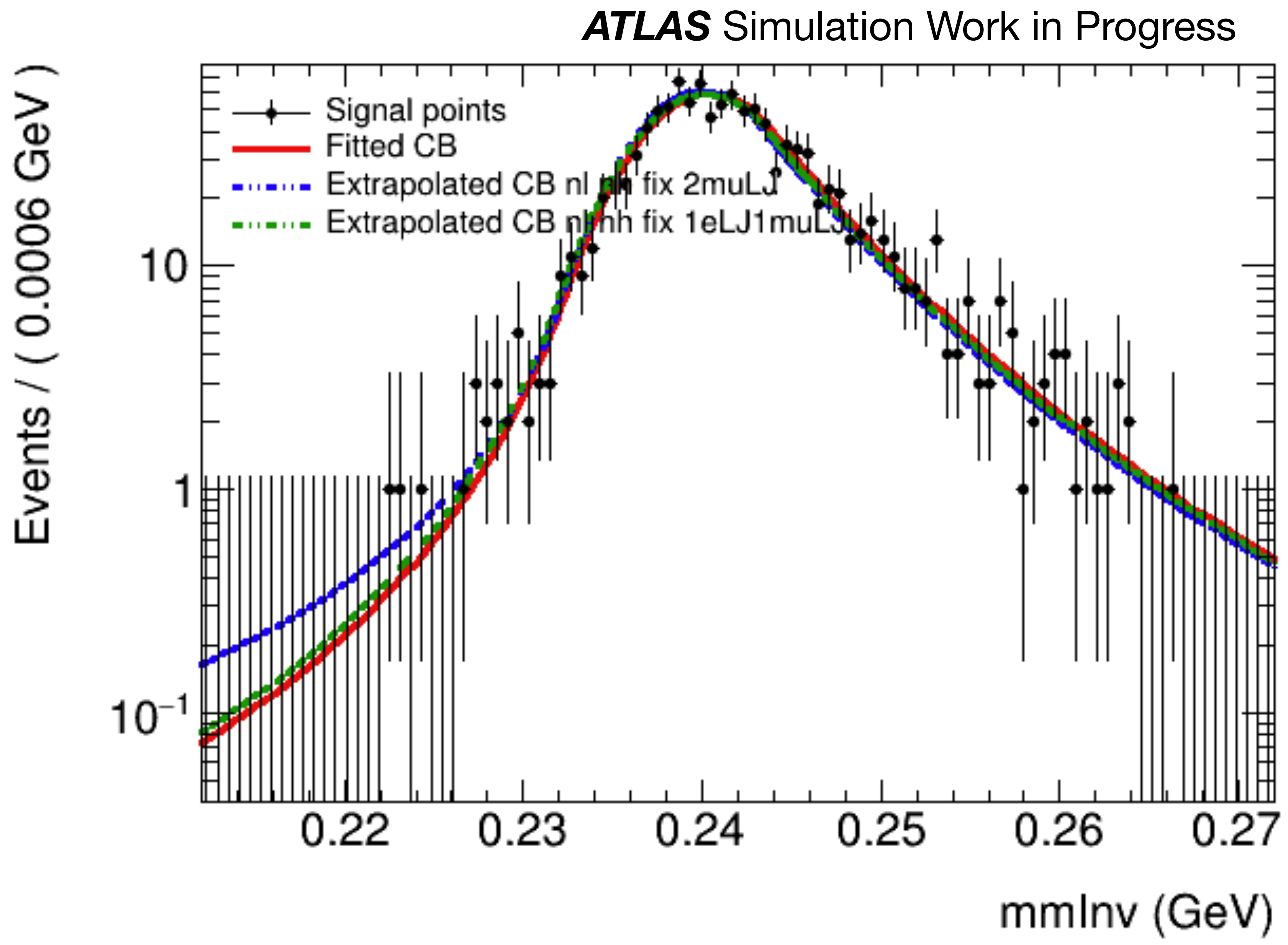

# Signal shape modelling: FRVZ

240 MeV

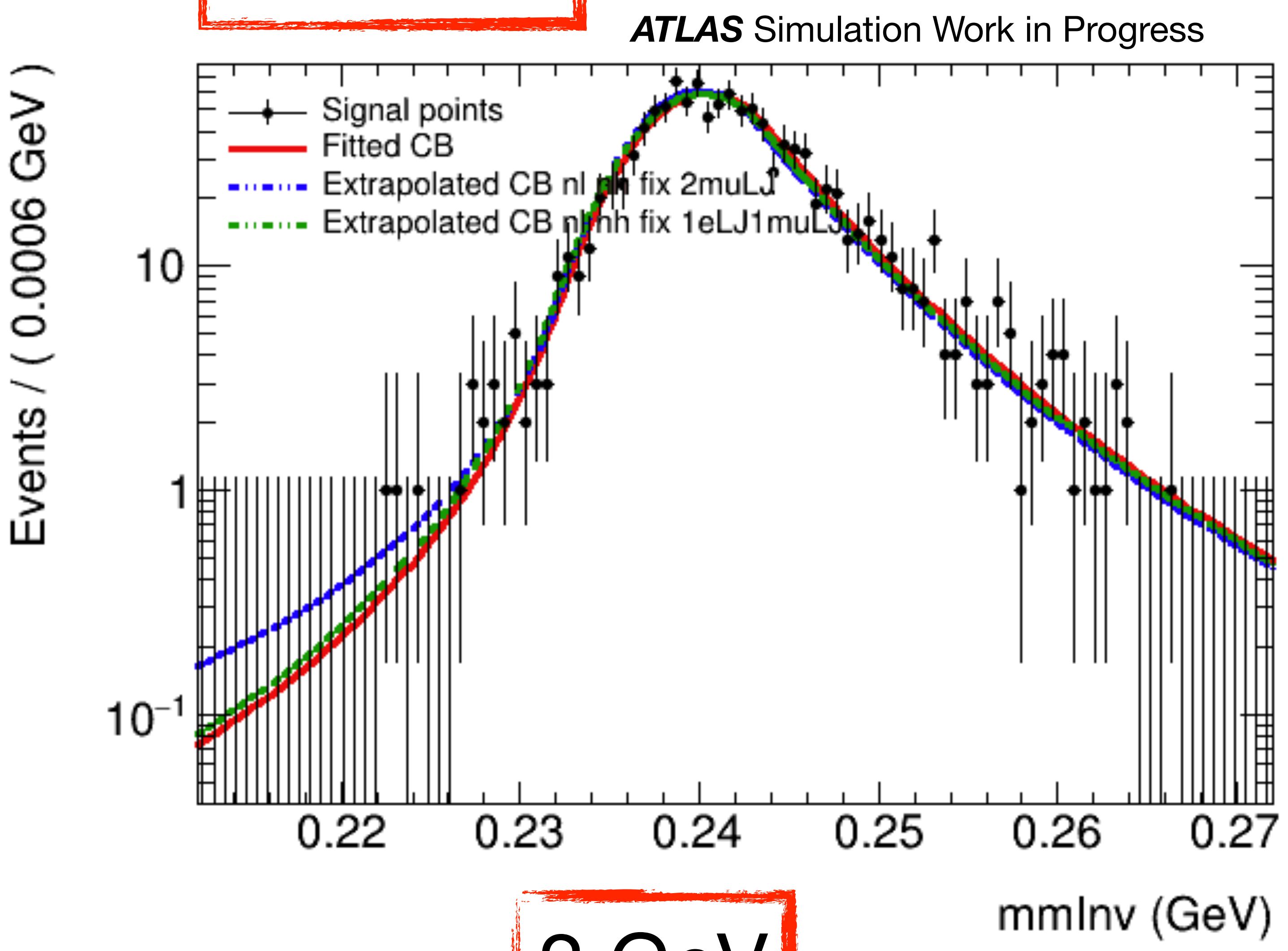


400 MeV

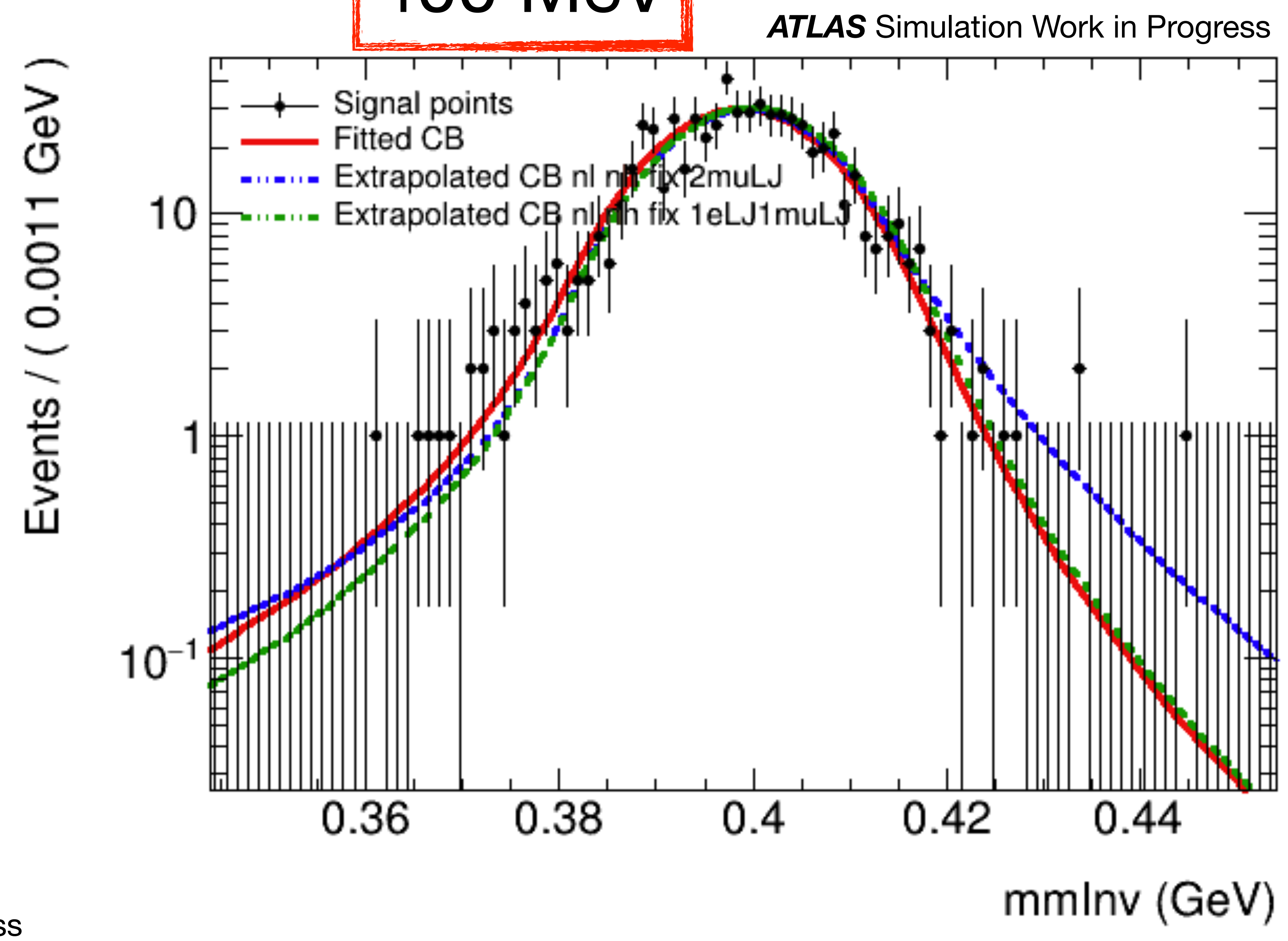


900 MeV

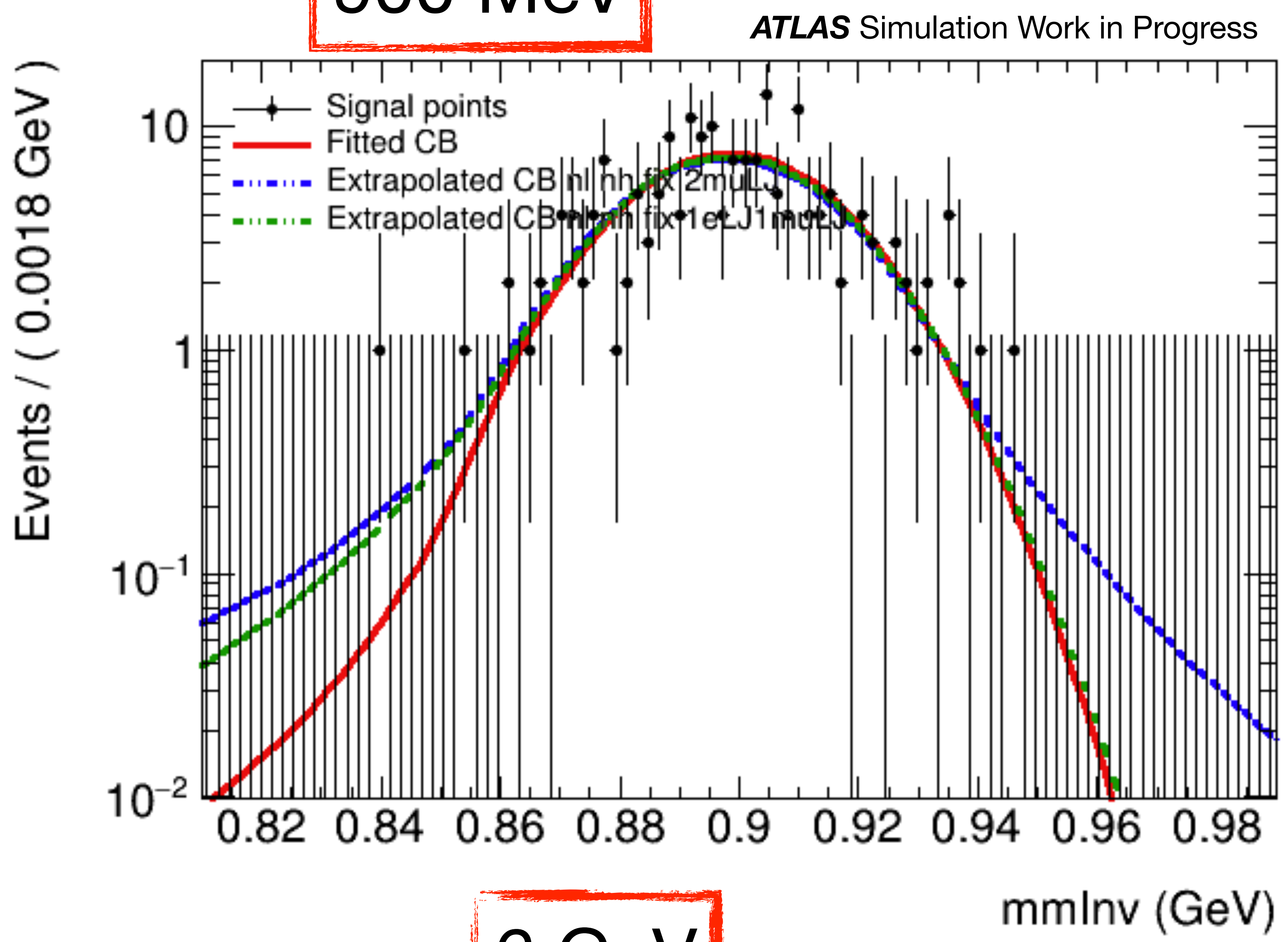


2 GeV

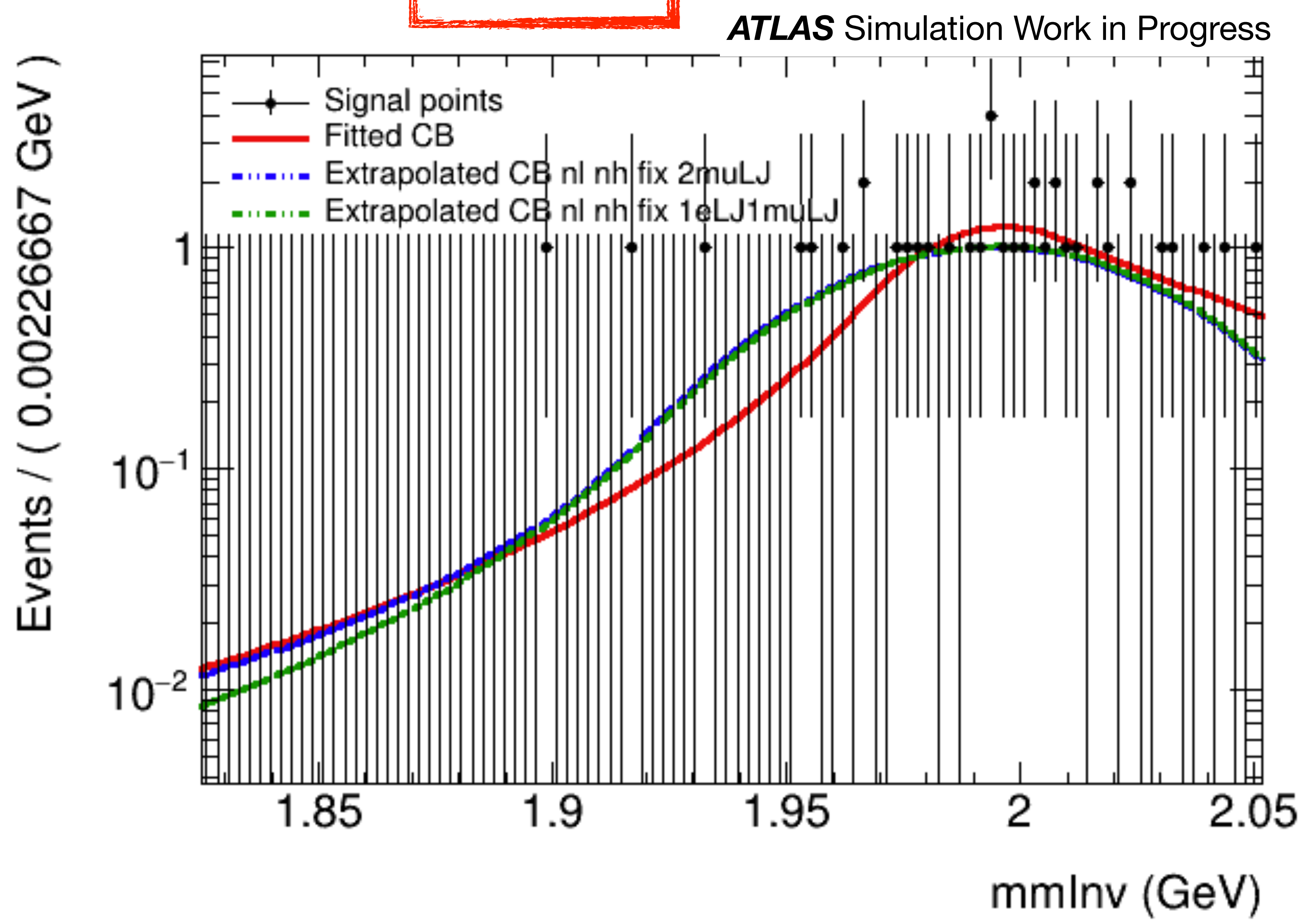


Fit DSCB

DSCB extrapolated 2$\mu$LJ

DSCB extrapolated $\mu$LJ-eLJ

6 GeV

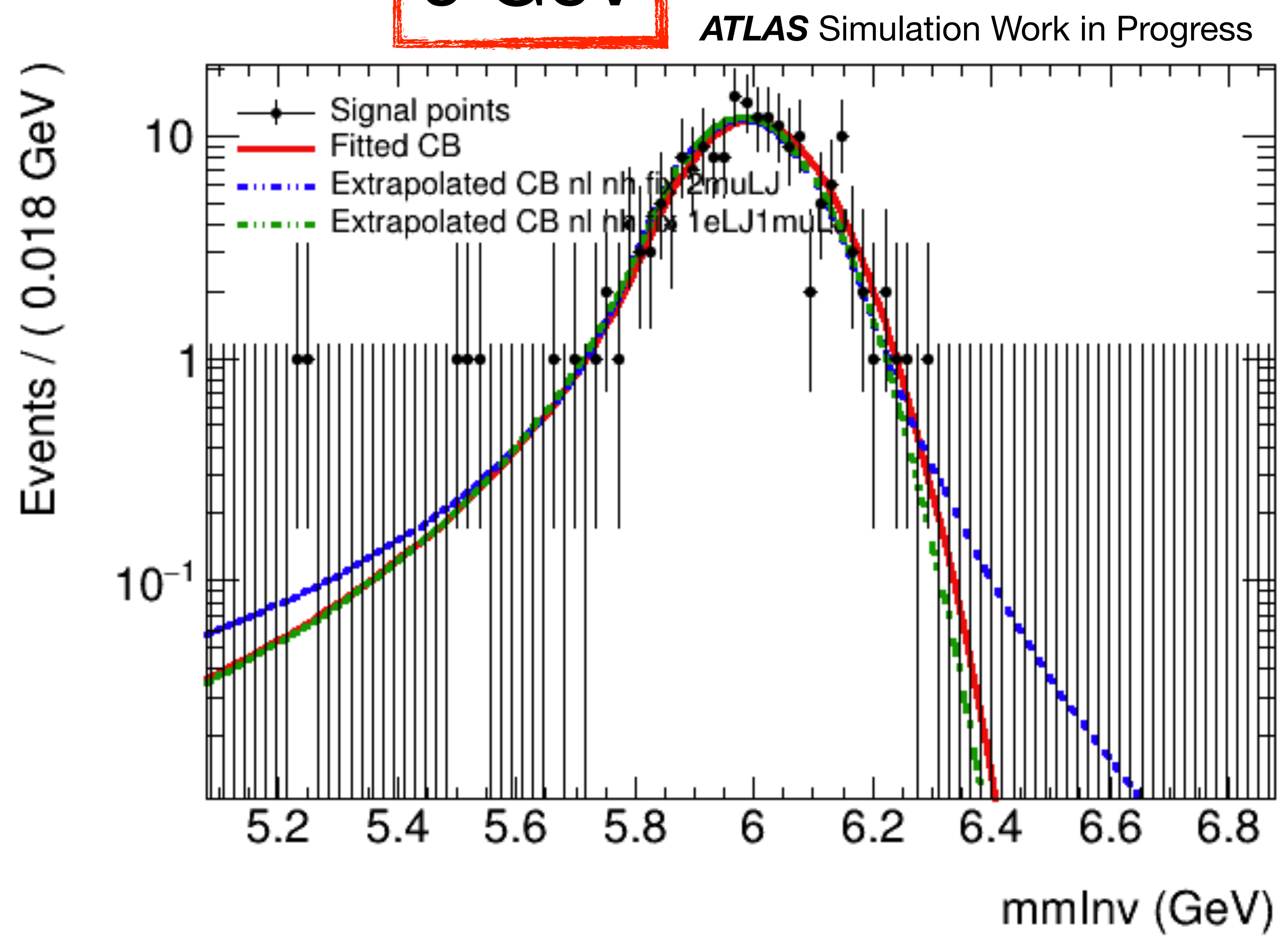

# Parameter extrapolation: FRVZ

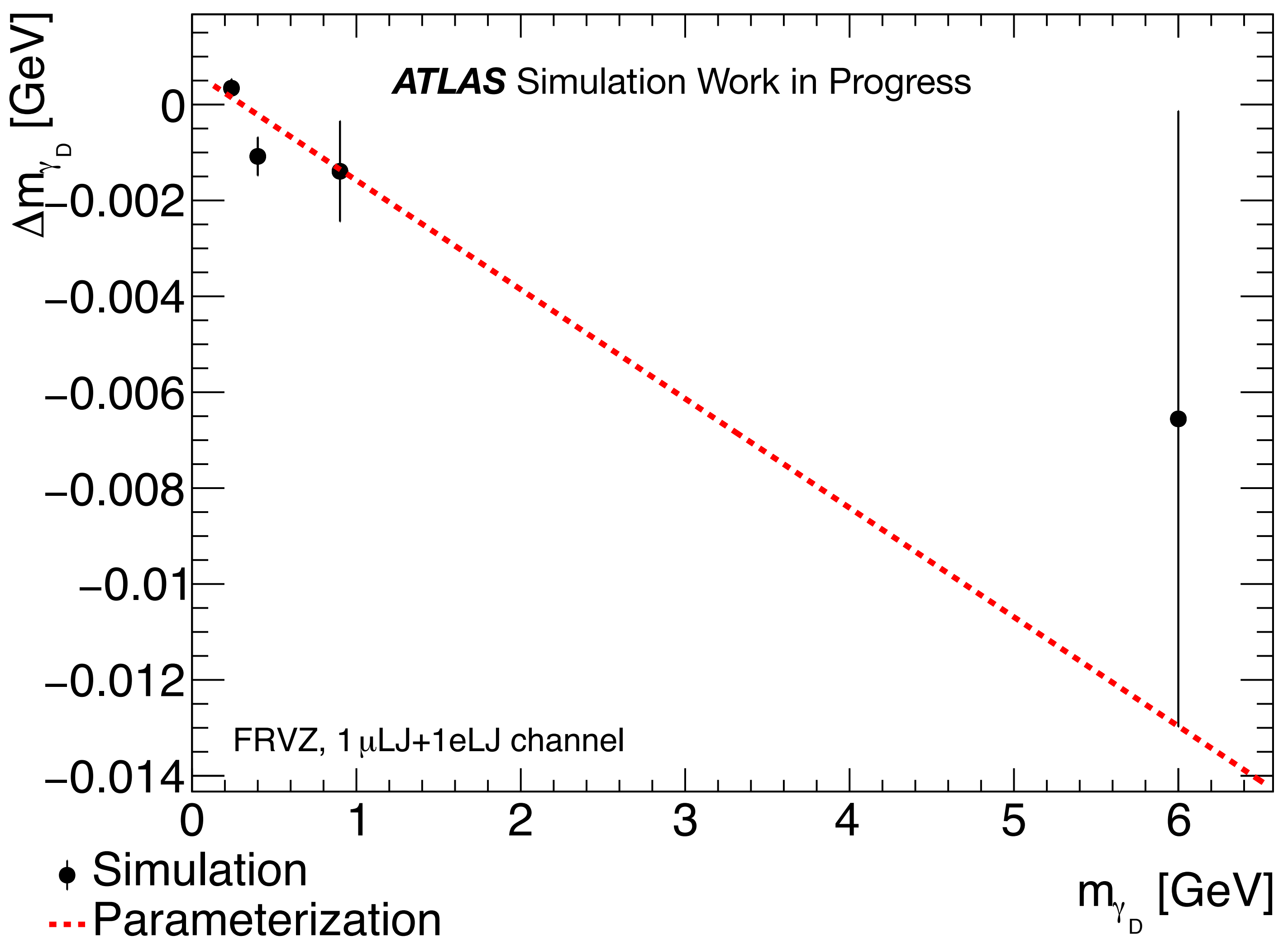


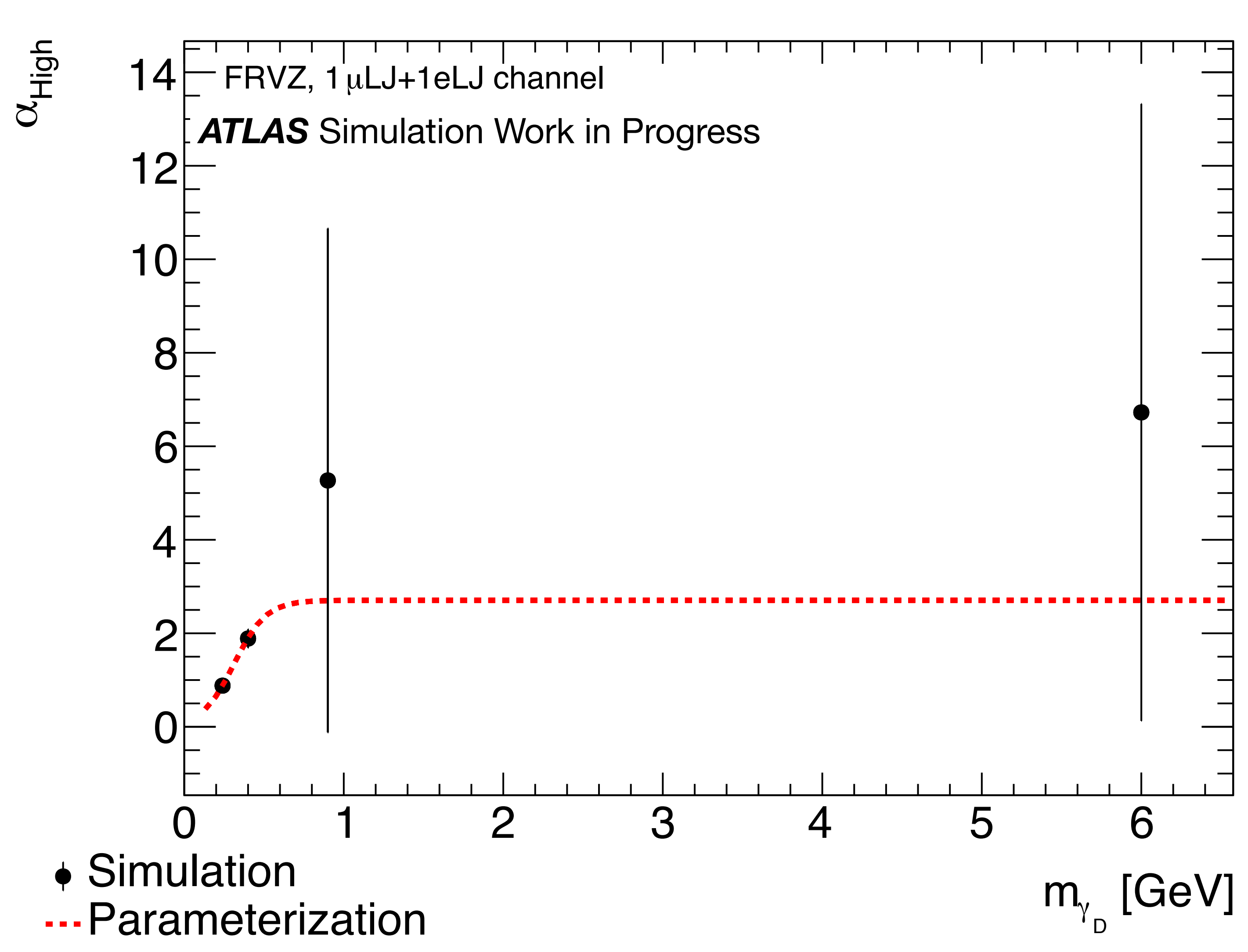


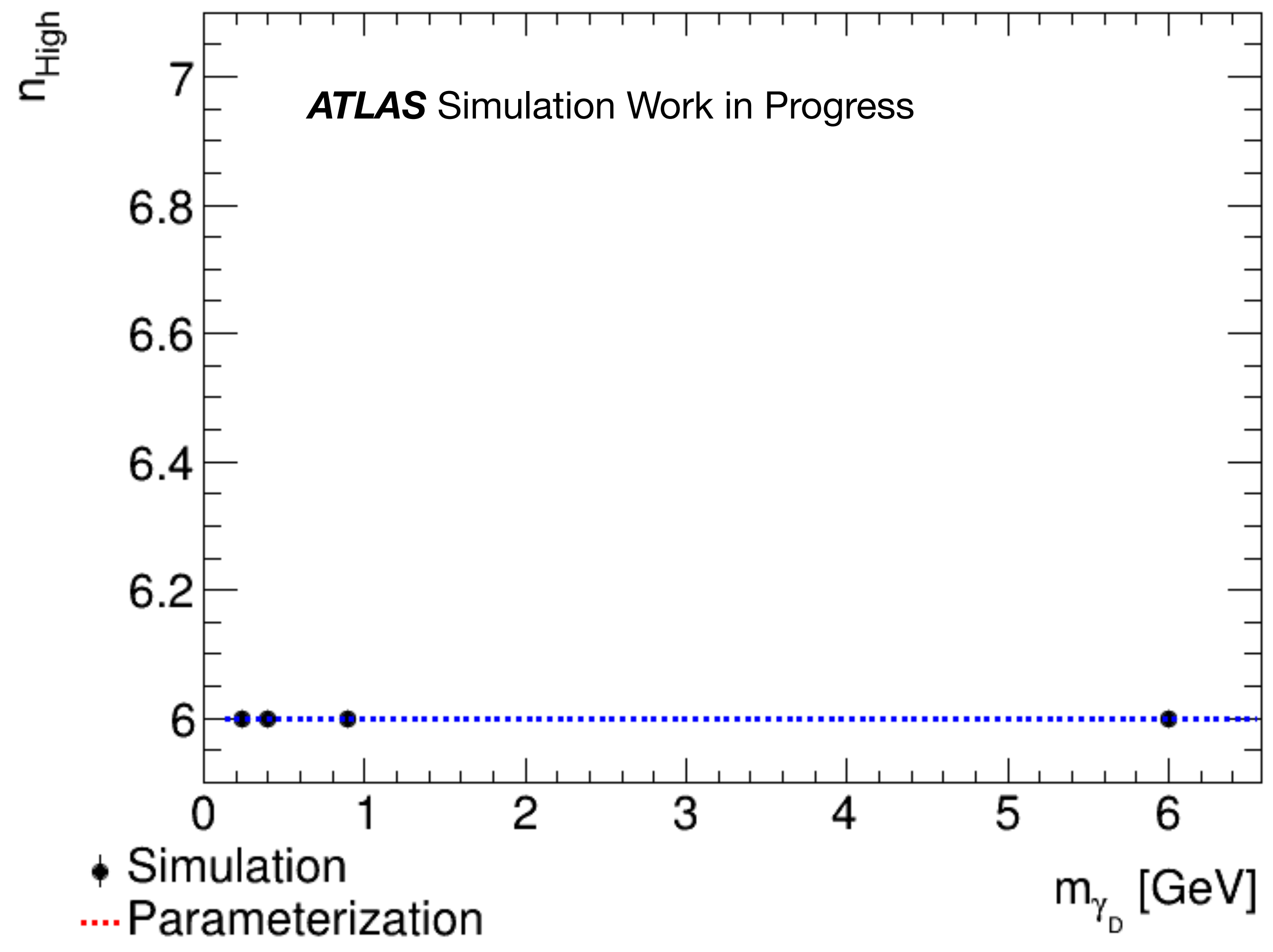


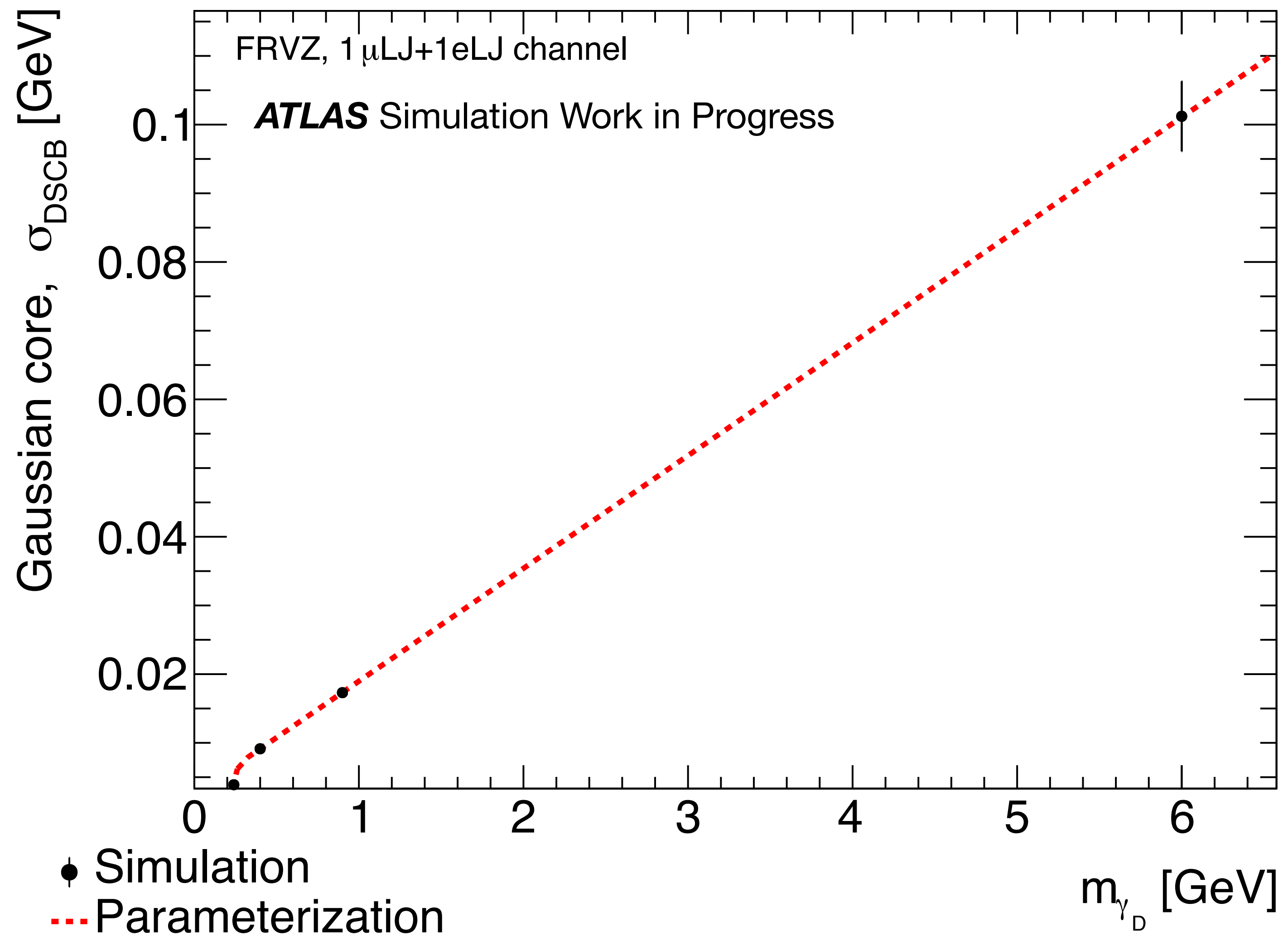


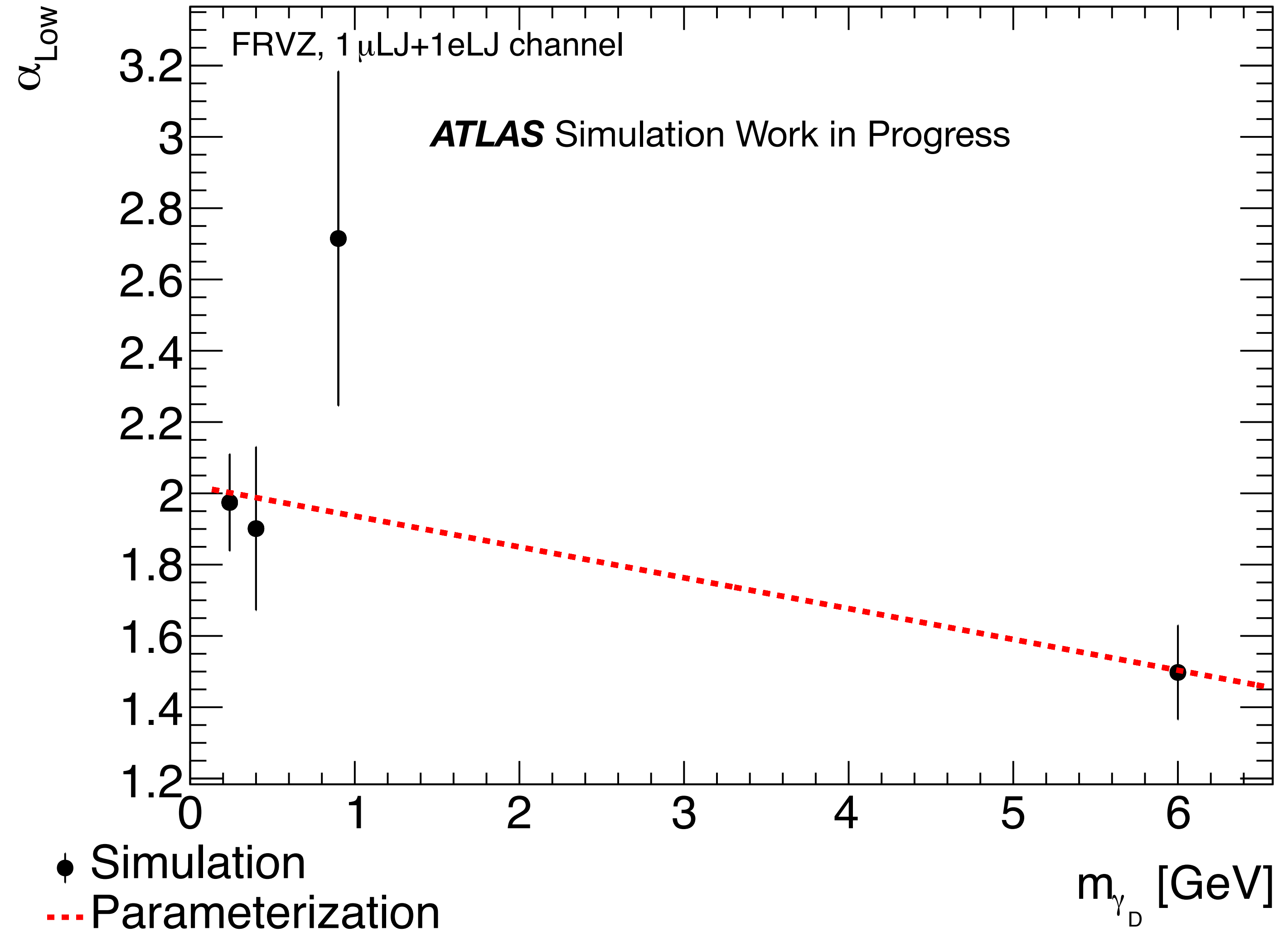


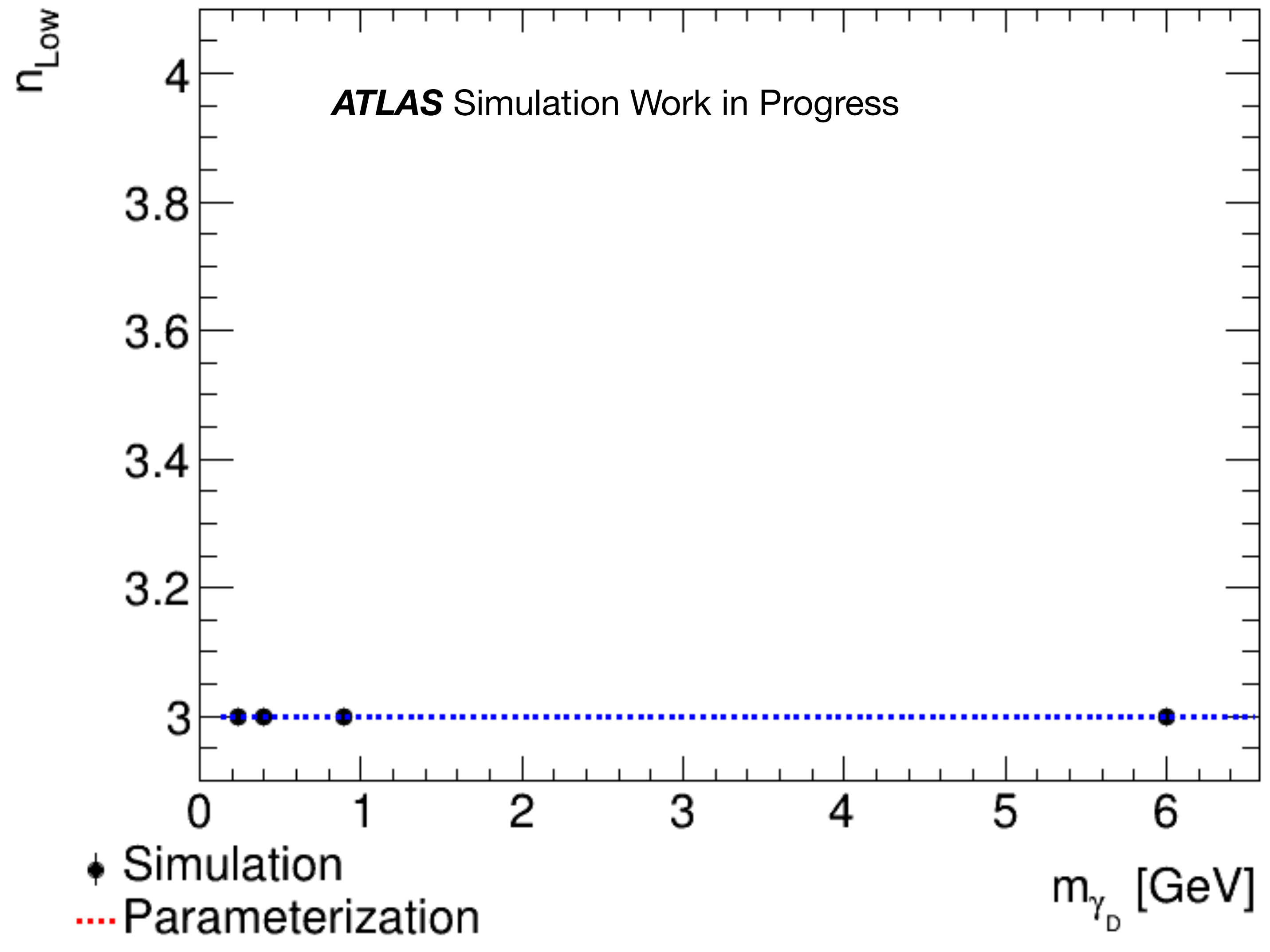

# Signal shape modelling: HAHM

400 MeV

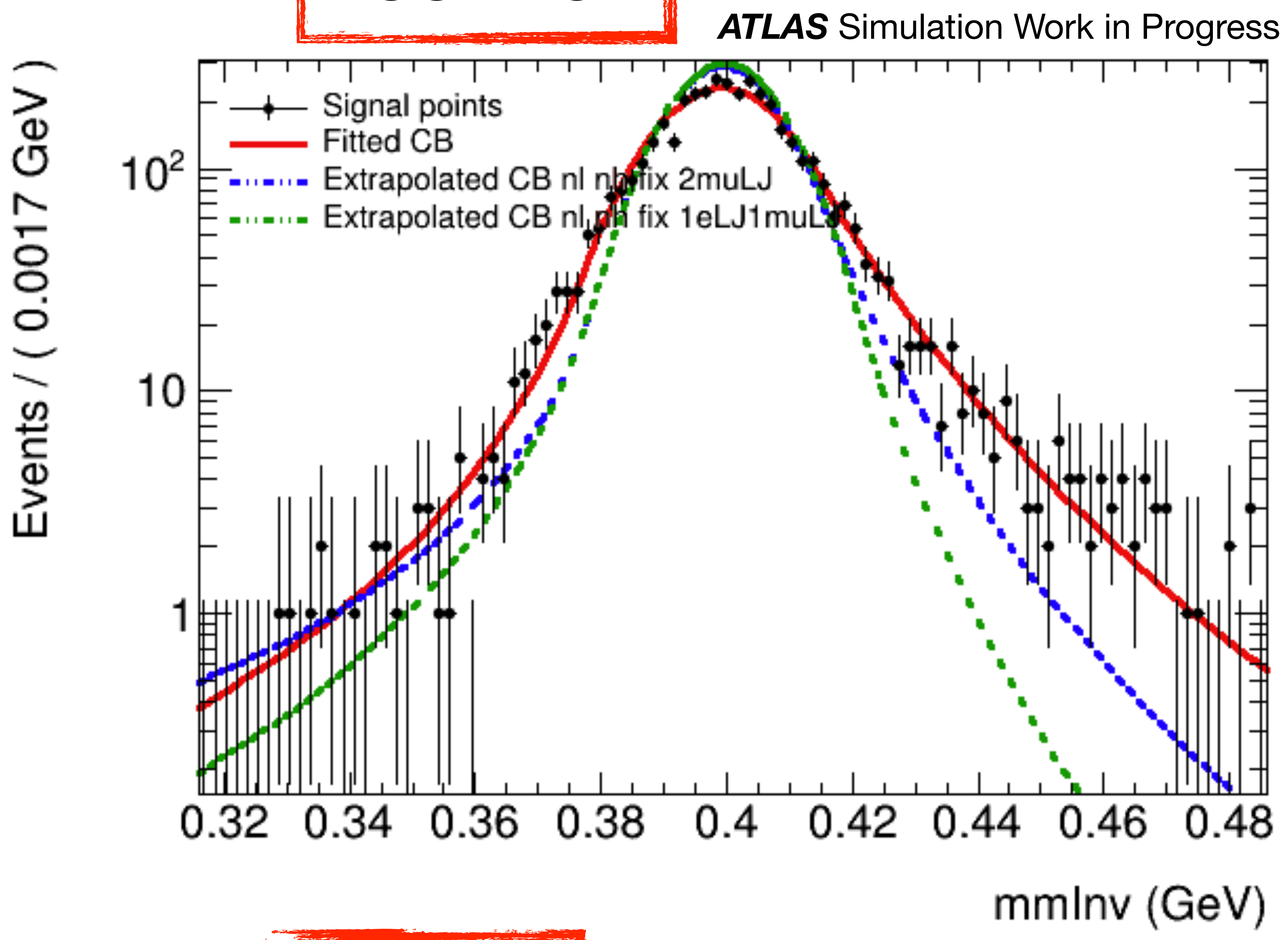


10 GeV

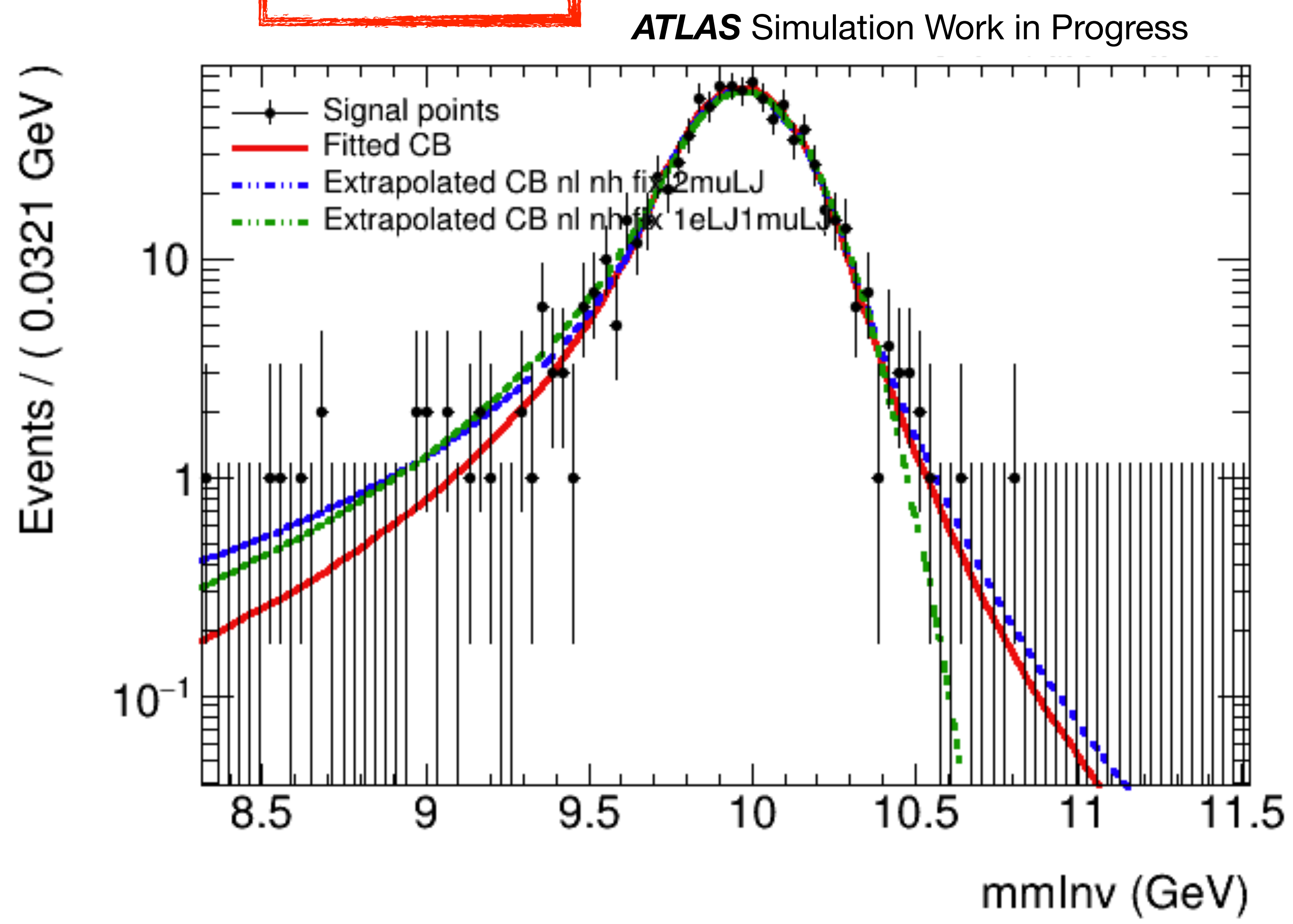


2 GeV

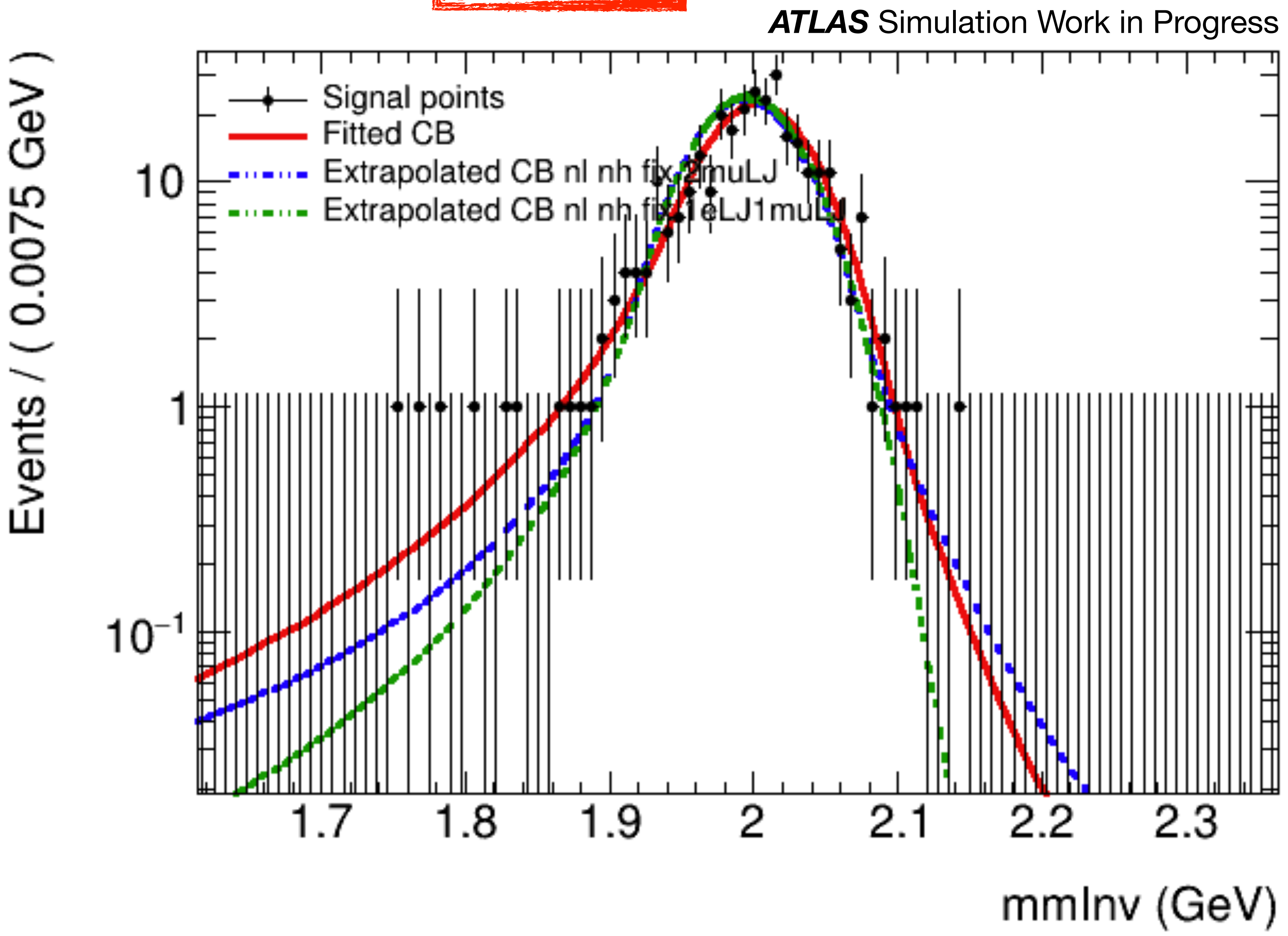


Fit DSCB

DSCB extrapolated 2$\mu$LJ

DSCB extrapolated $\mu$LJ-eLJ

# Parameter extrapolation: HAHM

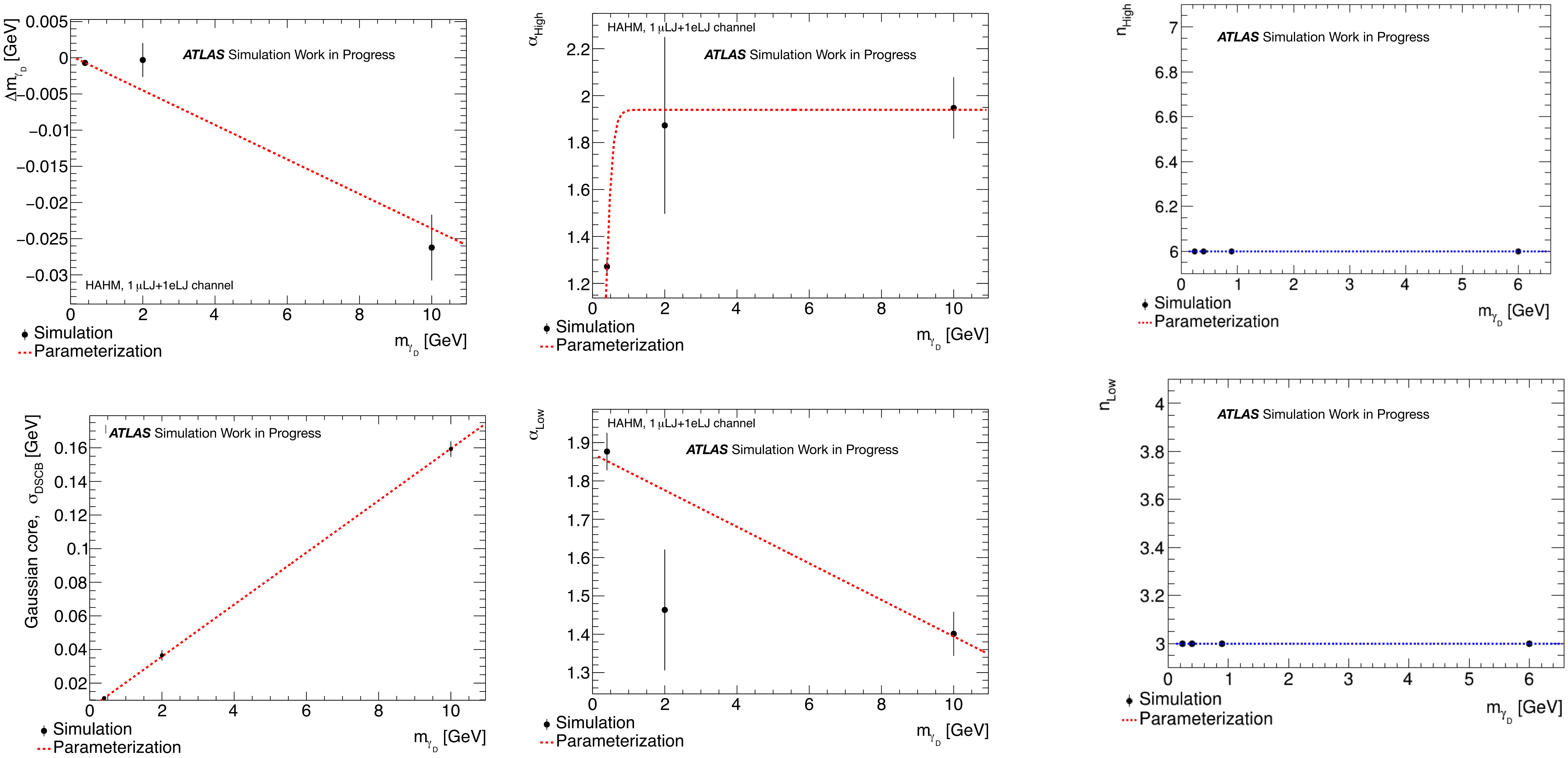

# Injection test

Check if the signal rendering 'injected' agrees with the fitted one

Slight dependence of the fit on modelling (Using muonic channel parameterization)

Mismodelling covered by 5% uncertainty

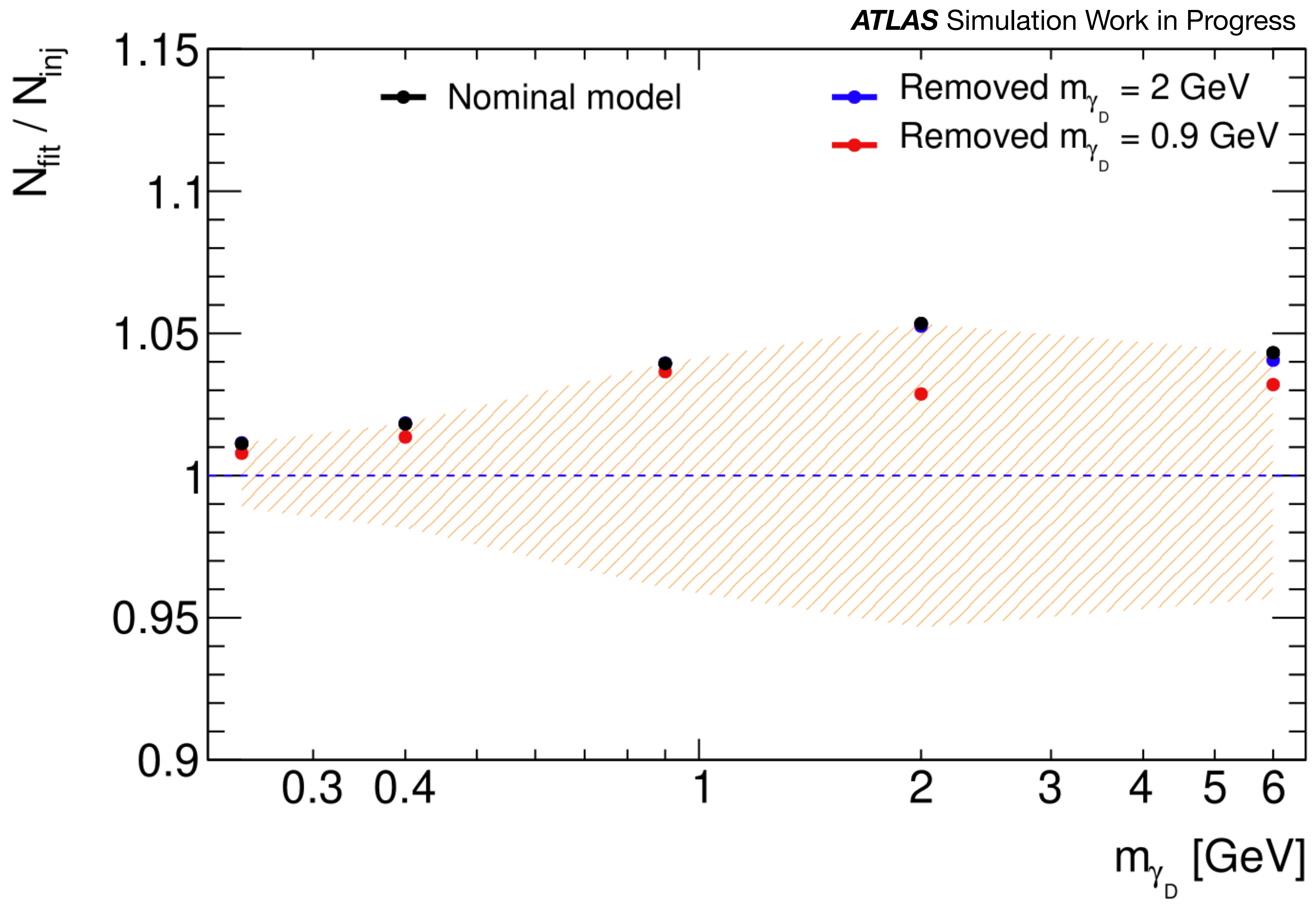

# Acceptance X Efficiency

$$\mathcal{A}\times\epsilon|_{\mu\text{LJ}-e\text{LJchannel}} = \mathcal{A}\times\epsilon|_{\gamma_d\to 2\mu,\gamma_d\to 2e} BR(\gamma_d \to 2\mu) BR(\gamma_d \to 2e) \times 2$$

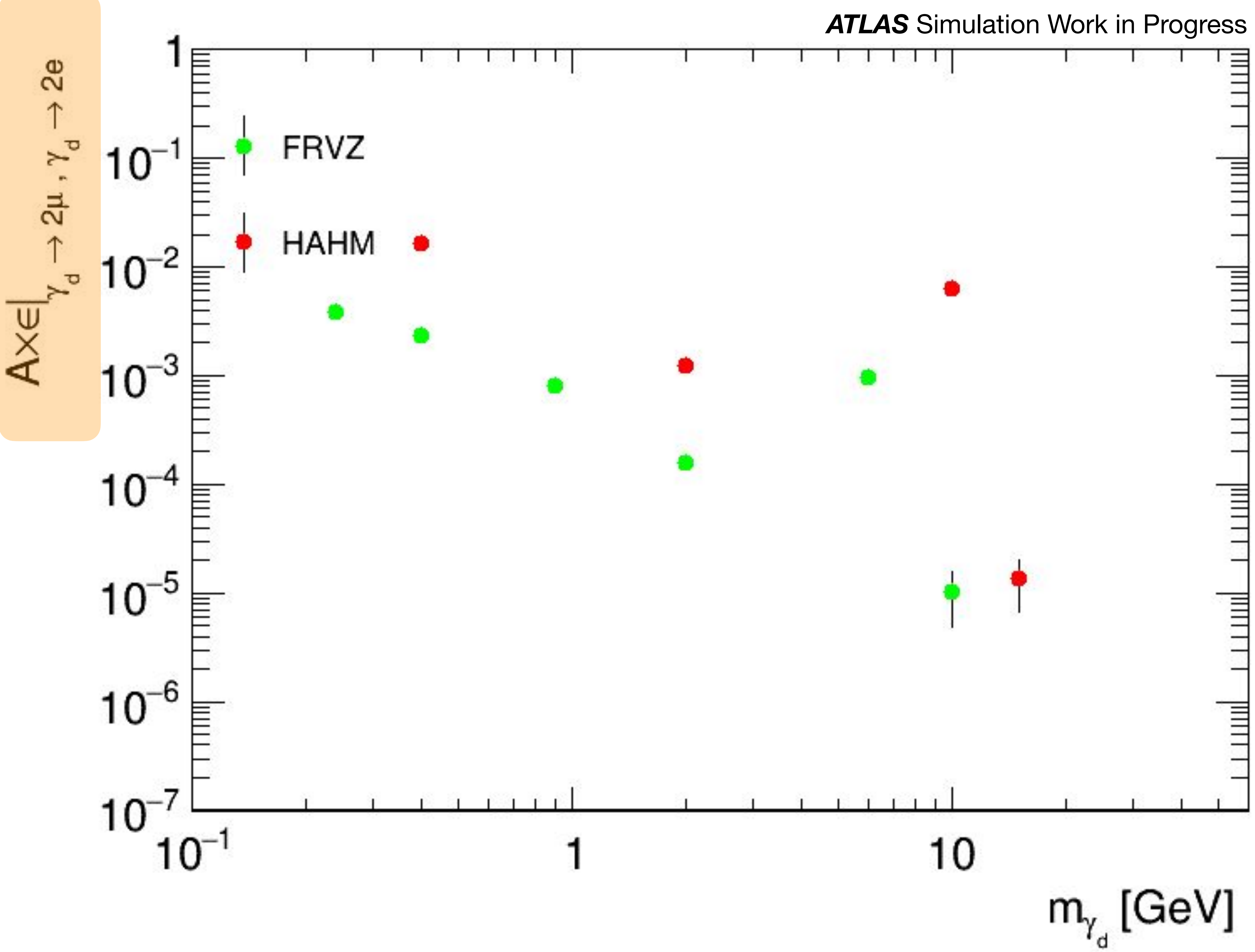


$A\times\epsilon$ can change due to:

- $BR(\gamma_d \to 2\mu), BR(\gamma_d \to 2e)$
- $\Delta R$ of decay products —> Efficiency of reconstruction of the LJs
- $p_{\mathrm{T}}$ of leptons —> acceptance of triggers

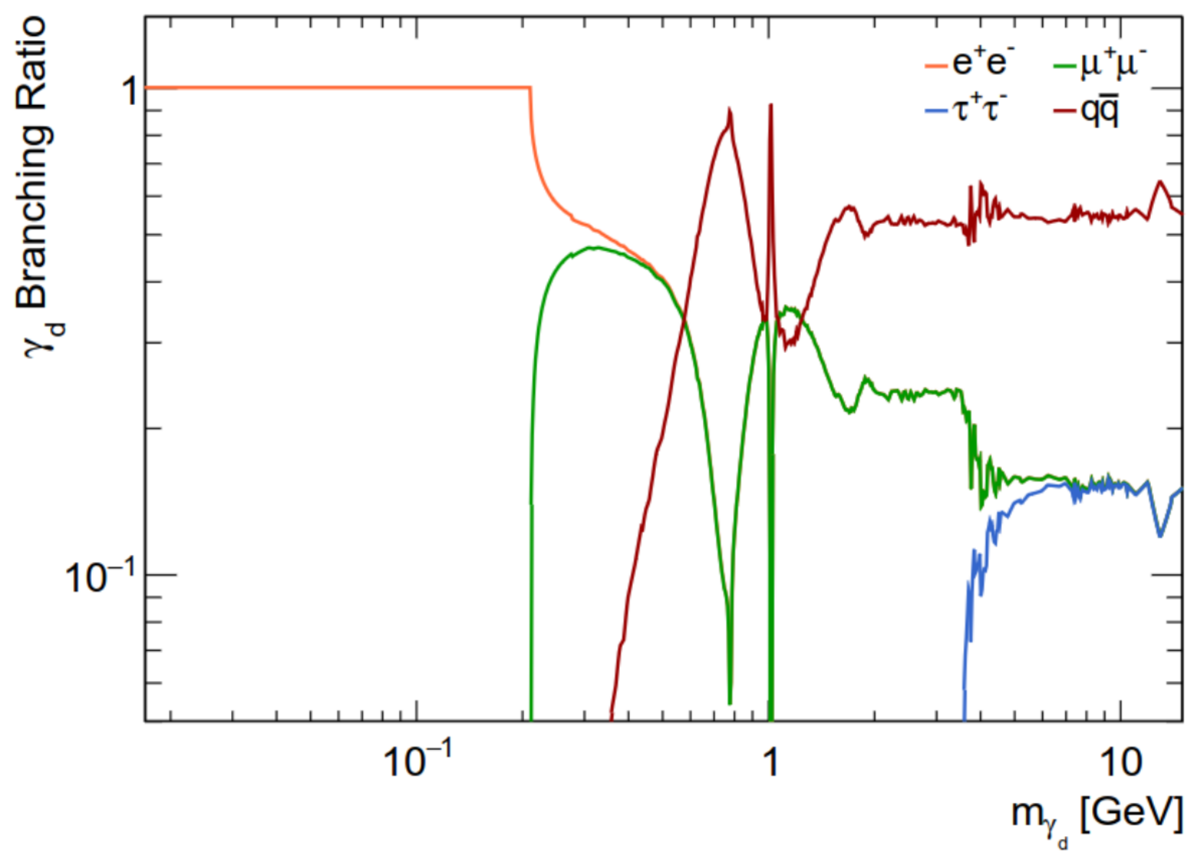

# Acceptance X Efficiency: 1 electron in eLJ

$$\mathcal{A} \times \epsilon|_{\mu\text{LJ}-e\text{LJchannel}} = \mathcal{A} \times \epsilon|_{\gamma_d \to 2\mu, \gamma_d \to 2e} BR(\gamma_d \to 2\mu) BR(\gamma_d \to 2e) \times 2$$

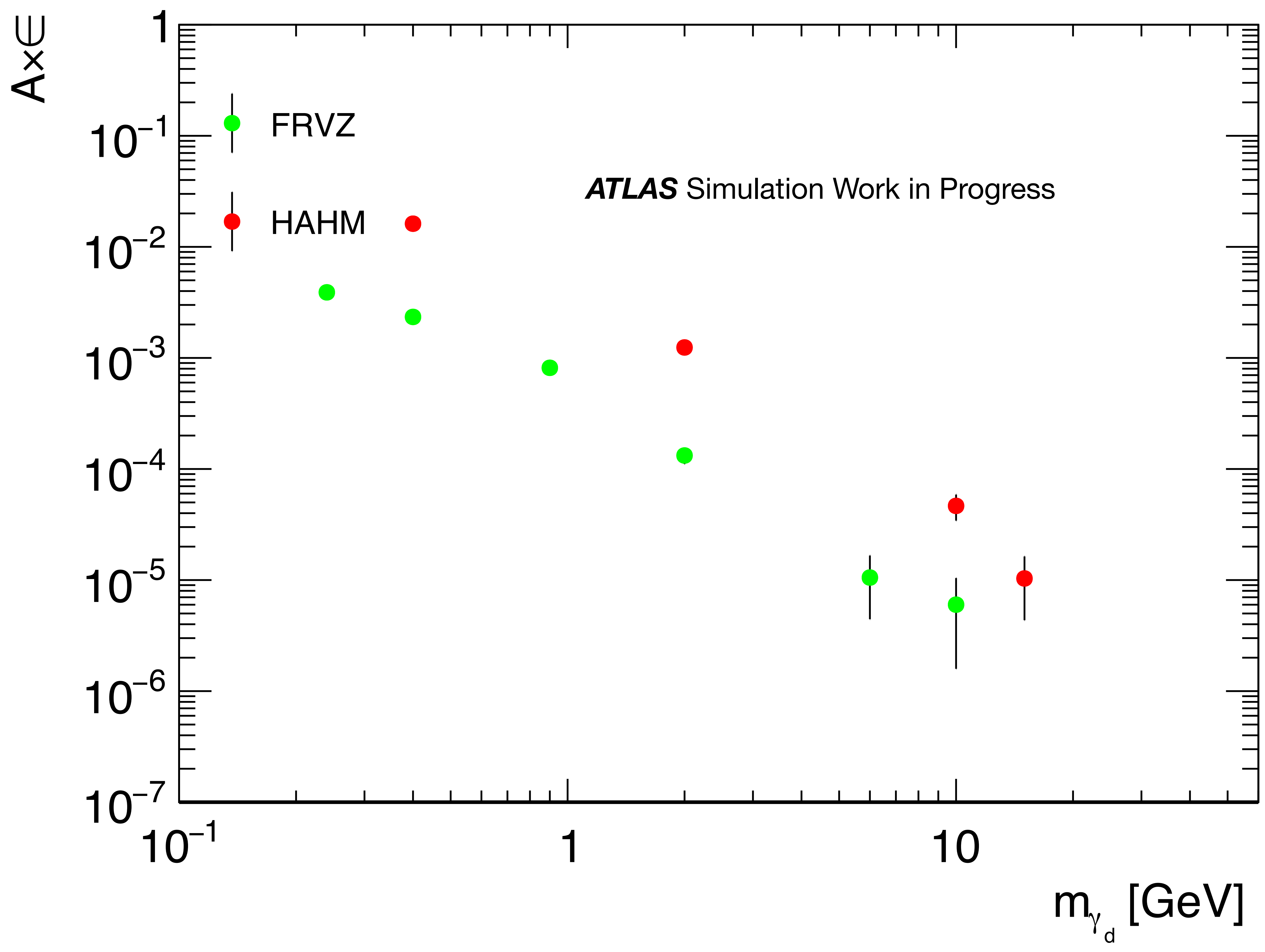


$A \times \epsilon$ can change due to:

- $BR(\gamma_d \to 2\mu), BR(\gamma_d \to 2e)$
- $\Delta R$ of decay products —> Efficiency of reconstruction of the LJs
- $p_T$ of leptons —> acceptance of triggers

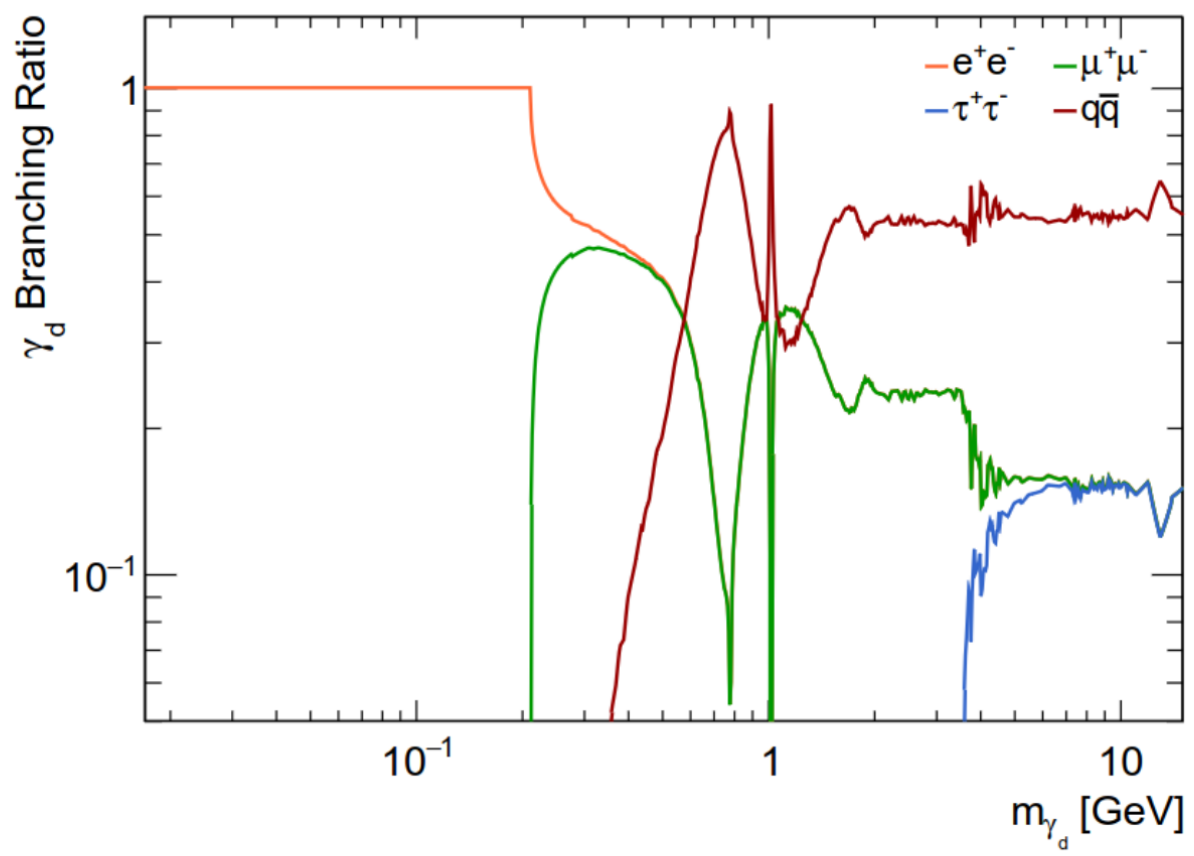

# Acceptance X Efficiency: 2 electrons in eLJ

$$\mathcal{A} \times \epsilon|_{\mu\text{LJ}-e\text{LJchannel}} = \mathcal{A} \times \epsilon|_{\gamma_d \to 2\mu, \gamma_d \to 2e} BR(\gamma_d \to 2\mu) BR(\gamma_d \to 2e) \times 2$$

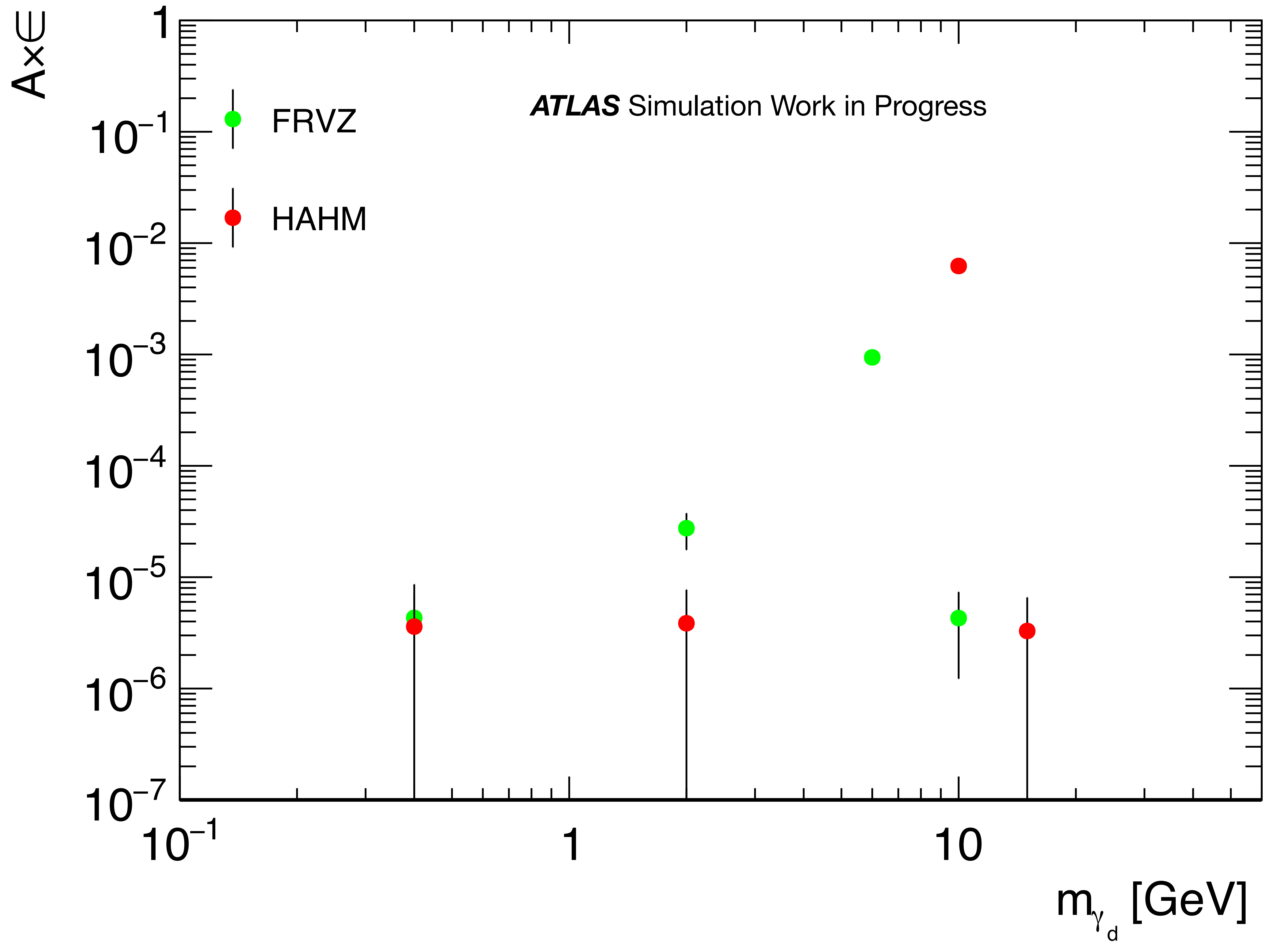


$A \times \epsilon$ can change due to:

- $BR(\gamma_d \to 2\mu), BR(\gamma_d \to 2e)$
- $\Delta R$ of decay products —> Efficiency of reconstruction of the LJs
- $p_{\text{T}}$ of leptons —> acceptance of triggers

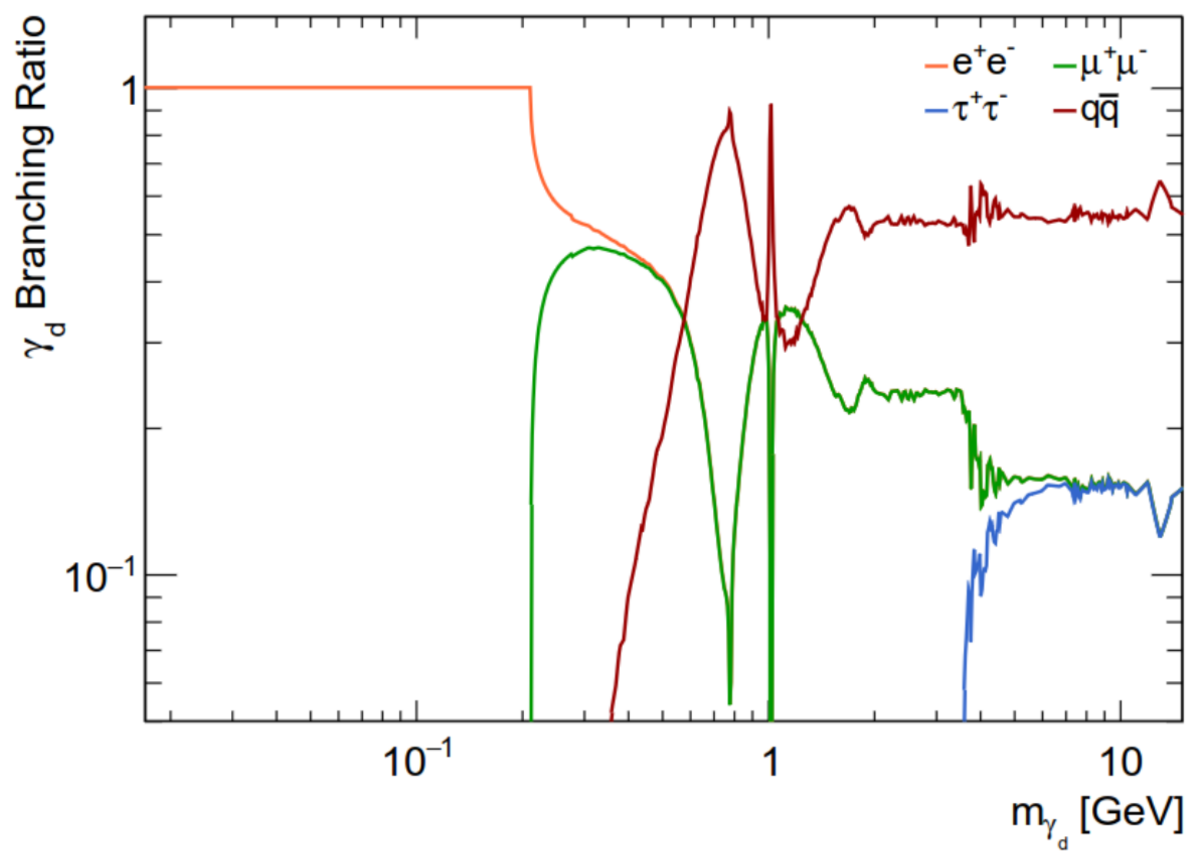

# Spurious Signal

Poor background —> risk of induced background (Spurious Signal)

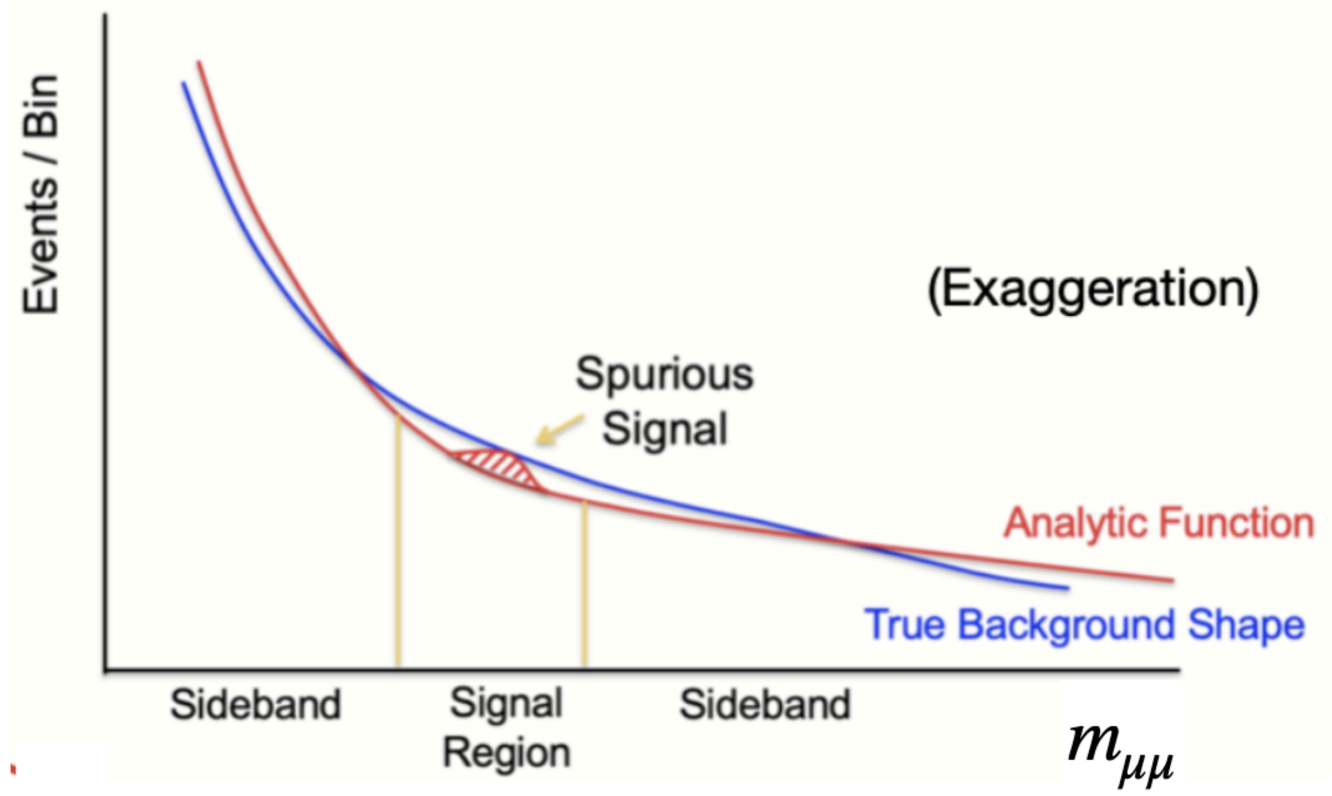


Smoothed template

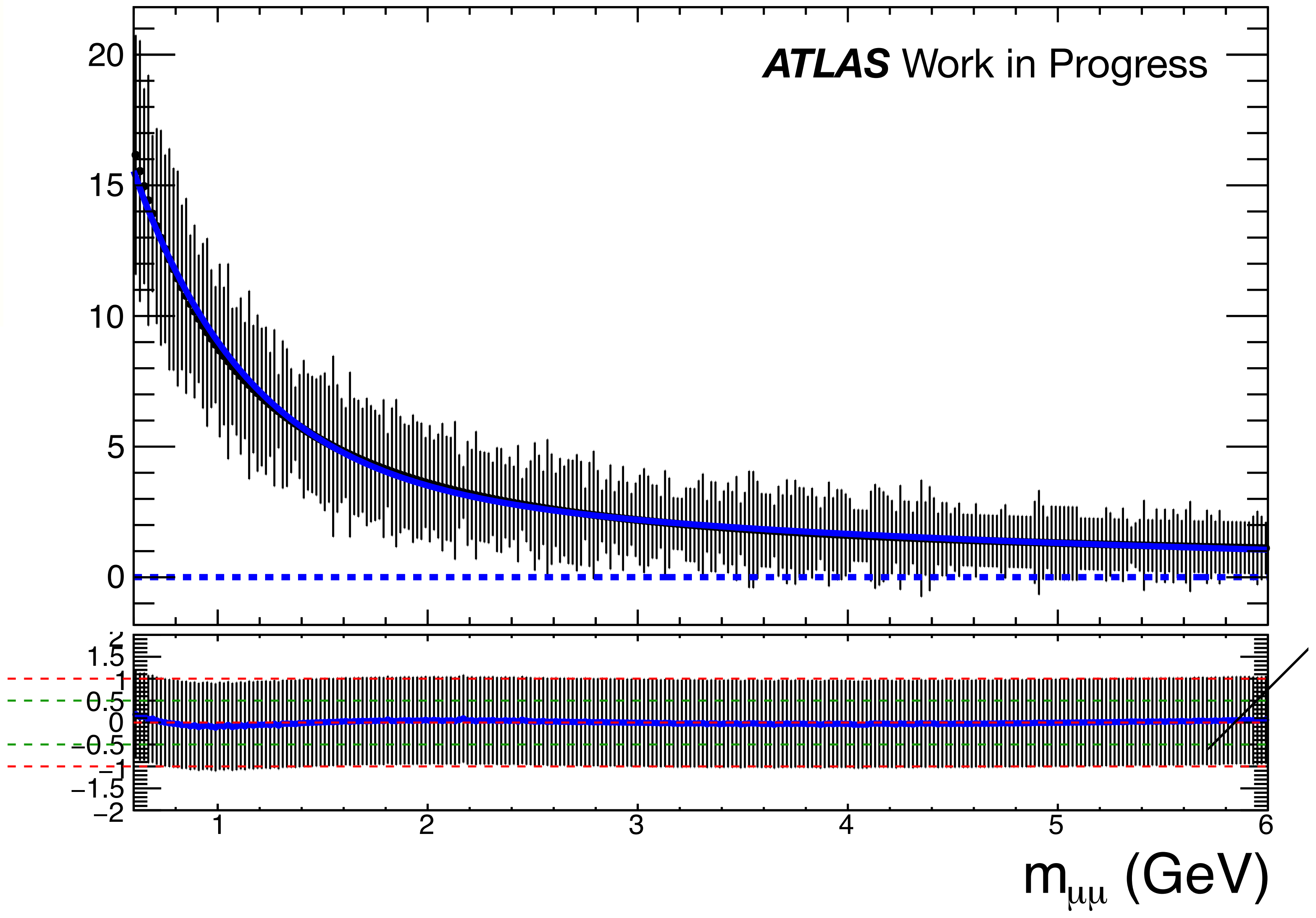


SS **before** and **after smoothing**

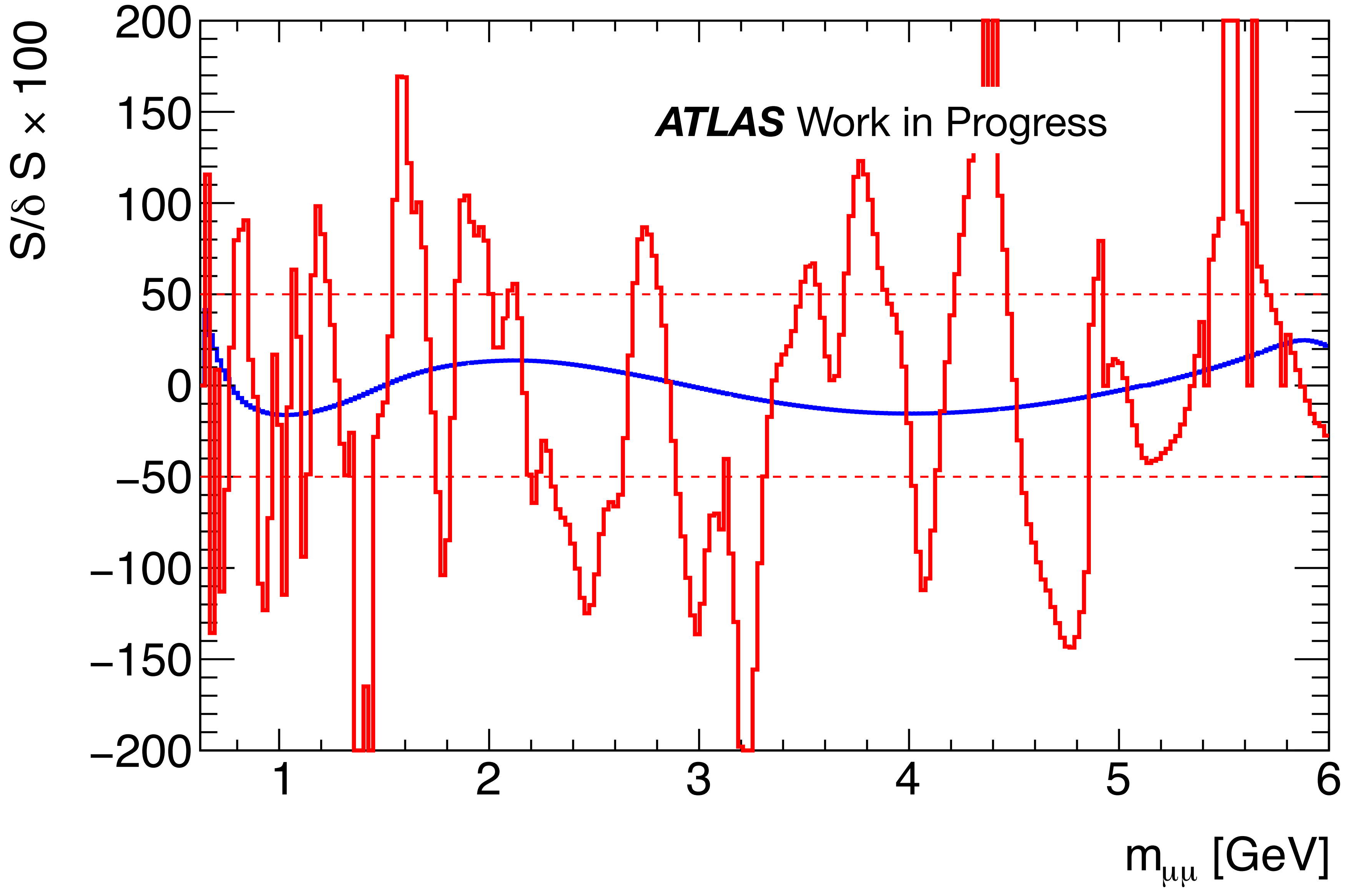


Systematics must be in $0.5\sigma_{stat}$

Systematics of Spurious Signal calculated via fit S+B on template of only background → Very sensible to statistical fluctuations

▶ **Smoothed template**

# Systematics

| $m_{\gamma_d}$ (GeV) | triggers (%) | $\mu$LJ reconstruction (%) | $\mu$LJ isolation (%) | $\mu$LJ TTVA (%) | eLJ reconstruction (%) | eLJ ID (%) | eLJ isolation (%) | PRW (%) | egamma resolution (%) | egamma scale (%) | muon ID (%) | muon MS (%) | muon scale (%) | Total (%) |
|---|---|---|---|---|---|---|---|---|---|---|---|---|---|---|
| 0.24 | 0.77 | 0.06 | 1.10 | 0.04 | 0.38 | 0.53 | 0.07 | 2.17 | 0.23 | 0.29 | 0.12 | 0.22 | 0.12 | 2.68 |
| 0.40 | 0.49 | 0.04 | 1.16 | 0.04 | 0.36 | 0.48 | 0.06 | 1.33 | 0.15 | 0.01 | 0.18 | 0.06 | 0.35 | 1.98 |
| 0.90 | 0.63 | 0.08 | 1.14 | 0.07 | 0.25 | 0.26 | 0.03 | 6.56 | 0.56 | 0.58 | 0.52 | 0.03 | 0.04 | 6.77 |
| 2 | 0.65 | 0.01 | 1.00 | 0.19 | 0.69 | 1.33 | 0.91 | 7.59 | 4.75 | 4.71 | 0.04 | 0.03 | 0.03 | 10.34 |
| 6 | 1.84 | 0.10 | 0.55 | 0.03 | 1.37 | 3.98 | 2.66 | 2.66 | 0.06 | 0.32 | 0.32 | 0.69 | 0.66 | 6.06 |

Table 8.5: Summary table of the systematic uncertainties on FRVZ signal MC events in the $\mu$LJ- $e$LJ channel.

| $m_{\gamma_d}$ (GeV) | triggers (%) | $\mu$LJ reconstruction (%) | $\mu$LJ isolation (%) | $\mu$LJ TTVA (%) | eLJ reconstruction (%) | eLJ ID (%) | eLJ isolation (%) | PRW (%) | egamma resolution (%) | egamma scale (%) | muon ID (%) | muon MS (%) | muon scale (%) | Total (%) |
|---|---|---|---|---|---|---|---|---|---|---|---|---|---|---|
| 0.40 | 0.28 | 0.10 | 0.53 | 0.04 | 0.36 | 0.25 | 0.02 | 0.01 | 0.04 | 0.07 | 0.06 | 0.06 | 0.17 | 0.78 |
| 2 | 0.15 | 0.12 | 0.56 | 0.01 | 0.37 | 0.26 | 0.04 | 3.9 | 0.02 | 0.48 | 0.01 | 0.00 | 0.00 | 4.00 |
| 10 | 0.35 | 0.16 | 0.28 | 0.01 | 1.14 | 0.42 | 0.06 | 0.43 | 0.04 | 0.11 | 0.04 | 0.00 | 0.00 | 1.38 |

Table 8.6: Summary table of the systematic uncertainties on HAHM signal MC events in the $\mu$LJ- $e$LJ channel.

# Isolation for boosted muons

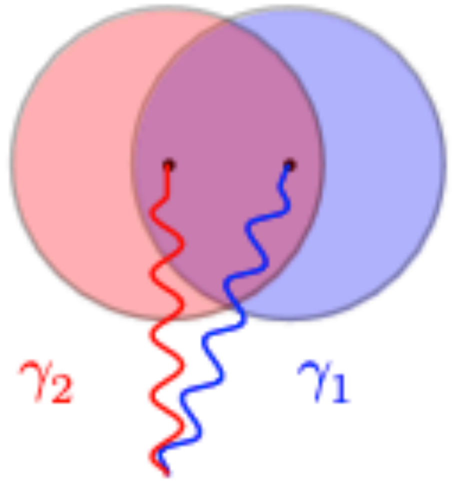


**Recommended isoWP: PflowLoose VarRad:** $\texttt{ptvarcone30} + 0.4 * \texttt{neflowisol20} < 0.16 p_T^{\mu}$,

$\mu$ in $\mu$LJ fails standard iso WP (ptvarcone30) → corrected isolation developed

Corrected isolation: as ptvarcone30, removing track belonging to close-by muon (isoCloseByTool)

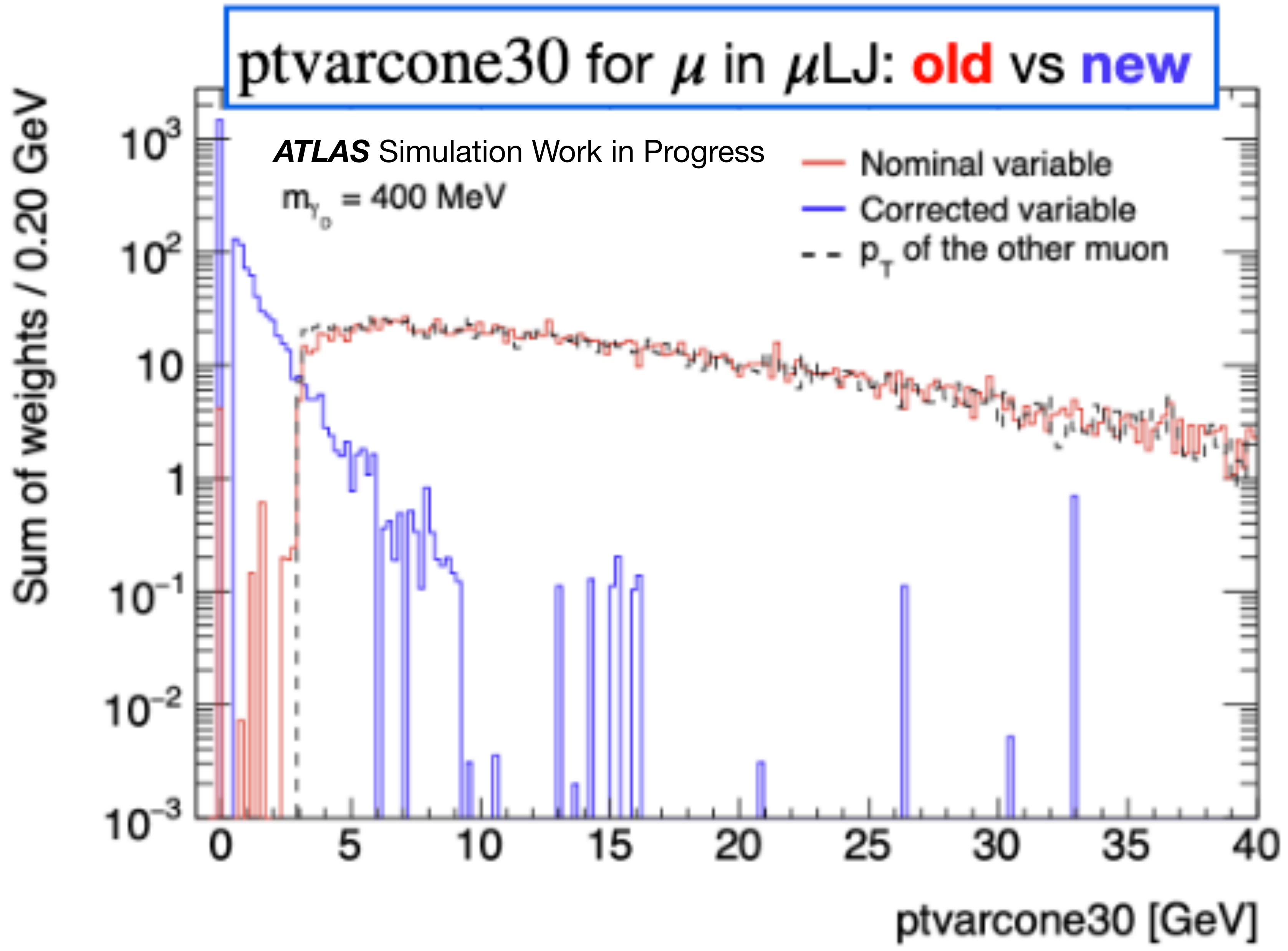


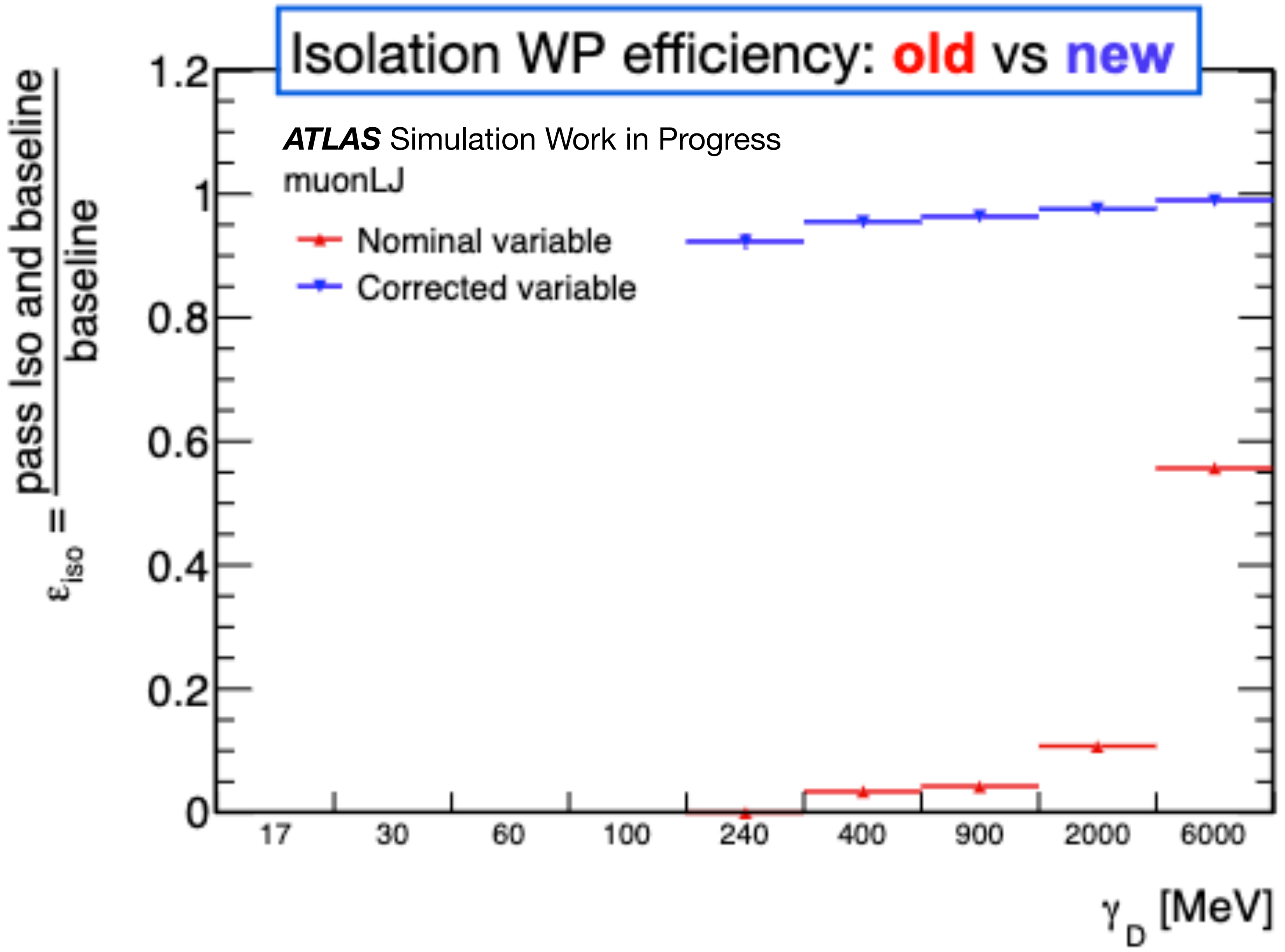


Used by HZZ analysis as well!

**Efficiency increased up to 90 % !!**

# Triggers muonic channel

| Type | Data-taking periods | Trigger |
|---|---|---|
| di-muon | 2015 | HLT_mu18_mu8noL1 |
| | 2015 - 2016 A | HLT_2mu10 |
| | 2016 A | HLT_2mu10_nomucomb |
| | 2016 A-D3 | HLT_mu20_mu8noL1 |
| | 2016 B-end - 2017 - 2018 | HLT_2mu14 |
| | 2016 B-D3 | HLT_2mu14_nomucomb |
| | 2016 D4-end - 2017 - 2018 | HLT_mu22_mu8noL1 |
| tri-muon | 2015 - 2016 B-D3 - 2017 - 2018 | HLT_3mu6 |
| | 2015-2018 - all periods | HLT_3mu6_msonly |

Table 6.1: List of muon triggers used in the $\mu$LJ–$\mu$LJ channelfor the corresponding data-taking periods.

# Signal region muonic channel

| Cuts | $m_{\gamma_d}$ = 0.24 GeV | $m_{\gamma_d}$ = 0.4 GeV | $m_{\gamma_d}$ = 0.9 GeV | $m_{\gamma_d}$ = 2 GeV | $m_{\gamma_d}$ = 6 GeV | $m_{\gamma_d}$ = 10 GeV | $m_{\gamma_d}$ = 15 GeV |
|---|---|---|---|---|---|---|---|
| None | 337900±700 | 337900±700 | 337900±700 | 331200±1100 | 349300±1000 | 337800±700 | 337600±700 |
| $2\mu$LJ | 8760±100 | 11020±120 | 8650±100 | 3300±40 | 422±12 | 145±14 | 40±7 |
| Trigger | 5080±80 | 6700±90 | 5230±80 | 2482±33 | 400±12 | 139±13 | 40±7 |
| Trigger matching | 3460±60 | 4560±70 | 3580±70 | 1839±29 | 344±11 | 137±13 | 37±7 |
| $q_{\mu\text{LJ}} = 0$ | 3460±60 | 4560±70 | 3580±70 | 1839±29 | 344±11 | 137±13 | 30±6 |

Table 7.1: Signal events remaining after each cut applied in the $\mu$LJ-$\mu$LJ channel. Events are generated according to the FRVZ model and are normalized assuming a branching ratio $B(\text{H} \rightarrow 2\gamma_d + \text{X}) = 0.05$.

| Cuts | $m_{\gamma_d}$ = 0.4 GeV | $m_{\gamma_d}$ = 2 GeV | $m_{\gamma_d}$ = 10 GeV | $m_{\gamma_d}$ = 15 GeV | $m_{\gamma_d}$ = 25 GeV |
|---|---|---|---|---|---|
| None | 337800±700 | 337800±700 | 337600±700 | 337600±700 | 337800±700 |
| $2\mu$LJ | 22390±170 | 19780±160 | 3490±70 | 297±20 | 52±8 |
| Trigger | 19920±160 | 17850±150 | 3440±70 | 294±20 | 52±8 |
| Trigger Matching | 17390±150 | 15610±140 | 3350±70 | 289±19 | 50±8 |
| $q_{\mu\text{LJ}} = 0$ | 17380±150 | 15610±140 | 3350±70 | 289±19 | 50±8 |

Table 7.2: Signal events remaining after each cut applied in the $\mu$LJ-$\mu$LJ channel. Events are generated according to the HAHM model and are normalized assuming a branching ratio $B(\text{H} \rightarrow 2\gamma_d) = 0.05$.

# Control region muonic channel

| Cuts | $m_{\gamma_d}$ = 0.24 GeV | $m_{\gamma_d}$ = 0.4 GeV | $m_{\gamma_d}$ = 0.9 GeV | $m_{\gamma_d}$ = 2 GeV | $m_{\gamma_d}$ = 6 GeV | $m_{\gamma_d}$ = 10 GeV | $m_{\gamma_d}$ = 15 GeV |
|---|---|---|---|---|---|---|---|
| None | 337900±700 | 337900±700 | 337900±700 | 331200±1100 | 349300±1000 | 337800±700 | 337600±700 |
| $1\mu$LJ + $0e$LJ | 77380±310 | 89480±340 | 83170±330 | 55840±270 | 21570±150 | 12530±130 | 3750±70 |
| Triggers | 4970±80 | 6550±90 | 6520±90 | 3330±40 | 2273±35 | 3220±60 | 1510±40 |
| Trigger matching | 585±27 | 1980±50 | 2810±60 | 1515±26 | 1372±24 | 2430±60 | 1170±40 |
| Electron veto | 581±27 | 1960±50 | 2800±60 | 1508±26 | 1361±23 | 2410±60 | 1170±40 |
| 2 signal muons | 2.5±1.8 | 2.7±1.6 | 3.0±1.8 | 2.6±1.1 | 558±14 | 1190±40 | 655±28 |
| $\Delta R_{\mu\mu} > 1.8$ | 2.5±1.8 | 1.9±1.4 | 1.3±1.3 | 1.1±0.6 | 0.6±0.4 | 39±7 | 240±16 |
| $\lvert m^{\mathrm{imb}}\rvert > 0.2$ | 2.5±1.8 | 1.9±1.4 | 1.3±1.3 | 1.1±0.6 | 0.6±0.4 | 28±6 | 196±15 |
| $\Delta\phi_{\mu\mathrm{LJ}-\mu\mu} > 2.8$ | 1.3±1.3 | 0.0±0.0 | 1.3±1.3 | 0.4±0.4 | 0.27±0.27 | 0.8±0.8 | 0.0±0.0 |
| $q_{\mu\mathrm{LJ}} = 0$ | 0.0±0.0 | 0.0±0.0 | 1.3±1.3 | 0.0±0.0 | 0.27±0.27 | 0.0±0.0 | 0.0±0.0 |

Table 7.3: Signal events remaining after each cut applied in the CR of the $\mu$LJ-$\mu$LJ channel. Events are generated according to the FRVZ model and are normalized assuming a branching ratio $B(\mathrm{H} \to 2\gamma_d + \mathrm{X}) = 0.05$.

| Cuts | $m_{\gamma_d}$ = 0.4 GeV | $m_{\gamma_d}$ = 2 GeV | $m_{\gamma_d}$ = 10 GeV | $m_{\gamma_d}$ = 15 GeV | $m_{\gamma_d}$ = 25 GeV |
|---|---|---|---|---|---|
| None | 337800±700 | 337800±700 | 337600±700 | 337600±700 | 337800±700 |
| $1\mu$LJ + $0e$LJ | 107700±400 | 115500±400 | 53910±260 | 16480±150 | 3380±70 |
| Trigger | 9060±110 | 9950±110 | 12770±130 | 4800±80 | 1070±40 |
| Trigger matching | 3130±60 | 4300±70 | 10280±110 | 4100±70 | 875±34 |
| Electron veto | 3130±60 | 4290±70 | 10220±110 | 4080±70 | 870±33 |
| 2 signal muons | 3.4±2.0 | 6.2±2.6 | 5730±80 | 2500±60 | 505±25 |
| $\Delta R_{\mu\mu} > 1.8$ | 2.3±1.6 | 3.5±2.0 | 8.9±3.0 | 58±8 | 144±13 |
| $\lvert \mathrm{m}^{\mathrm{imb}}\rvert > 0.2$ | 2.3±1.6 | 3.5±2.0 | 5.8±2.4 | 2.3±1.6 | 3.3±1.7 |
| $\Delta\phi_{\mu\mathrm{LJ}-\mu\mu} > 2.8$ | 1.3±1.3 | 2.5±1.8 | 5.8±2.4 | 1.0±1.0 | 1.2±1.2 |
| $q_{\mu\mathrm{LJ}} = 0$ | 0.0±0.0 | 0.0±0.0 | 0.0±0.0 | 1.0±1.0 | 1.2±1.2 |

Table 7.4: Signal events remaining after each cut applied in the CR of the $\mu$LJ-$\mu$LJ channel. Events are generated according to the HAHM model and are normalized assuming a branching ratio $B(\mathrm{H} \to 2\gamma_d) = 0.05$.

# Trigger strategy electronic channel

| Periods | Single-electron triggers |
|---|---|
| 2015 | HLT_e24_lhmedium_L1EM20VH<br>HLT_e60_lhmedium<br>HLT_e120_lhloose |
| 2016-2018 | HLT_e26_lhtight_nod0_ivarloose<br>HLT_e60_lhmedium_nod0<br>HLT_e140_lhloose_nod0 |

Table 6.2: Choice of lowest unprescaled single electron trigger list used in the $e$LJ–$e$LJ selection and the corresponding data-taking periods.

| Periods | Di-electron triggers |
|---|---|
| 2015 | HLT_2e12_lhvloose_L12EM10VH |
| 2016 | HLT_2e17_lhvloose_nod0 |
| 2017 (only B5-B8) | HLT_2e24_lhvloose_nod0 |
| 2017 (except B5-B8) | HLT_2e17_lhvloose_nod0_L12EM15VHI |
| 2018 | HLT_e60_lhmedium_nod0 |

Table 6.3: Choice of lowest unprescaled di-electron trigger list used in the $e$LJ–$e$LJ selection and the corresponding data-taking periods. During the accidentally prescaled periods B5-B8 (runs 326834-328393 with an effective reduction of 0.6 fb-1), HLT_2e24_lhvloose_nod0 is used instead of HLT_2e17_lhvloose_nod0_L12EM15VHI.

# Signal region electronic channel

FRVZ

| $m_{\gamma_d}$ [GeV] | 0.017 | 0.03 | 0.06 | 0.1 | 0.24 | 0.4 | 0.9 | 2 | 6 |
|---|---|---|---|---|---|---|---|---|---|
| 2 $e$LJs | 1900±22 | 1500±20 | 1100±17 | 830±14 | 210±7 | 54±4 | 8.5±1.4 | 1.2±0.5 | 7.9±1.3 |
| Trigger Matched | 1700±20 | 1300±18 | 960±15 | 730±13 | 200±7 | 53±4 | 8.5±1.4 | 1.2±0.5 | 7.5±1.2 |
| Leading track $p_T > 5$ GeV | 1600±20 | 1300±18 | 940±15 | 710±13 | 200±7 | 53±4 | 8.1±1.4 | 0.9±0.4 | 7.2±1.2 |
| $e$LJ $\eta < 1.5$ | 1100±16 | 820±14 | 610±12 | 420±10 | 130±6 | 36.0±2.9 | 5.6±1.1 | 0.38±0.27 | 4.8±1.0 |
| $\Delta\Phi(e\text{LJ}, e\text{LJ}) > 2$ | 720±13 | 550±12 | 410±10 | 300±9 | 72±4 | 17±2 | 3.2±0.9 | / | 4.3±1.0 |
| Z mass veto | 580±12 | 450±11 | 330±9 | 250±8 | 57±4 | 11.0±1.6 | 2.4±0.8 | / | 2.5±0.7 |
| $q_{e\text{LJ}} = 0$ | 580±12 | 450±11 | 330±9 | 250±8 | 57±4 | 11.0±1.6 | 2.4±0.8 | / | 2.5±0.7 |
| $m_{e\text{LJ}} > 20$ MeV | 200±6.9 | 290±8.6 | 310±8.9 | 240±7.7 | 57±3.7 | 11.0±1.6 | 2.2±0.72 | / | / |
| $\|m^{\text{imb}}\| < 0.8$ | 200±6.9 | 290±8.6 | 310±8.9 | 240±7.7 | 57±3.7 | 11.0±1.6 | 2.0±0.68 | / | / |

HAHM

| $m_{\gamma_d}$ [GeV] | 0.017 | 0.1 | 0.4 | 2 | 10 | 15 | 25 |
|---|---|---|---|---|---|---|---|
| 2 $e$LJs | 8400±46 | 3300±29 | 470±11 | 8.5 ±1.4 | 230 ±7.5 | 48 ±3.4 | 12 ±1.8 |
| Trigger Matched | 8300±46 | 3200±28 | 470±11 | 8.5 ±1.4 | 230 ±7.4 | 46 ±3.3 | 12 ±1.7 |
| Leading track $p_T > 5$ GeV | 8200±46 | 3200±28 | 460±11 | 8.2 ±1.4 | 220 ±7.4 | 44 ±3.2 | 11 ±1.7 |
| $e$LJ $\eta < 1.5$ | 5500±37 | 1700 21 | 280±8.5 | 5.9 ±1.1 | 140 ±5.7 | 20 ±2.1 | 4.6 ±1.2 |
| $\Delta\Phi(e\text{LJ}, e\text{LJ}) > 2$ | 4400±33 | 1300±18 | 180±6.8 | 2.1 ±0.69 | 130 ±5.6 | 4.8 ±1 | 0.68 ±0.39 |
| Z mass veto | 4200±32 | 1200±17 | 170±6.6 | 2 ±0.69 | 120 ±5.5 | 2.5 ±0.7 | 0.22 ±0.22 |
| $q_{e\text{LJ}} = 0$ | 4200±32 | 1200±17 | 170±6.6 | 2 ±0.69 | 120 ±5.5 | 2.3 ±0.69 | / |
| $m_{e\text{LJ}} > 20$ MeV | 1800±21 | 1100±117 | 170±6.6 | 2 ±0.69 | 120 ±5.5 | 2.3 ±0.69 | / |
| $\|m^{\text{imb}}\| < 0.8$ | 1800 ±21 | 1100±117 | 170±6.6 | 2 ±0.69 | 120 ±5.2 | 0.33 ±0.24 | / |